The role of sleep-oscillations in the emergence of hippocampal-dependent memory during postnatal development.

Doctorado en Neurociencias
María Alexandra García Pérez

Thesis submitted to the Pontificia Universidad Católica de Chile
in fulfillment of the requirements for the degree of Doctor in Neurosciences.

Advisors:
José Luis Valdés PhD,
Lab. Aprendizaje y Memoria y Neuromodulación
Pedro Maldonado PhD, *Lab. Neurosistemas*
Francisco Aboitiz PhD, *Lab. LaNCE*

Approved on March 10, 2022

PONTIFICIA UNIVERSIDAD CATÓLICA DE CHILE
Doctorado en Neurociencias

El Comité de Tesis, constituido por los Profesores abajo firmantes, aprueba la Defensa Pública de la Tesis Doctoral titulada:

The role of sleep-oscillations in the emergence of hippocampal-dependent memory during postnatal development.

Aprobación Defensa:
MARÍA ALEXANDRA GARCÍA PÉREZ

Calificándose el trabajo realizado, el manuscrito sometido y la defensa oral, con nota 7,0 (Siete coma cero)

Dr. Mauricio Cuello
Director de Investigación y Doctorado
Escuela de Medicina
Pontificia Universidad Católica de Chile

Dr. Felipe Heusser
Decano
Facultad de Medicina
Pontificia Universidad Católica de Chile

Dra. Claudia Sáez
Sub-Directora
Dirección de Investigación y Doctorado
Escuela de Medicina
Pontificia Universidad Católica de Chile

Dr. Francisco Aboitiz D.
Jefe Programa Doctorado en Neurociencias
Director de Tesis
Facultad de Medicina
Pontificia Universidad Católica de Chile

Dr. Pedro Maldonado
Co-Director de Tesis
Escuela de Medicina
Universidad de Chile

Prof. José Luis Valdés
Co-Director de Tesis
Facultad de Medicina
Universidad de Chile

Prof. Claudio Pérez Leighton
Profesor Evaluador Interno
Facultad de Ciencias Biológicas
Pontificia Universidad Católica de Chile

Prof. Jorge Campusano
Profesor Evaluador Interno
Facultad de Ciencias Biológicas
Pontificia Universidad Católica de Chile

Prof. Alexia Núñez
Profesor Evaluador Externo
Facultad de Ciencias
Universidad de Chile

Santiago, 10 de marzo de 2022.-

RESUMEN (Español e Inglés):

English:

Hippocampus-dependent memories emerge late during postnatal development, correlating with hippocampal maturation. During sleep, the two-stage memory formation model states that through the hippocampal-neocortex dialogue, cortical slow-oscillations (SO), thalamocortical Spindles, and hippocampal sharp-wave ripples (SWRs) gets synchronized, allowing the consolidation of episodic memories. However, evidence supporting these hypotheses during the first weeks of development is still lacking. Here, we performed successive object-in-place tests during the temporal window of memory emergence. We recorded the in vivo activity of SO, Spindles, and SWRs during sleep immediately after learning, and we found that hippocampus-dependent memory appears at P32 independently of task overtraining.

Interestingly, we observed that those animals with better performance had a higher density and duration of Spindles and a lower density of SWRs. Furthermore, we observed changes in the SO-Spindles and Spindles-SWRs temporal-coupling during the 3-6 postnatal week. Our results provide novel evidence regarding hippocampus-dependent memory onset and explain how adult consolidation models fit in the early stages of postnatal development.

Spanish:

Las memorias dependientes del hipocampo surgen tardíamente en el desarrollo postnatal y en paralelo con la maduración del hipocampo. El modelo de formación de la memoria en dos etapas afirma que durante el sueño ocurre un diálogo entre el hipocampo y la neocorteza, donde las oscilaciones lentas corticales (SO), los *Spindles* talamocorticales y los *Sharp-wave ripples* del hipocampo (SWR) se sincronizan, permitiendo la consolidación de los recuerdos de tipo episódicos. Sin embargo, este modelo no ha sido validado en etapas tempranas del desarrollo. En esta tesis, se evaluó la aparición de la memoria dependiente de hipocampo mediante la exposición sucesiva a la prueba conductual de reconocimiento de objeto-lugar. Junto con esto, se registró la actividad *in vivo* de SO, Spindles y SWRs durante periodos de sueño inmediatamente posteriores a la evocación en la tarea de objeto-lugar, donde encontramos que la memoria dependiente del hipocampo aparece en el día postnatal 32, independientemente del sobre-entrenamiento previo de la tarea.

Curiosamente, observamos que los animales con mejor rendimiento tenían una mayor densidad y duración de los *Spindles* y una menor densidad de SWRs. Además, observamos cambios en el acoplamiento temporal entre SO-Spindles y Spindles-SWRs durante esta ventana temporal. Nuestros resultados aportan nuevas evidencias sobre el inicio de la memoria dependiente del hipocampo y explican cómo se ajustan los modelos de consolidación adulta en las primeras etapas del desarrollo postnatal.

The role of sleep-oscillations in the emergence of hippocampal-dependent memory during postnatal development.

Doctorado en Neurociencias
María Alexandra García Pérez

Thesis submitted to the Pontificia Universidad Católica de Chile
in fulfillment of the requirements for the degree of Doctor in Neurosciences.

Advisors:
José Luis Valdés PhD,
Lab. Aprendizaje y Memoria y Neuromodulación
Pedro Maldonado PhD, *Lab. Neurosistemas*
Francisco Aboitiz PhD, *Lab. LaNCE*

Approved on March 10, 2022

"My own brain is to me the most unaccountable of machinery - always buzzing, humming, soaring roaring diving, and then buried in mud. And why? What's this passion for?"
— Virginia Woolf

"When you make the finding yourself - even if you're the last person on Earth to see the light - you'll never forget it."
— Carl Sagan

"Develop enough courage so that you can stand up for yourself and then stand up for somebody else"
— Maya Angelou

Index

List of Figures

List of Supplementary Figures

List of Tables

List of Equations

I

Abstract

Hippocampus-dependent memories emerge late during postnatal development, correlating with hippocampal maturation. During sleep, the two-stage memory formation model states that through the hippocampal-neocortex dialogue, cortical slow-oscillations (SO), thalamocortical Spindles, and hippocampal sharp-wave ripples (SWRs) gets synchronized, allowing the consolidation of episodic memories. However, evidence supporting these hypotheses during the first weeks of development is still lacking. Here, we performed successive object-in-place tests during the temporal window of memory emergence. We recorded the in vivo activity of SO, Spindles, and SWRs during sleep immediately after learning, and we found that hippocampus-dependent memory appears at P32 independently of task overtraining.

Interestingly, we observed that those animals with better performance had a higher density and duration of Spindles and a lower density of SWRs. Furthermore, we observed changes in the SO-Spindles and Spindles-SWRs temporal-coupling during the 3-6 postnatal week. Our results provide novel evidence regarding hippocampus-dependent memory onset and explain how adult consolidation models fit in the early stages of postnatal development.

II

2.0 Introduction

This thesis proposed investigating the onset of hippocampal-dependent memory during the postnatal period between P26 and P32. In parallel, to characterize the oscillatory profile during sleep, to answer whether sleep oscillations play a role in the consolidation of hippocampal-dependent memory during development? To facilitate the reading, we will divide the introduction into some main topics: hippocampus-dependent memory, ontogeny of episodic memory, sleep oscillations, and the active system consolidation theory, which will be deepened to contextualize the state of the art regarding this research question.

2.1 Hippocampus-dependent memory

The hippocampus is one of the most studied subcortical structures, located deep in the medial temporal lobe (MTL). Since the human case study H.M., a patient who suffered anterograde amnesia after removing the MTL [1], became one of the main foci of neuroscientific research linking it to memory formation [2].

In rodents, the hippocampus is a large, cashew-shaped structure that lies just below the neocortex. In general, the hippocampal circuitry or "trisynaptic loop" is well known and has been widely described to consist of unidirectional, excitatory

pathways that traverse from de entorhinal cortex to the dentate gyrus, CA3, and CA1 to the come back to the same cortex (Fig.1).

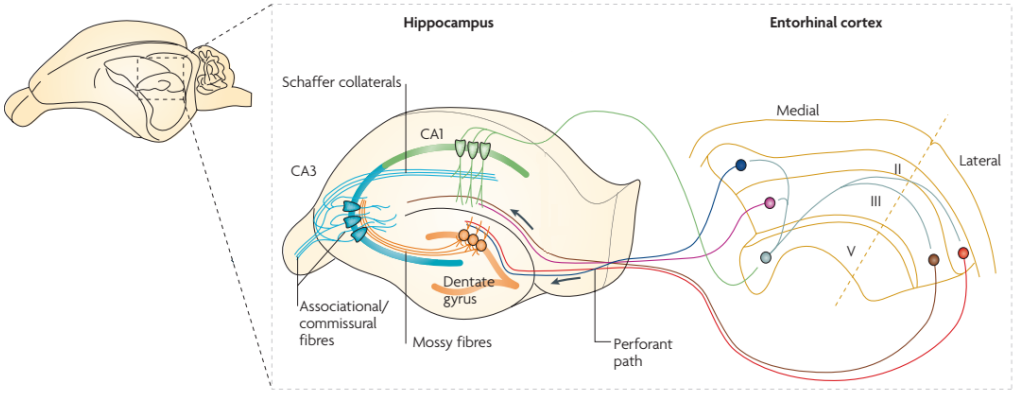

Figure 1: Basic anatomy of the hippocampus. The wiring diagram of the hippocampus is traditionally presented as a trisynaptic loop. In a simplified view, the primary input is carried by axons of the perforant pathway, which send polymodal sensory information from layer II/III of the entorhinal cortex to the dentate gyrus. These axons establish excitatory synaptic contact with the dendrites of the granule cells from the dentate gyrus and the lateral and medial entorhinal cortex. In turn, the granule cells project, via their axons (the mossy fibers), to the apical dendrites of the CA3 pyramidal cells projecting to the CA1 pyramidal cells via Schaffer's collaterals and to the CA3 and CA1 pyramidal cells. Some additional direct connections between CA3/CA1 and the entorhinal cortex are shown. *Modified from [3]*

.

Memories are constructed in three well-defined stages: acquisition of information (encoding), reorganization of this information for short/long-term storage (consolidation), and recall of the learned information (retrieval) [4]. The hippocampus is well known to be a brain structure that supports multiple types of memory [5]. It is even more essential for episodic memory, also known as "autobiographical"; used when we refer, store, and recall facts or events by answering three questions: "what happened", "where did it happen" and "when did it happen" [6]. Episodic memory requires the integration of a single event with its specific contextual information. At its core, the circuit requires higher association areas to process sensory information (neocortex), areas to communicate

with the hippocampus (parahippocampal region), the hippocampus to integrate and retrieve information about the episode, and the executive regions to produce appropriate behavior (prefrontal cortex) [7].

The hippocampus plays a critical role in the spatial and non-spatial component of episodic memory processing - "where did it happen" - by creating internal representations of space that it uses as a "spatial map" to guide navigation-based behavior [6, 8-9]. Both encoding and recall are spatial context-dependent processes - "where it happened" - meaning that memories are created using external environmental cues as reference. When memory involves a spatial component, contextual or temporal associations depend on interactions between areas that remain remarkably similar across mammalian species [10]: perirhinal cortex, hippocampus, and medial prefrontal cortex [7, 10-12].

The most consistent evidence for hippocampal involvement in memory functions has been obtained using spatial memory tasks for navigation [13, 14]. In rats, a significant proportion of hippocampal pyramidal cells known as "place cells", because they discharge only at specific positions in an experimental environment, have shown spatial firing correlates [15, 16]. In addition, rodents with partial hippocampal lesions show severe impairments in the acquisition of spatial navigation tasks [17, 18]. Similarly, rats with complete hippocampal lesions cannot perform tasks even when distal cues are used as spatial references [19, 20]. On the other hand, human studies of functional imaging have shown that the evocation of episodic memories, particularly with spatial composition, activates the hippocampus [21, 22]. These results strongly suggest that the hippocampus plays a critical role during the encoding and retrieval of spatial memory.

2.2 Ontogeny of episodic memory

The emergence of episodic memory has been related to the "maturation" of the hippocampus [23, 24]. This term refers to the continuous physiological changes during postnatal development until the adult physiological profile is reached. In humans, it has been argued that children younger than 4 or 5 years cannot form episodic memories [25]. However, this form of memory shows continued development throughout early and middle childhood, although rudimentary episodic memory skills seem to be in place by age three years [26]. Interestingly, more recent findings have suggested that it is the ability to retain, rather than form, episodic memories that would be triggering this controversy, evidenced in experiments on 3-year-olds that showed good manifestation of episodic memories with short, but not long, retention periods [27].

In this regard, animal models and recognition memory tasks, such as novel-object recognition (NOR) or object-in-place recognition (OPR) (Fig. 2), are advantageous for studying the neurobiology of different expressions of episodic memory, as they usually involve a single-trial training phase and allow the assessment of different components of this memory [28, 29]. Westbrook et al. (2014) reported in rodents that the hippocampus-independent novel-object recognition tasks (i.e., NOR) occur earlier in development, in the pre-weanling stage (Fig.3), around postnatal day 17 (P17) followed by hippocampus-dependent discrimination task (i.e., OPR) [29].

Within a hippocampus-dependent task, there are further distinctions to consider, first related to retention times, appearing earlier those memories using short retention periods (assessed after 5 min) around P17-P21 [29], and then long-term retention memories (referred to up to 24 h) around P26-P31 [28-30]. Along with this, spatial memories representations concerning with the own body

(egocentric) came earlier than memories using distant spatial cues (allocentric), being the latest form of episodic memory to emerge during the transition to adolescence in rats, P38 [31]. Thus, we can see that reaching a consensus on when memory appears is not an easy task as it depends on multiple factors; such as whether or not it depends on the hippocampus, the nature of the task, and the behavioral parameters chosen, the animal model, the spatial cues used, the retention time between the encoding and recall phases of the behavioral task, among others.

Spatial memories are the last form of episodic memory to emerge, probably because the systems that support them take longer to mature. These memories require fully developed hippocampal place cells, medial temporal lobe grid cells, head direction cells, boundary cells, between other neuronal systems to provide all the spatial information needed by the animal [9, 32]. Contreras et al. (2019) recently showed that some glimpses of spatial memory emerge from P18, but it was not until P38 reflected as the canonical displaced object exploration preference relative to the familiar object as has been widely observed in adult rats [31]. They also showed that around P18-P38, there is a specific developmental shift, in which rats manifest changes in the exploration preference from familiar to a novel location. Thus, postulating allocentric memories as the latest type of memory to emerge postnatally [31].

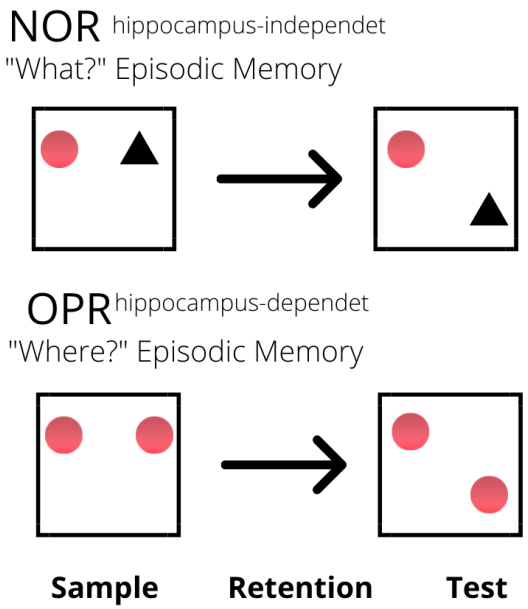

Figure 2: Recognition memory task. Novel object recognition (NOR) is the hippocampus-independent task used to evaluate episodic memory "what" component. The hippocampus-dependent object-in-place (OPR) is used to assess the spatial component "where" of episodic memory. Sample: the first exposition to the objects, Retention: time , between the sample and test, which usually can range from 5 min-48h. Test: the last part of the task, when the rodent is challenged to discriminate the displaced object.

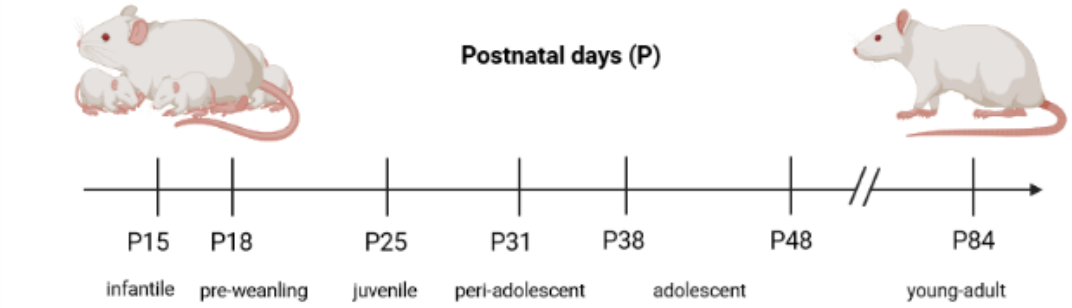

Figure 3: Rat developmental stages. Different postnatal days (P) representing different developmental stages. Infantile: P15, pre-weanling: P18; juvenile: P25, peri-adolescent: P31; adolescence: P38, P48, and young adult: P84. *Adapted from [31].*

2.3 Sleep Oscillations

One of the main functions of sleep is to isolate the brain from the body and the environment, and contrary to what one would first think, the brain is busy at night. Since the earliest electrophysiological studies, attempts have been made to understand the oscillatory behavior of the brain, arguing that there must be a good reason why complex brains have developed an elaborate sleep choreography.

In humans, at least five stages of sleep have been identified. The rapid eye movement (REM) phase and four subsequent phases called the non-REM (NREM) state, N1 to N4. REM sleep is characterized by an oscillatory profile similar to wakefulness (high frequency and low amplitude), rapid eye movements, atonia, and high-voltage hippocampal theta activity (5-8 Hz) [33]. It usually makes up 20-25 percent of total sleep time in healthy adults, and indicates the end of a non-REM/REM sleep cycle. On the other hand, the NREM stage is based primarily on the relative number of sleep spindles and large-amplitude delta (1–4

Hz) activity on cortical electroencephalogram (EEG) recordings [33, 34]. Stage 1 is the transitional phase between wakefulness and sleep. It consists of a relatively low voltage EEG with mixed frequencies. Stage 2 is characterized by the appearance of sleep spindles and K-complexes. Stage 3 is a mixture of Spindles and delta waves (20-50 percent), while stage 4 is characterized by a predominance of delta activity with only traces of Spindles. Stages 3 and 4 are often referred to as slow-wave or delta sleep. Although the classification of sleep stages is useful, the temporal boundaries of these stages are not precise. Typically, four to five NREM/REM cycles occur in a night with a period of 70-90 minutes each [35]. These five stages are organized in a periodic sequence, characterized on a hypnogram as the macrostructure of sleep.

It is important to note that in rodents, sleep architecture is rather polyphasic and fragmented. NREM or REM sleep periods may be interrupted by random micro-vigilant states without necessarily having a definite continuity between these cycles as described in humans [36, 37]. In addition, in rodents, it is impossible to determine the 4-stages of NREM sleep, indicating only one that receives the name and is characterized by high-amplitude cycles of delta waves and sleep spindles (Fig. 4) [33].

Oscillations have quantifiable parameters that allow their study and characterization, such as their frequency, amplitude, duration, among others. In adults, these parameters are usually more or less stable, and characteristic of each oscillation or oscillatory event over time, and we take them as a reference, denominating them as “mature”. Therefore, it is understood that these oscillations may change their parameters in previous “immature” stages of development or pathologies and consequently modulate the functions usually attributed to them.

Here we will focus on describing the characteristic oscillations of NREM

sleep: slow cortical oscillations (SO), thalamic Spindles (SPs), and hippocampal sharp-wave ripples (SWRs) (Fig.4b). SOs (0.5-4 Hz) are the hallmark of cortical LFP during non-REM sleep [38]. It is characterized as a phenomenon generated in the frontal cortex and propagates as traveling waves [39, 40] with descending periods of membrane hyperpolarization followed by ascending states of membrane depolarization and increased cortical activity [38, 41, 42]. SO begin to appear as discontinuous and short slow oscillation cycles once the cortex has completed its anatomical development, from the second postnatal week in rodents (P11-P12) [43]. SO amplitude correlates positively with sleep homeostatic pressure [44] and decreases in successive NREM episodes, being highest during the first hours of sleep [45]. Furthermore, it has been shown that SO amplitude is modulated by learning experiences; for example, sleeping immediately after completing a motor task improves performance and correlates with an increase in SO amplitude in the cortical areas involved [46]. On the contrary, a decrease in SO amplitude has been described in the visual cortex after visual deprivation [47]. In both rodents and humans, a slow oscillatory activity follows an inverted U-shape during development, which is thought to reflect cortical synaptic changes, first increasing and peaking due to synaptogenesis, and then decreasing during adolescence and adulthood due to refinement or pruning of synaptic connections [43, 48, 49]. Interestingly, recent studies have shown that SO density decreases with age and even more so in Alzheimer's patients, intensifying its role with memory consolidation [50].

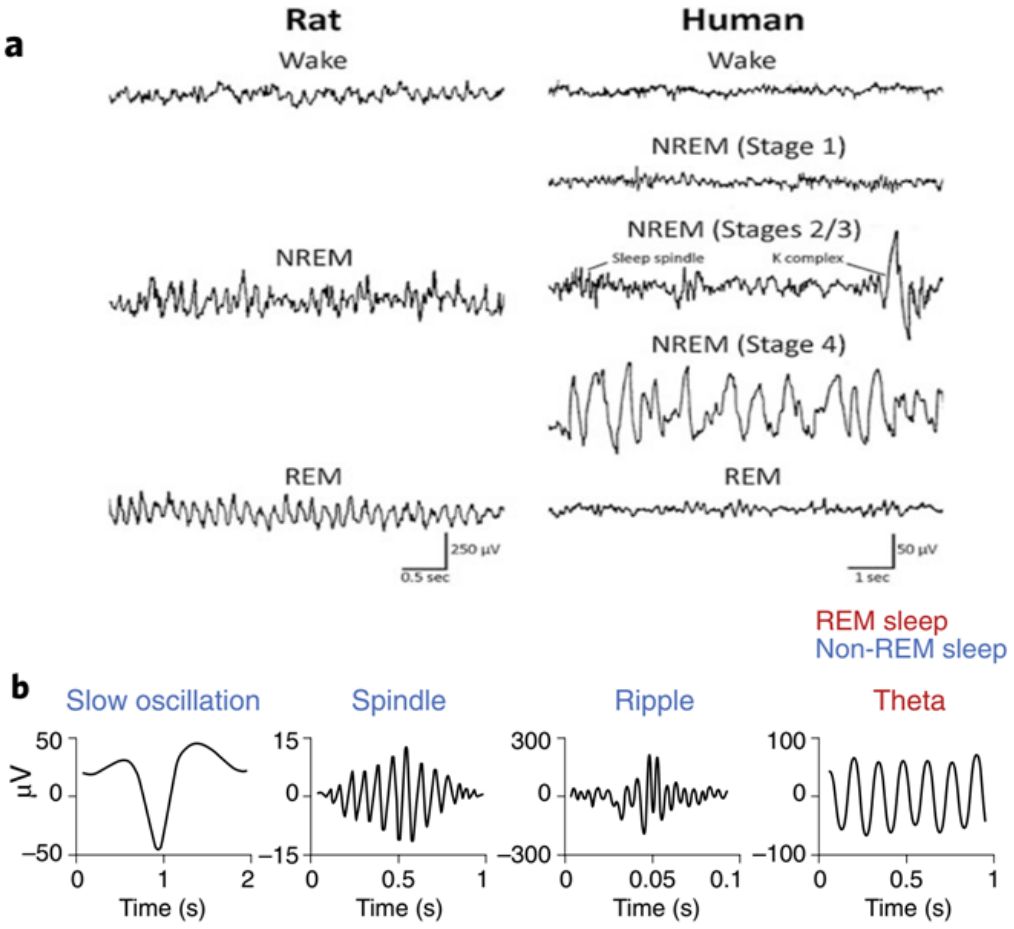

Figure 4: Sleep architecture. (a) Electroencephalographic (EEG) recordings of vigil states (wakefulness, NREM, and REM sleep) in rats and humans. Wakefulness in both species is characterized by low-amplitude, high-frequency cortical activity. NREM sleep in the rodent is usually not differentiated between stages and has a large delta amplitude (1-4 Hz). NREM sleep in humans is classified into four stages. In the first stage, they are showing alpha and theta activity. Sleep spindles (7- 14 Hz) and K-complexes are observed in stages 2 and 3 of NREM sleep. In stage 4 of NREM sleep, also known as slow-wave sleep, strong delta activity (1-4 Hz) of large amplitude is observed. The EEG returns to a profile similar to wakefulness, with low-amplitude, high-frequency activity. (b) Neocortical slow oscillations, thalamocortical spindles, and hippocampal ripples are electrophysiological signatures of non-REM sleep. Theta oscillations are prominent during REM sleep, particularly in the rodent hippocampus (5-8 Hz). *Modified from [33, 34].*

Spindles are transient (1-3 s) oscillations in the 7-18 Hz range present in the thalamus and neocortex [38, 51, 52]. Spindles start appearing during NREM sleep

at P14, presenting changes in frequency and duration, and by P18, the EEG is adult-like [53]. Spindles usually follow the K-complexes, recognized as an abrupt negative deflection in the EEG during NREM sleep. Like SOs, Spindles in the human brain also tend to occur locally [54], generated independently of cortical input in the thalamic reticular nucleus [55]. However, they can also be observed synchronously in the cortex [56-58]. On the other hand, Spindles densities are positively correlated with learning in rats and humans [59-61].

SWRs are discrete, short (30-120 ms) LFP events that occur in the hippocampus (CA1) during NREM sleep and awake immobility [62-65]. SWRs occur stochastically and locally by a depolarization of CA1 pyramidal cells resulting from synaptic input in CA3 generating a "sharp-wave", followed by rapid oscillatory ripples (100-300 Hz). The characteristic SWR oscillations appear on P14, with a stable frequency throughout development [66]. However, their amplitude increases during the third postnatal week, growing to reach an adult-like profile by P20 [66]. Several studies have demostrated the role of SWRs in episodic memory consolidation using closed-loop online detection/suppression of SWRs during immobility [67] or during sleep after learning [68, 69], which transiently impaired subsequent memory performance. Similarly, suppression of SWRs induced by optical stimulation of non-serotonergic neurons in the medial raphe resulted in the abolition of fear memory [70].

2.4 The active system consolidation theory

The mechanisms by which memory is consolidated remain primarily unknown. However, much research has pointed towards sleeping as a memory promoter since it improves episodic memory when taken immediately after encoding [71-73]. The sleep-oscillatory-activity contribute mainly to hippocampal-dependent memory consolidation [72-74]. There are two main widespread hypotheses in which sleeps rhythms plays as the subjacent "off-line" consolidation mechanism. First, the "Two-stage memory formation mechanism" [75] states that during wakefulness, memories are initially encoded as a temporary and labile buffer in the hippocampus and then gradually transferred to long-term storage in the neocortex, allowed by the coordination of sleep-oscillatory rhythms [75, 76]. Secondly, "The active system consolidation theory" [76] complemented and updated the first theory, deepening the hippocampal-cortical dialogue. Stating that memory transference into the long-term storage occurs by the phase-locking of the three hallmarks oscillatory patterns of NREM: the slow cortical waves (< 1 Hz), the thalamic spindles (9-16 Hz), and the hippocampal sharp-wave ripples (SWRs, 100-250 Hz) (Fig.5) [77-79].

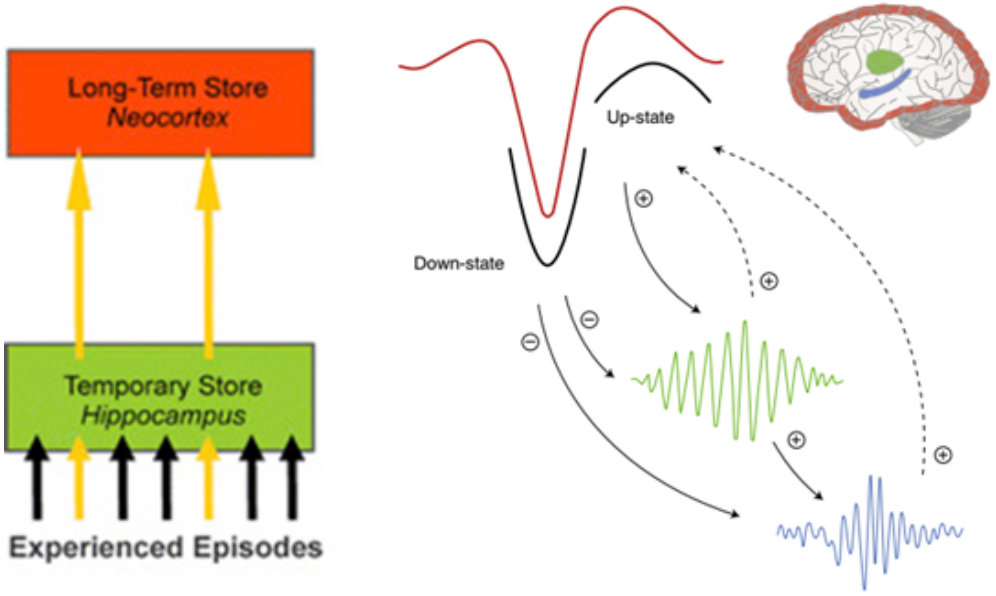

Figure 5: Active system consolidation model. Memory consolidation during NREM sleep is based on a dialogue between the neocortex and the hippocampus, where labile memories stored in the hippocampus are transferred to the cortex for long-term storage. This process occurs under the control of slow neocortical oscillations (red) that, in turn, command sharp-wave ripples (blue) and thalamocortical Spindles (green), allowing the formation of a loop of synchronous events. The spindle is coupled in the up-state of the SO, thus recruiting SWRs, and allowing synaptic plasticity events that allow memory consolidation. Both Spindles and hippocampal ripples can also induce SOs in the prefrontal cortex. *Modified from: [34, 80].*

More recent studies have explored these hypotheses in several models, Latchoumane et al. reported in mice that via optogenetics and thalamic stimulation during sleep, SPs that were aligned to the up-state of slow oscillation were responsible for an improvement in the consolidation of hippocampus-dependent memories [79]. Furthermore, it highlighted those slow oscillations alone were not sufficient to explain this mechanism, but rather the importance of these three oscillatory events for memory consolidation to occur. On the other hand, SWRs alone have been described as events that play a fundamental role in the consolidation of memories, as their suppression during post-learning sleep worsened hippocampal-dependent spatial memory consolidation [68]. Likewise, the disruption of SPs-SWRs coordination also worsens the

post-sleep spatial memory [81].

In this line, Maingret et al. made an essential contribution by determining for the first time a causal relationship between the temporal coupling of slow oscillations, Spindles and ripples with the hippocampus-dependent memory consolidation in rats. Utilizing a cortical electrical stimulation protocol, they enhanced and decreased the synchrony between these three oscillations, observing that memory consolidation was significantly improved when these events were coupled [82].

However, up to date, all these studies have focused on adult animals, remaining unexplored how the oscillatory patterns change along with after-birth development; particularly, how "The active system mechanism" and "The active system consolidation theory" fits with the postnatal emergence of hippocampus-dependent memories. Slow-wave oscillations, spindles, and SWRs become detectable by around the second postnatal week (P14) [43, 53] and, studies in rodents have shown that these oscillations continue maturing postnatally by changing some parameters until they adopt the adult-like form [49, 66, 83]. Altogether, these oscillatory changes co-occur with the emergence of spatial-memory abilities and the rat sensorimotor repertoire [5, 84], which may explain episodic memory developmental onset.

Consequently, we hypothesized that the synchronization of cortical slow-oscillations, thalamic Spindles, and hippocampal sharp-wave ripples supports spatial memory consolidation during the transition of juvenile to adolescence during sleep. As episodic memory has been reported to emerge at different postnatal days, we want to focus on the behavioral switch between P25-P38 previously described [31] and evaluate if the early overtraining of the task could anticipate its expression.

To evaluate how sleep oscillations relate to the emergence of episodic memory in a rodent model, we choose as experimental approach: a hippocampus-dependent recognition memory task known as Object-in-place recognition, OPR, a spontaneous exploration task, which requires making an association between an object and a place by using spatial cues as guidance and providing an index of incidental contextual learning and memory [28, 85]. These will be complemented with *in-vivo* electrophysiological recordings while performing the OPR task.

Finally, according to our hypothesis, the objectives of this thesis consider three stages: first, implementing an episodic-spatial memory task that emerges later in postnatal development. Second, to identify sleep periods and characterize oscillatory patterns after a recognition memory task. Third, to elucidate a correlation between the postnatal emergence of hippocampus-dependent memory consolidation and sleep oscillatory profile suggest a possible underlying mechanism.

III

3.0 Hypothesis and Objectives

3.1 Hypothesis

The cardinal sleep oscillations: cortical slow-waves, thalamic spindles, and hippocampal sharp-wave ripples synchronize during postnatal development and support spatial memory consolidation.

3.2 General Objective

To characterize the postnatal development of synchronicity of sleep oscillatory patterns: slow-wave sleep, spindles, and sharp-wave ripples and correlate them with the behavioral performance of spatial memory consolidation.

3.3 Specific Objectives

1.- Implement a hippocampus-dependent memory task in which performance evolves during the early stages of development.

2.- Record and characterize the cortical, hippocampal, and thalamic oscillatory activity at sleep state along with the development.

3.- Establish relationships between behavioral performance and sleep architecture for the spatial memory task.

IV

4.0 Methods

4.1 Animals

Forty male Long-Evans rats were used for the experiments. Rats were grouped according to postnatal day (P), and an OPR task was performed with a group of juvenile rats (n = 12) between day 26 and 32, which were successively tested in P26, P28, P30 and P32. P26, P28(n = 12), and P30, P32 (n = 11). Adults rats also performed the OPR test as reference (P90, n=17). An additional group at P32 (n = 11) was included, which underwent OPR testing without prior task overtraining (P32-NoRep).

All litters were born in the facilities of the Centro de Investigaciones Médicas (CIM) of the Pontificia Universidad Católica. The offspring were kept with their mother until weaning (P19). The animal colony was maintained at an ambient temperature of 22^{o}C, with a 12 h/12 h light/dark cycle (lights on at 8:00 h). All rats had free access to food and water during the experiments. All procedures involving experimental animals were performed according to the Humane Care and Use of Laboratory Animals Policy of the U.S. Public Health Service, reviewed and approved by the university (Scientific Ethical Committee for Animal Care and Environment, CEC-CAA) and national (National Commission

for Scientific and Technological Research, CONICYT) bioethics committees according to the Ethics Committee (protocol CEC ID:180430001 and CBA 1108 FMUCH).

4.2 Experimental procedures and task

All procedures were performed between 8:00-14:00 h (i.e., ZT0-ZT6, light on at 8.00 A.M). During the handling phase, animals were gently handled for at least 10 min on five consecutive days. For the next two consecutive days twice daily (AM/PM), in the habituation phase, rats were allowed on the first day to freely explore the empty open field in groups of no more than four rats for 20 min. Followed by 30 min on the pot to sleep, and an additional 10 min customized with active supervision by gentle handling for each rat. On the second day, rats explore as a group the empty arena, and then with an object, followed by personalized exploration (10 min) of the arena plus the object. Immediately after that, the rats were left in the resting pot for 30 min. The same protocol was repeated during the second habituation in the afternoon (PM).

The object-in-place spatial object recognition task consisted of an encoding and recall phases, separated by a 3-hour consolidation interval. During the encoding phase, two copies of the same object were placed in two adjacent corners 10 cm or 15 cm away from the walls, depending on the open field used: a smaller one (40x40x40 cm for P26-P32 rats), and a larger one (80x80x40 cm for adult rats).

Rats were randomly released in front of a wall and allowed to explore the arena and objects for 5-min. The trial was discarded if the rats expressed a preference for one of the two objects during the encoding phase. The rats were then placed in the resting pot during the 3 h retention interval. In this phase,

electrophysiological recordings were performed for the implanted rats (n= 4). The recall phase took place immediately after that. One of the objects was moved a new location, while the other remained in the exact (familiar) location as in the encoding phase. The recall phase comprised another 5-min interval during which the rat could explore the objects and the arena.

The memory index was defined as the exploration time of the displaced object divided by the total exploration time of both objects (Equation 1). Rats were considered exploring an object whenever their head was facing toward and within 2 cm of the object. Exploration time was measured from video recording, using a semi-automated MATLAB routine in single-blind.

$$\frac{\text{displaced object} - \text{familiar object}}{\text{displaced object} + \text{familiar object}} \tag{1}$$

Equation 1: Memory Index

When the Memory Index was close to 1 meant that the exploration of the displaced object was greater than that the familiar one. On the other hand, when it was close to -1 the animals prefer the familiar object over the displaced one; and when it was close to 0 no objects were preferred.

Importantly, between the encoding and recall phase the entries to the arena were randomized, with the rat always facing the respective wall of the arena to avoid the entry position being used as a proximal cue [73, 84]. Object locations during the recall phase were balanced between rats, and the objects and arena were arduously cleaned with alcohol 70 % at each stage.

4.3 Apparatus and objects

The OPR task was performed by using a dark gray square open field. Two different sizes of the arena were used depending on the age of the rats. The juvenile

group (P26, P28, P30, and P32) performed the task in a smaller arena (40 cm x 40 cm with 40 cm high walls), and the adult P90 group performed in a larger arena (80 cm x 80 cm with 40 cm high walls). The objects were glass bottles of different shapes filled with bedding chip. Objects must had sufficient weight so that the rats could not dislodge them. Two size pairs of objects were used depending on age, for the P26-P32 groups, the height of the objects was 10-18 cm, and for the P90 group, it was 22-29 cm. At the test room distal cues were used to facilitate spatial location, fluorescent lamps placed on the ceiling were covered with butter paper to provide indirect light, white noise was played at a constant intensity during all procedures to mask any disturbing sounds. Objects and the open field were thoroughly cleaned between trials with a 70 % ethanol solution. The resting box used in the retention interval was a 35 cm x 35 cm pot, 45 cm high, covered with fluffy material to facilitate the rats sleeping in it.

4.4 Behavioral data collection

The rat behavior was videotaped during the encoding and recall stages for subsequent offline quantification using a semi-automated custom MATLAB routine. First, the locomotor trajectory was determined using the open-source video tracking system IdTracker [87]. The frame rate of the camera (frame rate per second, FPS) was calculated as the number of frame of the video/ video duration, usually 30 FPS, to collect the instantaneous position along the track and the animal trajectory. Next, the animal instantaneous speed was quantified as the mean displacement between adjacent frames divided by the frame time.

Exploration was defined when the rat directed its nose toward the object and sniffed. Climbing on an object or sitting next to it without any sign of active exploration was omitted. The object memory index, which represents the standard way of assessing OPR memory in adult rats, was calculated and is defined by the

previously described formula (Equation 1). Note that the memory index only provides meaningful data if the animal shows minimal amounts of exploration of the two objects. Therefore, only rats that had explored both objects for at least 2 s during the encoding phase were included in the analyses. Total distance traveled, object latency, and whole object exploration time (cumulative and non-cumulative) during the encoding and recall phase were used as indicators of motor activity and anxiety.

4.5 Surgery

Electrophysiological signals were acquired using tetrodes, groups of four twisted 17 μm polyimide-coated ni-chrome wires (AM Systems; WA, USA). The final impedance of each wire was adjusted to $\sim$ 1 MOhm measured in gold solution at 1 kHz with an impedance tester (model Omega-tip-Z, WPI; MA, USA). Microdrives were composed of two bundles of four stainless-steel cannula each (27 G; Components Supply Co, FL, USA). One tetrode was inserted in the bundle targeting the Medial parietal association cortex (MPtA), two tetrodes targeting the hippocampus, and one tetrode targeting the thalamus. Each tetrode was cemented to a single movable shuttle fixed with a screw to allow independent depth regulation (one twist of the screw: $\sim$ 300 μm). Tetrodes were connected to a 16 channels-printed circuit board assembled to an Omnetics connector.

The rats (at P20, n = 4) were initially anesthetized with isoflurane (4 % isoflurane with 100 % O2) before being placed in a stereotaxic frame, a previous injection of lidocaine hydrochloride (2 %) was performed at the base of the ear. During the surgery, anesthesia was maintained using isoflurane (1–2 % isoflurane with 100 % O2). The temperature was kept at 37°C throughout the procedure using a heating pad [88]. After incision in the scalp, two burr holes were drilled in the right hemisphere at stereotaxic coordinates targeting parietal cortex (MPtA)

(-3.5 mm AP, 2.6 mm ML, 1.5 mm DV from Bregma), region CA1 of the hippocampus (-3.5 mm AP, 2.6 mm ML, and 2.5 mm DV from Bregma), and posterior nucleus of the thalamus (-3.5 mm anterior, 2.6 mm ML, and 5 mm DV from Bregma). The calculations of the stereotaxic coordinates were adjusted to the proportional size of the developing skull for that postnatal stage, which approximated 90 %. The dura was removed, and the electrodes were lowered to the cortical surface. Two ground wires were attached to skull screws, and the microdrive was fixed to the skull with dental acrylic. The recording electrodes were progressively lowered until they reached their targets and adjusted every day until P26 to optimize yield and stability.

After surgery, animals were maintained in individual cages in a room with temperature (22°C) and humidity controlled with food and water ad libitum. Rats were allowed to recover for three days after surgery before beginning the 2-days habituation protocol and then the behavioral experiments. During recovery, weight and general health were monitored daily, and animals received an intraperitoneal dose of analgesic (Ketoprofen, 5 mg/kg/day) and antibiotic (Enrofloxacin, 10 mg/kg/day). Microdrives allowed stable recording for up to three months.

4.6 Recordings

On day P26, rats started the OPR protocol (n = 4), the microdrives were connected to a headstage (model RHD 16-Ch Intan Tech, CA, USA). Neural signals were amplified (200-fold), digitized (sampled at 20 kHz) filtered at 0.5-500 Hz, and monitored through an amplifier board (RHD2000 evaluation system; Intan Tech, CA, USA). All analyses were conducted offline. LFP was downsampled at 1000 Hz. Tetrodes were individually lowered to target regions for several days until detection of single units in the cortex ($\sim$ 1000-1500 μm depth) and detection of sharp-waves ripples in hippocampal CA1($\sim$ 2500 μm depth) was evident. The tetrode leading to

the thalamus was lowered as calculated by the rat brain atlas ($\sim$ 5000 μm depth) [89]. Once the tetrodes had reached their desired locations, behavioral experiments were initiated.

4.7 Sleep classification

Each LFP channel was segmented into nonoverlapping 5 s windows during the episodes where the animal was immobile. The power spectral density was computed and averaged over each window over the cortical delta/SO (0.5–4 Hz) and hippocampal theta (4–8 Hz) frequency bands. Then a K-means classifier was used to cluster epochs into two clusters, NREM sleep and REM/awake [82, 90]. Only long ($>$ 30 s, 5 consecutive windows) epochs of sleep were analyzed. The classified windows were further confirmed by visual inspection.

4.8 Data analyses

4.8.1 Event Detection

SO detection. Cortical LFP signals during NREM sleep epochs of each animal were filtered between 0.5 and 4 Hz. A slow oscillation event was identified if the following criteria were met (adapted from [91, 92]): (i) two consecutive negative-to-positive crossings of the signal occurred within 0.2 to 1 s; (ii) of these events in an individual rat, the peak to trough amplitude of each event was higher than mean 3 SD and lower than 6 SD.(iii) of these events, the trough amplitude was higher than 1.5 SD and lower than 4 SD of the mean above the full average signal.

Spindle detection. Cortical LFP signals were band-pass filtered between 9 and 17 Hz. A smoothed envelope was calculated by computing the magnitude of

the Hilbert transform of this signal and then convolving it with a Gaussian kernel ($\alpha = 2.0$). Next, we determined two thresholds for Spindle detection based on the mean and SD of the SPs band envelope during NREM sleep (lower: 1 SD; upper: 2 SD). Events in which the envelope exceeded the upper threshold for at least one sample, and the power exceeded the lower threshold for at least 500 ms were considered Spindles. Finally, Spindles that were sufficiently close in time (300 ms) were combined, similar to other previous reports [82, 90].

SWRs detection. For SWRs detection, the normalized LFP signal recorded in the dorsal CA1 region of the hippocampus was band-pass filtered between 150-250 Hz. The squared magnitude of its Hilbert transform was calculated to improve the detection of small amplitude SWR according to Maingret et al (2016). SWRs were defined as events when its amplitude was at least 2SD above the mean power envelope of the signal, and the peak of the SWR signal was higher than 5SD, lasting from 30 to 100 ms [82].

4.8.2 Events coupling analyses

SO-Spindle To detect SO-Spindle coupling events, the down-state of the SO and the beginning of the Spindle were taken to generate the histogram of coupled event, using a time window of -500 to +500 ms time lag from the SO down-state (max. lag). The coupled events in the days for each rat were analyzed as the total events (pool) throughout the development (P26-P42). The events that exceeded values of the average of 1000 permutations of the time stamps of the SPs start and SO valleys (MonteCarlo analysis) were considered as significant. The slow oscillations LFP grand average was generated by averaging all the SO events in all the NREM epoch for each postnatal day, all events were centered on the valley of the events.

SO-SWRs From the cortical and hippocampal events recorded, SO and SWRs troughs were taken to generate the histogram of coupled events. Taking -500 and 500 ms of the SO descending state (maximum lag). Coupled events throughout the days were quantified for each rat and the total number of events throughout the development (P26-P42). Events that exceeded the mean values of 1000 permutations of the timestamps of the SO and SWRs troughs (MonteCarlo analysis) were considered significant. SO grand average was generated by averaging all the data across each day, and centered on the valley of the events.

Spindle-SWRs From the cortical and hippocampal events recorded, the peak of the SPs and the SWRs trough were taken to generate the histogram of coupled events. Taking -500 and 500 ms of the SWRs descending state (maximum lag). Coupled events throughout the days were quantified for each rat and the total events throughout the development (P26-P42). Events that exceeded the mean values of 1000 permutations of the timestamps of the SWRs valleys and SPs peaks (MonteCarlo analysis) were considered significant. Spindle grand average was generated by averaging all the data across each day, and centered on the peak of the events.

4.8.3 Time-frequency Decomposition

Time-frequency analysis of the LFP was performed using the multitaper frequency transform for the frequency range of the SPs and SWRs (9-17 Hz and 100-250 Hz) from a cortical or hippocampal channel depending on the events to be evaluated. SO and SPs (cortical channel) and SWRs (hippocampal channel).

The complementary analysis for the time-frequency analysis took -1 to 1 second (max lag) of the falling state of each SO and determined a baseline period for each window in which there was no SO ranging from -4.5 to -2 and normalized

each window with respect to the baseline. The overall mean SO was plotted as a visual reference guide aligned at 0 in the down-state.

Statistical comparisons were performed through a non-parametric permutation test (MonteCarlo, n = 1000) using a cluster alpha of 0.02 and with a significance mask of $p<0.01$.

4.9 Histology

After completing the experiments, electrolytic lessions were conducted to determining the location of each tetrode, the mark was created by passing a small amount of current through each tetrode (50 μA for 10 s) in anesthetized rats (2 % isofluorane). On the next day, rats were anesthetized with isofluorane (4 %), and then transcardially perfused with saline solution (0.9 %, wt/vol) followed by 400 ml of 4 % paraformaldehyde in phosphate buffer saline (PBS, pH = 7.4). The brain was removed, postfixed overnight in 4 % paraformaldehyde in PBS, and then stored in PBS containing 0.2 % Sodium azide. In ice-cold PBS, the brains were cutted in the coronal plane at 80 μm, with a vibratome (World Precision Instruments, Sarasota, USA) in ice-cold PBS. For visualization of the electrolytic lesions, slices were stained with Nissl-staining, and images were acquired with a microscope (Nikon, Eclipse 2000).

4.10 Statistical analysis

All statistical analyses were performed using SigmaPlot (Systat Software Inc.) and custom scripts from MATLAB (The Mathworks, Inc.). Behavioral analyses: for memory index measurements along postnatal days non-parametric Two-sided Wilcoxon signed-rank test was used to compare each postnatal day

group against chance level. Two-sided Wilcoxon rank-sum test was used to compare between groups (i.e., juvenile vs adults). For memory index at the final time (5 min.), normality was evaluated with Kolmogorov-Smirnov test, differences between postnatal days were assessed with One-way repeated ANOVA measures analysis, followed by post-hoc Multiple Comparisons versus Control Group (P26) Bonferroni t-test. For travelled distance and total object exploration the one-way repeated ANOVA test and Friedman test was used. All results are reported as mean $\pm$ SEM. A $p < 0.05$ was considered significant. For correlational analyses, we calculated linear regressions by Spearman rank correlations. Squared spearman correlation coefficients (rho), and p-values are reported for effect sizes.

We used cluster-based random permutation testing [95] to correct for multiple comparison (MonteCarlo method), cluster alpha 0.05, max size criterion, 1000 iterations, critical alpha level 0.005 two-sided) for time-frequency analyses. We clustered the data in the frequency and time domain.

V

5.0 Results

5.1 Behavior

5.1.1 The onset of hippocampus-dependent memory through development

Hippocampal-dependent spatial memory is one of the latest forms of memory to emerge postnatally [9]. We assess the emergence of this memory between postnatal days 26 (P26) and P32 by successively exposing a hippocampal-dependent object recognition task, the object in place (OPR).

Previous reports have shown that spatial episodic memory begin to emerge prematurely from P17, and with longer-retention times since P26, and fully consolidated at P38 [29-31]. We evaluated a group of juvenile rats that started the task at P26, and then successively performed the task on days P28, P30 and P32, with a retention time of 3 h. Another group of adult rats (P90) was used as reference to compare the juvenile performance. We found that hippocampus-dependent memory appears on P32, reaching adult memory index (Fig. 7a).

Rodents from P26 to P30 showed no preference between objects in the recall phase (p = 0 .0830 or higher, Two-sided Wilcoxon signed-rank test, non-significant respect to chance, red asterisk, $*$); however showed significant differences against adults memory indexes indexes (p = 0.0431 or lower, Two-sided Wilcoxon rank sum test , significant between groups, blue triangles, $\triangle$). Notably, by the fourth consecutive day of exposure to the task at P32, rats were able to successfully distinguish the displaced object from the familiar (p = 0.042 or lower, Two-sided Wilcoxon signed-rank test, significant respect to chance, red asterisk, $*$), after the 3 h retention period, reaching adult-like discrimination index during almost the entire exposure to the task. These results suggest that only rats at P32 could consolidate episodic-like memories, and even more as adults.

As an representative example, we illustrated the trajectory on each P-day (Fig.7b), suggesting that the successful discrimination on P32 (Fig. 7a) was not due to differences on the trajectory.

5.1.2 Object-in-place recognition memory emerges gradually up to P32

Since we present the memory index throughout the entire time course of the OPR task, it was essential to determine whether the whole memory index at the final time (5 min) was still significant at the end of the task. Previous publications typically show these results by computing the memory index after the rodent completes the object recognition task (Equation 1).

Accordingly, we included the cumulative discrimination index at the end of the task (5 min) for each postnatal day. From day P26-P30, rats showed no preference for any object, with a discrimination index close to 0 in the recall phase (Fig. 8). However, the discrimination index gets positive values (close to 1) at P32

(p = 0.043, One-way repeated ANOVA, F(12; 3.057) followed by Multiple Comparisons versus Control Group Bonferroni t-test, p = 0.038, black asterix, $*$) (Fig. 8), indicating that only rats at P32 were able to discriminate the displaced object in the OPR task.

A linear regression analysis was performed between the values at the final time (5 min) of the OPR days (P26, P28, P30, and P32) to determine whether the rats improved their memory capacities over the days. Observing that there is a positive correlation between those variables (Linear regression, $r^2 = 0.170$; p = 0.004) (Fig. 8). These results suggest that although this capacity appears at P32, it would gradually develop during this time window until reaches the performance observed in adult rats.

5.1.3 Postnatal memory onset is independent of early overtraining.

Even though the previous results suggest that this kind of memory may emerge by P32 as a consequence of natural brain development at that postnatal stage, this positive discrimination index at P32 may be explained by overtraining in the OPR task. Therefore, to prevent any overtraining process, we decided to include another experimental group, which did not have previous experience in the OPR task (P32 NoRep group). This group of P32 NoRep rats (n = 11) followed the same previous protocol, habituation, and task. However, assessments at P26, P28, and P30 were excluded, and the task was only assessed at P32.

Interestingly, the P32 NoRep group showed a positive memory index respect to chance (p = 0.0186 or lower, Two-sided Wilcoxon signed-rank test, significant respect to chance, red triangles, $\triangle$). When compared with the previous P32 group, which also showed a positive discrimination index (p = 0.042 or lower,

Two-sided Wilcoxon signed-rank test, significant respect to chance, red asterisk, $*$) (Fig. 7a), there was no difference between the two groups (p = 0.057 or higher, Two-sided Wilcoxon rank sum test , non-significant between groups, blue triangles, $\triangle$) (Fig. 9a). These results discard the possibility that early overtraining of the OPR task could anticipate the onset of spatial memory capacities during development. This experiment was crucial to elucidate our hypothesis and verified that hippocampal-dependent recognition memory emerged specifically at postnatal day 32, independent of early task experience.

To further investigate whether these effects were not due to another developmental change (i.e., motor or preference), we quantified the total distance traveled (Fig. 9b), which showed no difference across days (p = 0.08, one-way repeated ANOVA F(12; 2,479), non-significant between P -days). Whole object exploration time (Fig. 9c) also was invariant across days (p = 0.609, Friedman test, F (12; 0,617), non-significant between P-days), suggesting that the onset of memory at P32 was not due to either of these factors.

Further, to verify whether these results were aligned with previous results observed in P32 with overtraining, we added the P32 Norep memory index at 5 minutes. We combined these results with the previous ones to the linear regression, observing that the correlation was maintained. Showing a positive relationship throughout the developmental window between P26 and P32 (r^2 = 0,154; p = 0,003) (Supplementary Fig.1).

5.2 Electrophysiology

5.2.1 Sleep oscillation detection.

Because sleep oscillations play a fundamental role in consolidating hippocampal-dependent memories [71-73], we evaluated the profile of slow oscillations, Spindles, and sharp-wave ripples along with the postnatal developmental window.

We successfully recorded extracellular LFP (n = 4) from the cortex (MPtA: medial parietal association area), and the dorsal hippocampus (CA1). However, tetrodes targeting the thalamus (posterior nucleus) did not reach their destination, as we could advise those electrodes reach more ventral areas of the hippocampus (DG and CA3) (Fig. 10a-b). However, thalamic spindles can also be detected in the cortex due to the corticothalamic networks [56]. Then we detected slow oscillations and spindles from cortical recordings and SWRS from hippocampal recordings [82, 90]. The electrical activity was recorded during the retention phase, where animals were left for three hours to prompt sleep.

Slow oscillations, SPs, and SWRs are characteristic events of the NREM sleep stage [38, 53, 62]. Therefore, it was essential to distinguish this sleep stage from REM or wakefulness. As described before [90], we successfully identified NREM episodes (Fig. 10 c-d) by determining theta/delta power ratio. We identified SPs and SOs events (Fig. 11) during NREM sleep using standard algorithms adapted for semiautomatic detection [90]. Briefly, we selected a representative LFP channel from the cortical region. Then, the signal was filtered in the low-frequency band (0.5-4 Hz) for SO detection and between 9-17 Hz for the spindle band. All positive-to-negative zero crossings in the 0.5-4 Hz frequency band were identified as SO, along with the preceding peaks and following valleys.

When the oscillation peak and trough met the established thresholds, and the time between peak and trough was between 200 and 1000 ms, it was considered SO. To minimize false positives, we focused on large amplitude SO. For SPs detections, periods in which the Spindle power exceeded the upper threshold (2 SD) and the lower threshold (1 SD) during 500 ms until 2000 ms were identified as Spindles (Supplementary Figure 2).

On the other hand, to quantify SWRs, the most synchronous oscillatory events in the hippocampus [86], we performed event detection using a representative hippocampal LFP channel and filtered in the frequency range of 100-250 Hz. In addition, each event had to comply with the established thresholds of duration (30-100ms) and amplitude (2 SD lower and 5 SD higher). As a result, these events were effectively detected and characterized, as shown in Fig. 11 and Supplementary Fig. 3.

5.2.2 The density of slow oscillations correlates positively with development between P26-P42.

The electrophysiology results were separated into two categories from the behavioral performance obtained: 1) Animals that discriminated the task n = 3, i.e., animals with a positive memory index on day P32. 2) All animals, i.e., all animals, independently of their memory index day P32 (n = 4) to analyze the profile of LFP oscillations along developmental.

First, as sleep in juvenile rats is highly variable and fragmented [36, 37], we wanted to determine whether the amount of NREM sleep would be a critical factor in determining our results. As seen in Figure 12 there was no correlation between the amount of NREM sleep and the memory index in both categories (Linear regression, All: r^2 = 0,00745; p = 0,779. Discriminate: r^2 = 0,0991; p = 0,376)

(Fig.12).

A straightforward step to elucidate our hypothesis is to determine any change in the electrophysiological parameters of NREM-oscillations between P26-P32. Therefore, we quantified the power, frequency, duration, and density of SO and Spindles until several days after the consolidation of memory (P42).

Regarding the density of slow oscillations (0.5-4 Hz), a positive linear relationship was observed between the number of SO-events per min during NREM sleep, and the developmental days contained in the P26-P42 window (Linear regression, r^2= 0.166; p = 0.023, "all" n = 4) (Fig. 13). In contrast, this result was not observed for animals who discriminated the task (Linear regression, r^2 = 0.083; p = 0.184), suggesting that this increase in SO-density could be a developmental change that occur independently of the successful discrimination at the behavioral task, or additional animals could be needed to more conclusive results.

We cannot observe any changes in the SO power, frequency, and duration throughout postnatal development (Supplementary Fig. 4) that would explain the observed behavioral results for both the "all" and "discriminate" categories (Table 1).

For cortical Spindles, no changes were observed at any parameter, and also no correlation with development days was observed for both groups of animals, independently their discriminated or not the task (Table 1) (Supplementary Fig. 5).

5.2.3 SWRs density and frequency decreases over the days of development.

To establish a possible role between hippocampal SWRs and memory consolidation [68]. We evaluated several parameters of these oscillatory events (power, frequency, duration, and density) during NREM sleep windows.

Notably, when quantifying the density of these events, we found a decrease in the density as a function of developmental days in the P26-P42 window in both categories (Linear regression, "all" r^2 = 0,176; p = 0,015 and "discriminate" r^2 = 0,284; p = 0,007). Because the effect is observed in both cases, we can suggest that this could be explained by: 1) a decrease independently of the behavioral task or 2) a clearer decrease associated with memory.

Additionally, we observed a decrease in the frequency of the SWRs oscillating in the range 195-235 Hz. For the animals that discriminated the task (Linear regression, r^2 = 0,204; p = 0,027), through linear regression analysis, it was determined that this decrease was related to the advancement in the postnatal days between P26-P42.

Regarding the other parameters of the SWRs, such as the power and duration no relationship was observed concerning development (Table 1, Supplementary Fig. 6).

5.2.4 Spindles duration and density correlate with better performance in the Object-in-place task.

Since some oscillatory parameters did not follow a linear relationship concerning developmental days. We wanted to know if, during the days when the hippocampus-dependent OPR task was conducted, some of these parameters could

get correlated. We could observe that for those animals with better performance coincides with longer spindles events (Linear regression, r^2 = 0,465; p = 0,030) and, with higher spindle densities (Linear regression, r^2 = 0,625; p = 0,007) (Fig. 15). Linear regressions were performed for all the spindle parameters against the memory index (Table 2). However, no other relation was found.

5.2.5 Decreased SWRs density correlate with better performance in the Object-in-place task.

The previous results show a decrease in the density of SWRs during development days (Fig. 14 a-b). Then we determine whether this decrease correlated to better or worse performance during the OPR task by analyzing the recordings of the four implanted rats. SWRs density values were obtained from the NREM sleep at the memory consolidation stage. These values were correlated with the corresponding pairs of memory index in the test stage of the OPR task. Interestingly, we observed that only for rats that discriminated the task at P32, the decrease in SWR density was related to a better memory index (Linear regression, r^2 = 0,406; p = 0,047) (Fig. 16). In contrast, when these results were analyzed for all rats, we could not observe the same effect (Linear regression, r^2 = 0,230; p = 0,097) (Table 2).

Therefore, despite the small experimental number, we hypothesize that a lower density of high-frequency hippocampal events may play a preponderant role in the consolidation of hippocampal-dependent memories. Linear regressions were performed for all the other SWRs parameters against the memory index (Table 2), and no other relationship was found.

5.2.6 SO-Spindle temporal coupling strengthens during development

Fundamental analysis to test the active model of memory consolidation [75, 76] in our hypothesis was to implement cross-correlation analysis between these three oscillatory events of NREM sleep. As previously reported, the alignment between spindles with the ascending phase of the SO may improve consolidation of hippocampus-dependent memories [79]. Therefore, we decided to quantify this parameter.

We select the Spindle events contained within +/- 500 ms from the down-state of the SO for all animals (n = 4) and all the NREM epochs. We observed a temporal coupling between these two events (SO-Spindles), where mostly all SO events nested spindles in their up-phase (Fig. 17 a), suggesting that SO would be commanding and containing the spindles in their ascending phase [79, 93].

In addition, we calculated the density of the coupled events during the course of the development (P26-P42). These correlations were corrected by MonteCarlo analysis, revealing that there was a significant difference between these distributions. Notably, we observed that the average number of coupled events per day has a positive linear relationship regarding the postnatal days (Linear regression, r^2 = 0,586; p = 0,0099) (Fig. 17 b), suggesting that SO-SPs coupling is strengthened during this stage of development. We did not observe a correlation with animals who discriminate the task (Fig. 17 c), reinforcing the idea that this effect would be a general effect of development.

Additionally, we analyzed SWRs events coupled to SO using the down-state of SO as 0 lag. We found no relationship between the temporal coupling of SO-

SWRs and the days of development for both categories (Linear regression, All:r^2 = 0,000378; p = 0,957; Discriminate: r^2 = 0,0154; p = 0,733) (Supplementary Fig. 7 a,b). These findings could indicate that although SWRs are driven by SO events [80], it would not be the temporal coupling between these events related to memory consolidation. One possibility could be that the SO-SWRs coupled events remain stable, being the SO-SPs tunning the most relevant event during this stage, or by the other hand, that the coupled events present are enough to account for memory consolidation besides SWRs event diminish along development.

5.2.7 Spindle-SWRs coupling decrease during development

The disruption of cortical Spindles and sharp-wave ripple coupling is critical for spatial memory [81]. We investigated the temporal coupling between those two events during the developmental window from P26 to P42. For this purpose, we count the SWRs events between +/- 500 ms around the peak of the Spindle (Fig. 18 a). The average of coupled events showed a decrease throughout the postnatal days for both categories (Linear regression, All: r^2 = 0,552; p = 0,014, n = 4; Discriminate: r^2 = 0,562; p = 0,02) (Fig. 18 b-c), suggesting that this correlation may be related to memory.

As the density of SWRs (Fig. 14 a-b) and Spindle-SWRs coupling (Fig. 18 a-b) is decreasing during this stage, unlike SO-SWRs coupling which remains stable, these results would suggest that the SWRs events would be the last to synchronize to SO-Spindle events, possibly being the capstone in memory consolidation during this stage.

A linear regression analysis was used to determine whether or not there was a relation between the SPs-SWRs temporal coupling and the performance in the hippocampus-dependent OPR task. However, it was impossible to observe any

relation between them (Supplementary Fig. 8) (Table 3). Thus, further studies are required to determine a better relationship between these two oscillatory events.

5.2.8 Spindles power increase at P32.

As the temporal coupling by itself, it was not correlated with the consolidation of memory. Therefore, it was necessary to analyze these events in more detail; for this purpose, spectrograms were made to visualize both temporal and spectral dimensions. We time-locked SPs and SWRs frequency bands to SO events during NREM windows within +/- 1 s of the SO down-state for all the OPR days (P26, P28, P30 and P32), and to observe possible changes in the days between tasks and after memory consolidation we considered from P26 until P42.

First, to see Spindles (9-17 Hz), we took the frequency range between 5-20 Hz. Then, to query the power of the spectrogram, we applied a spectrogram mask to highlight significant changes in the cluster power. We did not observe power modulations previous P32. Interestingly, we found a cluster power increase at 9-14 Hz on P32 ($p = 0{,}01$ or lower) (Fig. 19), specifically located at the up-state of the SO. These results suggest that the memory consolidation occurring at P32 could be related to a SPs time-locked power increase with SO.

Additionally, when looking at the entire time-window spectrograms between P26-P42, we found other significant spindle-range clusters at the rising portion of the SO at P27, P35, and P39 (Supplementary Fig. 10). However, the frequency range at P27 is higher than expected for spindle events, possibly indicating we are observing another oscillation. On the other hand, spectrograms at P35 and P39 are more or less in the desired Spindle frequency range, suggesting that this power modulation is maintained after the first week from the memory onset.

The same analysis was performed to evaluate SO-coupled SWRs events. For constructing the spectrograms we took the frequency range between 100 and 300 Hz. We found a cluster power increase only by P27 ($p < 0{,}01$), at the ascending

portion of the SO (Supplementary Fig. 9). From these results, we cannot conclude that memory consolidation was due to a SWRs-SO power modulation; however, we cannot exclude that the consolidation mechanism depends on other parameters of the coupled SWRs.

VI

Figures: Behavior

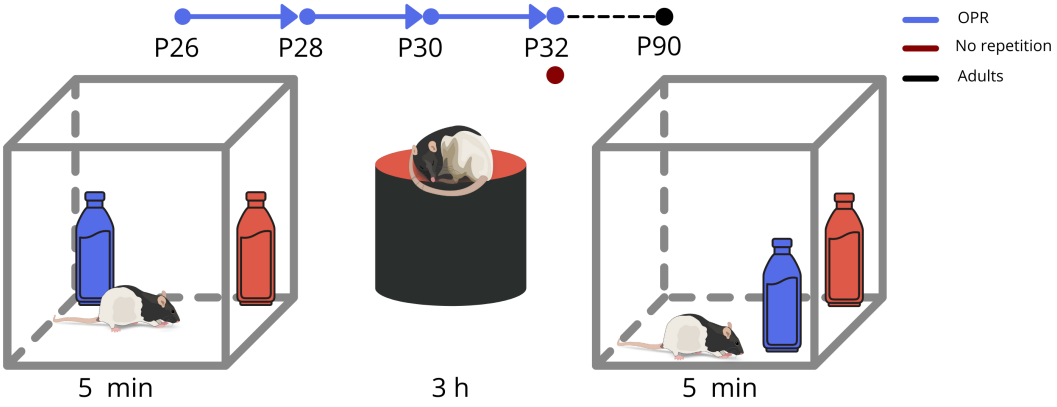

Figure 6: Experimental design. Three groups of rats were tested in an Object-in-Place Recognition (OPR) task on different postnatal days (P) representing different developmental stages. Group 1 (OPR test): P26, P28, P30 and P32; Group 2 (no repetition): P32 without previous exposures (P32 NoRep), and Group 3 (adult rats): P90 rats. For group 1 the task was performed intercalary days; otherwise, the rats were at their homecages. No repetition group performed the task only on day P32 without previous exposures but complying with the corresponding habituation and handling protocols. Adults performed the task at P90, and their memory index was used to reference adult-like memory performance for the other groups. The rats explored an arena with two identical objects for 5 minutes during the encoding phase, and again during the recall phase, a 3 hour retention interval was considered between both stages in a sleep-facilitating environment. In the recall phase, one of the objects was moved to a new location, while the other remained in the same familiar location as during the encoding phase. Each rat was placed in the arena facing and close to one of the walls. Different rat starting positions were used during the encoding and recall phases. Finally, the rat was placed in a pot covered with a soft cloth to prompt sleep (3h). *Rat figures were obtained from the GitHub repository [94] and used for making the scheme.*

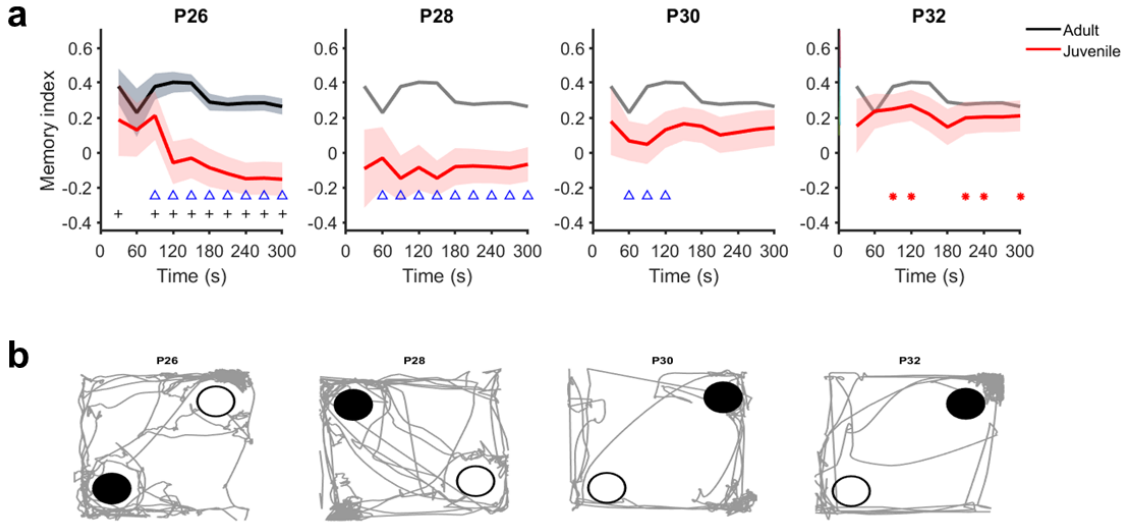

Figure 7: Object-in-place performance throughout postnatal development. (a) Object memory index (mean ±SEM) during the recall phase for each postnatal day (P26, P28, P30, P32, and P90). Positive memory index indicates preferential exploration of the object in a novel location; negative memory index indicates preferential exploration of an object in a familiar location. The memory index of the recall phase is shown for the entire duration of the task (30-second intervals for 5 min); for adults (P90), the same line was shown on the other following P-days as a reference (shown in gray). The memory index of juvenile rats was shown in red for each P-day (P26-P32). Black sign (+) represents the Two-sided Wilcoxon signed-rank test for adult memory index versus chance level (i.e., zero ($p = 0.034$ or lower). Asterisk in red ($*$) show juvenile memory index versus chance level (Two-sided Wilcoxon signed-rank test at different P-day, p = 0, 0420 or lower for P32). Blue triangle ($\triangle$) comparison between adults and juveniles at each P-day. (Two-sided Wilcoxon rank-sum test, p = 0.000828 or lower for P26, p = 0.0201 or lower for P28, and p = 0.0431 or lower for P30). P32 showed a significant preference for the object in the novel location, reaching a memory index similar to that of the adult group used as a reference, while the P26-P30 groups showed no preference between objects in comparison to displaced preference observed in the adult group. P26 and P28 n=12, P30 and P32 n=11. (b) Representative examples of individual trajectories in the open field each day (P26, P28, P30, and P32). The white circle represents the familiar object, which remains in the same position during the sample and test phase of the OPR, and the black circle shows the displaced object. This example comes from the same animal AG07 rat.

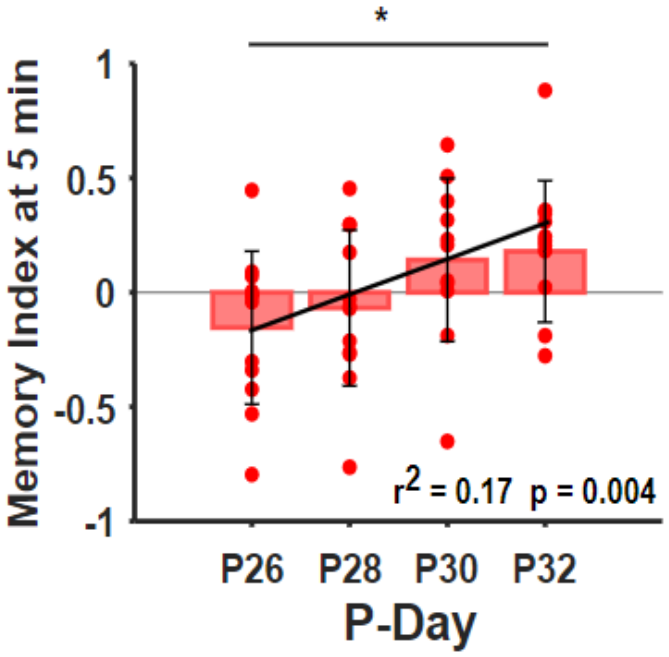

Figure 8: Memory index at 5 minutes. The cumulative memory index (Mean ±SEM) at final time (5 min) for each postnatal day (P26, P28, P30, and P32). Memory index becomes positive at P32. One-way repeated ANOVA measures analysis was performed, and Multiple Comparisons versus Control Group (P26) Bonferroni t-test, the asterisk in black, $*$, p = 0.043. P26 and P28 n = 12, P30 and P32 n = 11. Linear regression analysis was performed between the values of the OPR final time (5 min) values against P-days. A positive correlation between these variables was found (r^2 = 0,170; p = 0,004). P26 and P28 n = 12, P30 and P32 n = 11.

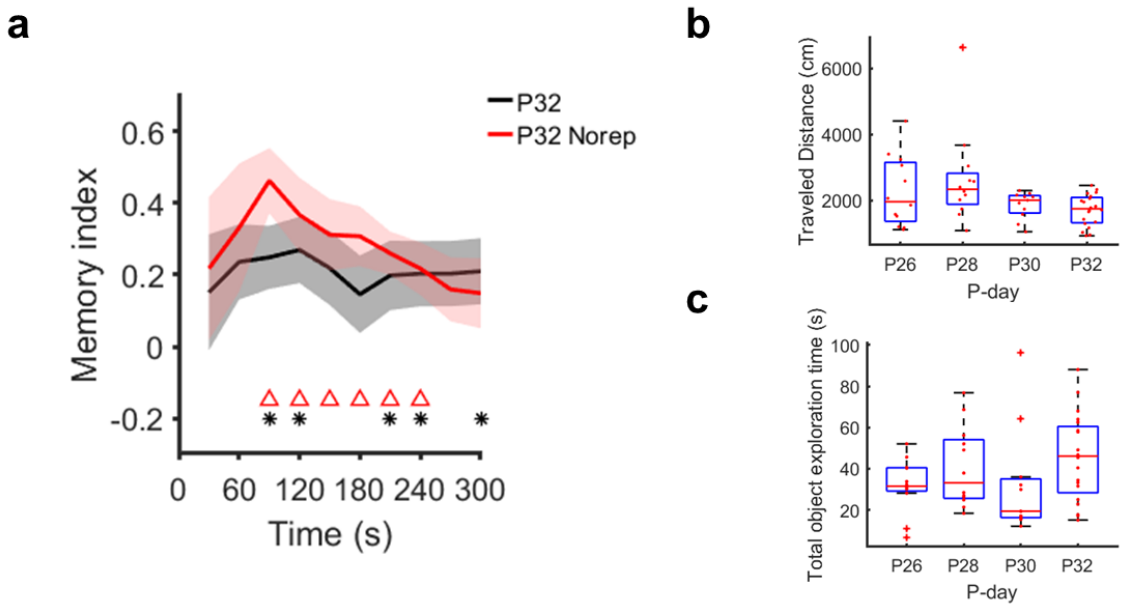

Figure 9: Memory index: overtraining vs. single exposure. (a) Memory index (mean ± SEM) for animals exposed to previous repetitions of the task at P32 (P32, black line), and animals who performed the task without previous exposure (P32 NoRep, red line). The positive memory index indicates preferential exploration for the displaced object; the negative memory index indicates the familiar object preferential exploration. The entire task-duration memory indexes were shown (each 30 seconds), for P32 rep (n = 11), and no repetition group at P32, (n = 11, P32 NoRep). Aterisk in black, $*$, p = 0.0420 or lower, two-sided Wilcoxon signed-rank test for P32 rep memory index against chance level, i.e. zero. Red triangle ($\triangle$), p = 0.0186 or lower, two-sided Wilcoxon signed-rank test for P32Norep memory index against chance level, i.e. zero. P32 and P32 NoRep showed no significant difference between them, p = 0.057 or higher, two-sided Wilcoxon rank-sum between both groups. (b) Traveled distance, median (± SEM) during the 5 min encoding phase for the different P-days, p = 0.08, One Way Repeated Measures Analysis of Variance F(12; 2,479), non-significant between P-days. (c) Total object exploration time, median (± SEM) for total object exploration time, p = 0.609, Friedman test, F(12; 0,617), non-significant between P-days. On each box, the central mark indicates the median, and the bottom and top edges of the box indicate the 25th and 75th percentiles, respectively. Outliers are plotted individually using the (+) symbol. For P26 and P28 n = 12, P30 n = 11, and for P32 n = 11.

Figures: Electrophysiology

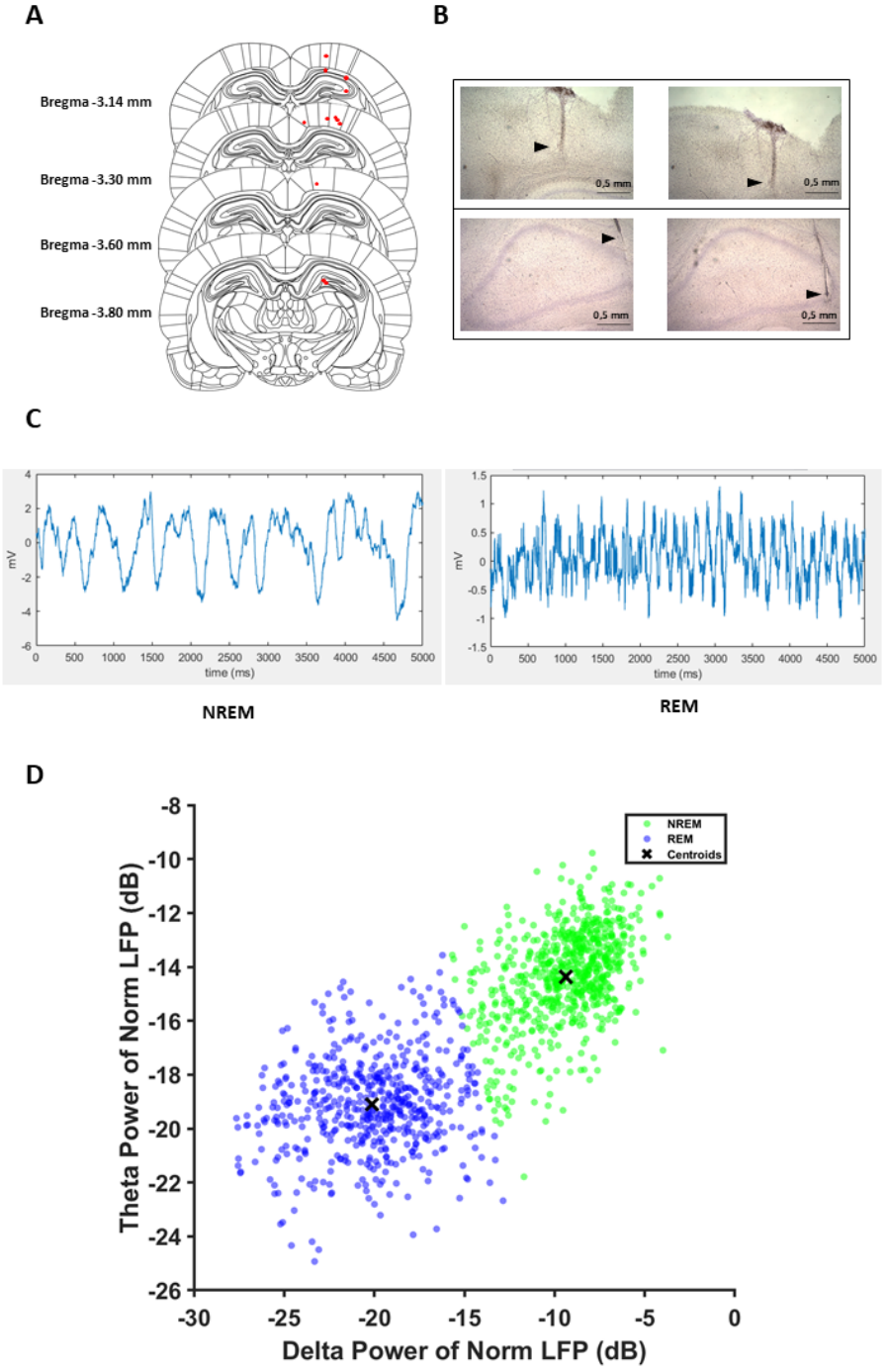

Figure 10: Sleep classification in both temporal domain and power spectral density (PSD). (Continue next page)

(a) Reconstruction of tip location of tetrodes targeting cortex, hippocampus, and thalamus (n = 4), at the coronal plane (Bregma -3.34 mm to -3.80 mm). *Adapted from GitHub repository: https://github.com/Ashu156/Rat-Brain-Atlas.git* (b) Nissl-stained brain sections of the rat brain as an example (Long Evans, cut sections 33 and 34, Bregma -3.34 mm to -3.80 mm, Scale bar: 500 μm). (c-d) Sleep classification in the time and power spectral density (PSD) domain. (c) At the left, LFP extract of slow oscillations characteristic of an NREM episode (5 s) and at the right an LFP, showing theta oscillations characteristic of a REM sleep episode (5 s). (d) Each point represents the PSD in the theta (4-8 Hz) and delta (0.5-4 Hz) frequency bands during 5 s windows. A k-means classifier was used to cluster the epochs into two groups: REM-wakefulness (blue) and NREM (green), according to [90]. Centroids are shown in both clusters (as a 'x' in black).

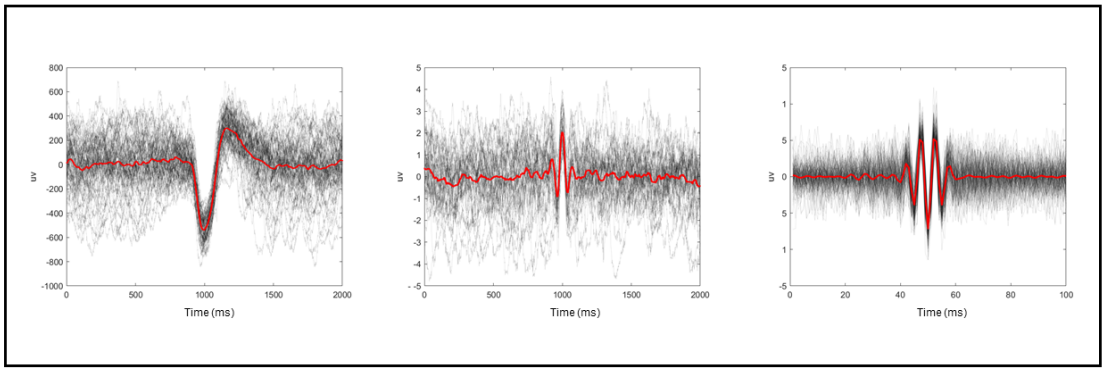

Figure 11: Grand average of sleep oscillations. Left, cortical slow oscillation (SO). Middle, cortical Spindle. Right, hippocampal sharp-wave ripple. The grand average was obtained as the mean events detected from each animal NREM sleep 5-sec windows every postnatal day. The figure shows the three sleep oscillations from the a representative animal.

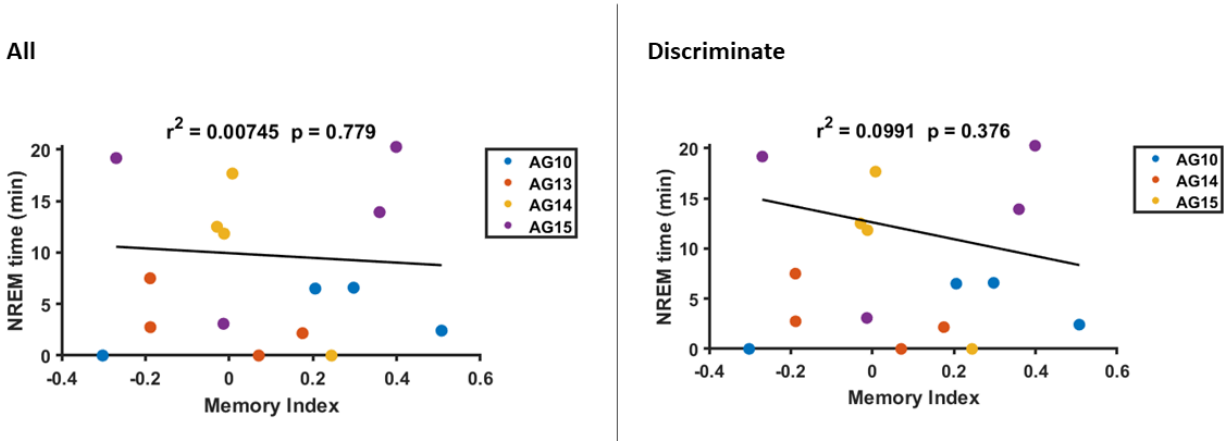

Figure 12: Correlation between time spent at NREM and memory performance. Left, NREM time (min) versus memory index for all animals (n = 4). No linear relationship was observed (Linear regression, r^2 = 0,00745; p = 0,779). On the right, animals that discriminated the task (n = 3), also no linear relationship was observed between these variables (Linear regression, r^2 = 0,0991; p = 0,376). These results show that rodent performance does not depend linearly on the amount of NREM sleep in both cases.

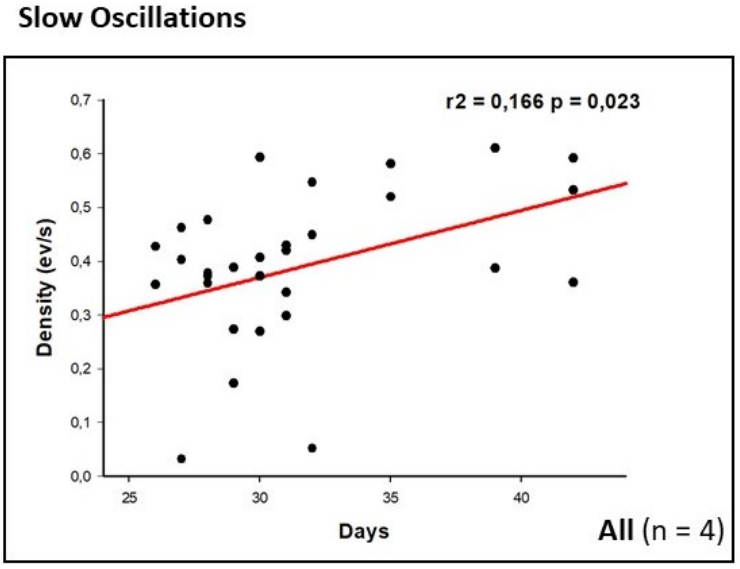

Figure 13: Slow oscillation density along postnatal days. SO density (events/min) was calculated during the periods of NREM in the retention phase (3 h). Linear regression between SO density and development days for all the implanted animals (black dots, n = 4). Days with missing dots are because the animal did not sleep (i.e., P26) at that time of recording or a rat damaged his registration implant (i.e., AG14 at P32). These results show a positive correlation between SO density and postnatal days. Linear regression was calculated for SO densities along the developmental days of recording (P26-P42). Linear regression, $r^2 = 0,166$ and p = 0,023.

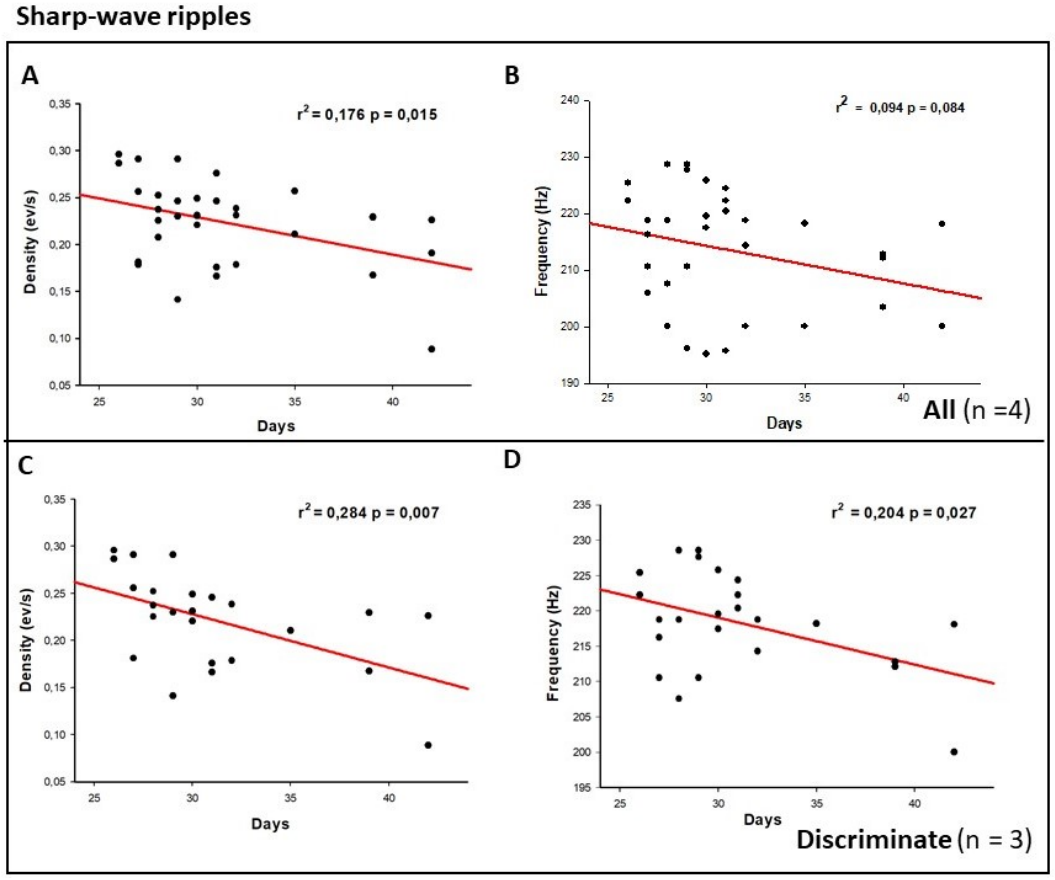

Figure 14: SWRs parameters that diminish throughout postnatal development during the NREM periods in the retention phase (3 h). All animals: (a) SWRs density (events/min), $r^2 = 0,176$ and p = 0,015, and (b) SWRs frequency (Hz) $r^2 = 0,094$ and p = 0,084. Discriminate animals: (c) SWRs density (events/min), $r^2 = 0,284$ and p = 0,007, and (b) SWRs frequency (Hz) $r^2 = 0,204$ and p = 0,027. Linear regression (red line) and individual SWRs density and frequency values per day for all the implanted animals (black dots, n = 4). Days of missing black dots occur because the animal did not sleep (i.e., P26) or a rat damaged his registration implant (i.e., AG14 at P32). These results show a negative correlation between SWRs density and postnatal days for both animal categories, conforming better to linearity for the animals that discriminated the task. SWRs frequency also show a negative correlation, but only for animals who discriminated the task.

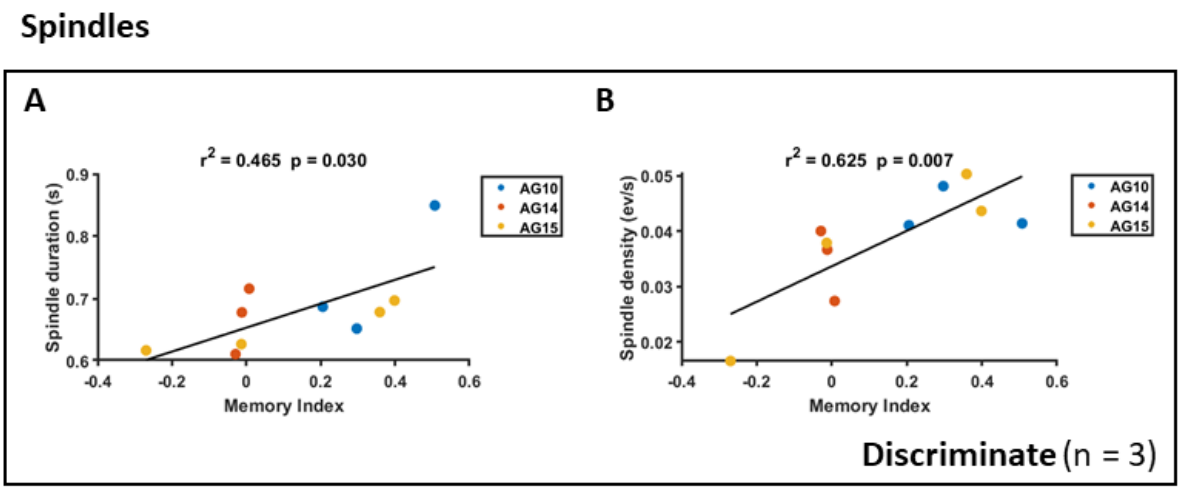

Figure 15: Spindle parameters and memory index. Linear regression was calculated for the spindle duration (s) and the memory index during OPR days. Spindle duration and density were determined during NREM periods in the retention phase. Every point for each animal was shown in different colors. Days with missing dots occur because the animal did not sleep (i.e., P26) or a rat damaged his registration implant (i.e., AG14 at P32). These results positively correlate the memory index with spindle duration and spindle density during P26 to P32. Linear regressions for spindle duration (discriminate) $r^2 = 0,465$ and p = 0,030. Spindle density (discriminate) $r^2 = 0,625$ and p = 0,007. All the other spindle parameters correlations did not show significance in neither animal categories, results are shown in Table 2.

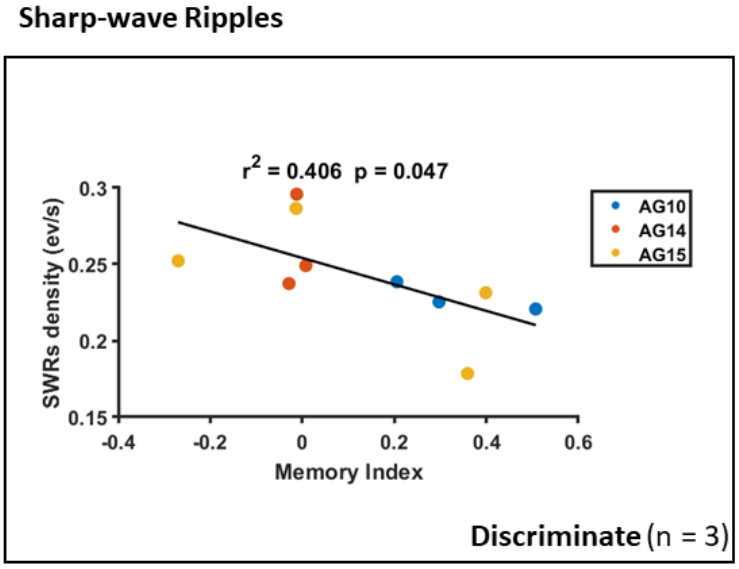

Figure 16: SWRs density and memory index. Linear regression was calculated for the SWRs density (events/min) and the memory index during OPR days. SWRs density was determined during the NREM periods. Each animal was shown in different dots colors. Days with missing dots occur because the animal did not sleep (i.e., P26) or a rat damaged his registration implant (i.e., AG14 at P32). These results show a negative correlation of the memory index and the SWR's density during P26 to P32 for animals who discriminated the task (n = 3). Linear regression, $r^2 = 0,406$ and p = 0,047. All the other SWRs parameters correlations did not show significance in neither animal categories, results are shown in Table 2.

/P-day	Power	Frequency	Duration	Density
S.O (All)	r^2 = 0,001 p = 0,865	r^2 = 0,038 p = 0,291	r^2 = 0,037 p = 0,303	**r^2 = 0,166 p = 0,023**
S.O (Discriminate)	r^2 = 0,028 p = 0,446	r^2 = 0,006 p = 0,735	r^2 = 0,003 p = 0,792	r^2 = 0,083 p = 0,184
Spindles (All)	r^2 = 0,112 p = 0,057	r^2 = 0,020 p = 0,430	r^2 = 0,009 p = 0,604	r^2 = 0,046 p = 0,232
Spindles (Discriminate)	r^2 = 0,135 p = 0,077	r^2 = 0,087 p = 0,161	r^2 = 0,027 p = 0,808	r^2 = 0,100 p = 0,131
SWRs (All)	r^2 = 0,005 p = 0,697	r^2 = 0,094 p = 0,084	r^2 = 0,012 p = 0,544	**r^2 = 0,176 p = 0,015**
SWRs (Discriminate)	r^2 = 0,087 p = 0,163	**r^2 = 0,200 p = 0,027**	r^2 = 0,001 p = 0,870	**r^2 = 0,284 p = 0,007**

Table 1: Oscillation parameters across postnatal days (P26-P42). Parameter correlation analyses were divided using all the animals (n = 4) or only those that discriminate the OPR task (n = 3). For each kind of oscillation, power, frequency, duration, and density were quantified. The r^2 and p value is detailed for each case. In red are shown the values that were significant (p < 0,05).

/ Memory Index	Power	Frequency	Duration	Density
S.O (All)	r^2 = 0,132 p = 0,204	r^2 = 0,011 p = 0,736	r^2 = 0,007 p = 0,779	r^2 = 0,007 p = 0,781
S.O (Discriminate)	r^2 = 0,013 p = 0,738	r^2 = 0,003 p = 0,884	r^2 = 0,005 p = 0,849	r^2 = 0,001 p = 0,929
Spindles (All)	r^2 = 0,150 p = 0,190	r^2 = 0,011 p = 0,733	r^2 = 0,166 p = 0,167	r^2 = 0,186 p = 0,141
Spindles (Discriminate)	r^2 = 0,295 p = 0,105	r^2 = 0,159 p = 0,254	**r^2 = 0,465 p = 0,030**	**r^2 = 0,625 p = 0,007**
SWRs (All)	r^2 = 0,148 p = 0,194	r^2 = 0,015 p = 0,664	r^2 = 0,039 p = 0,519	r^2 = 0,230 p = 0,097
SWRs (Discriminate)	r^2 = 0,116 p = 0,335	r^2 = 0,278 p = 0,117	r^2 = 0,056 p = 0,509	**r^2 = 0,406 p = 0,047**

Table 2: Oscillation-parameters correlation with behavioral performance along with the postnatal day (P26-P32). The correlation between oscillation parameter and behavior was divided into all (n = 4) and discriminate (n= 3), just as before. For each oscillation, power, frequency, duration, and density were quantified. The memory index was obtained from the test trials of the OPR task for each animal at 5 min. The r^2 and p value is detailed for each case. In red are shown the values that were significant ($p < 0{,}05$).

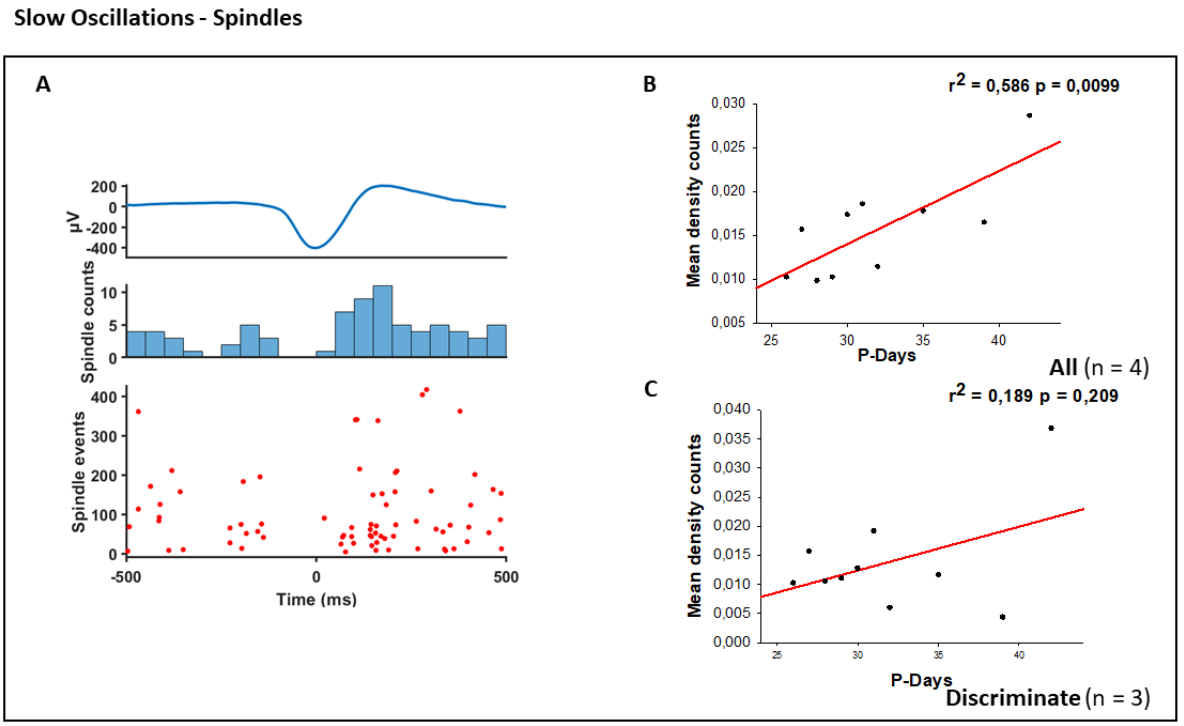

Figure 17: Increased SO-spindle temporal coupling over the course of development. (a) A representative example from one animal of SO-spindle coupling, on top, SO grand average waveform across postnatal days (blue line). The SO down-state was centred at 0. In the middle, a histogram showing the temporal coupling of cortical-Spindles related to the SO down-state with a time lag of 500 ms and with a MonteCarlo correction for chance. Below, a raster plot showing all the Spindle events related to the SO down-state around 0 lag. (b-c) Linear regression for the mean density count of SO-SPs coupled events(events/min) along with the postnatal days. Linear regressions showed a positive correlation of SO-Spindle coupling events and postnatal days (P26-P42) for all the animals (n = 4) $r^2 = 0,586$ and p = 0,0099. For the animals that discriminate the OPR task (n = 3) $r^2 = 0,189$ and p = 0,209.

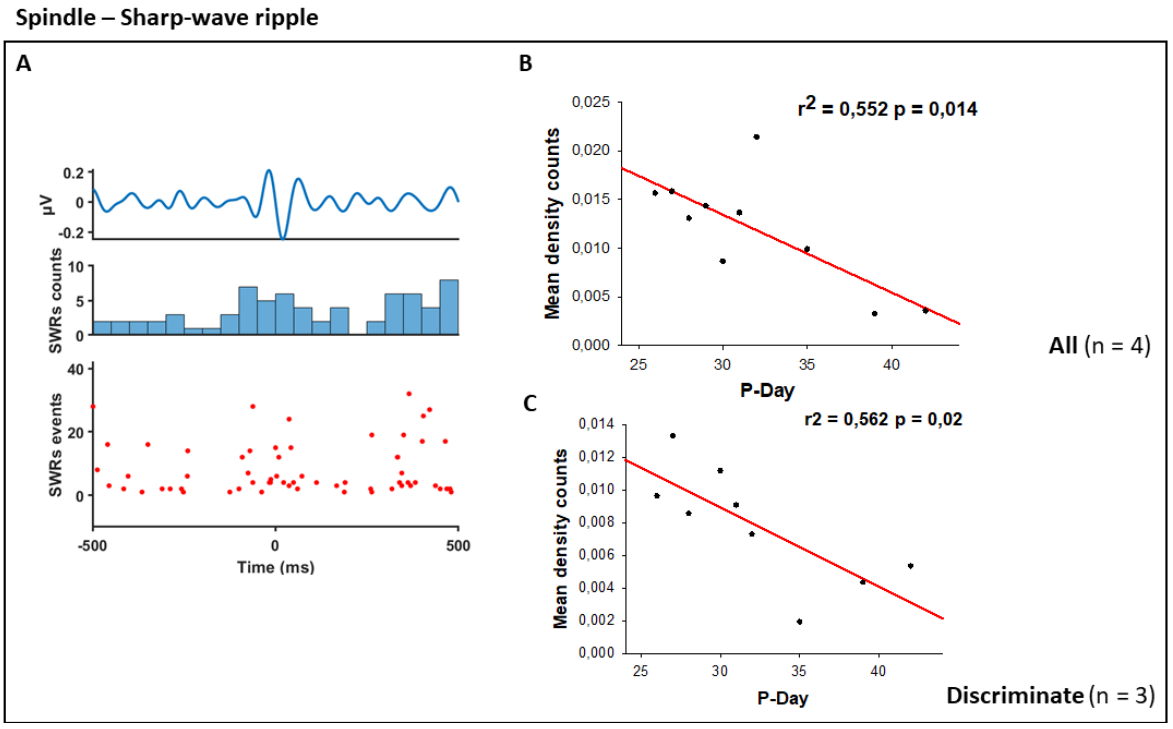

Figure 18: The Spindle-SWRs temporal coupling over the course of development is decreasing. (a) A representative example from one animal. On top of, Spindle grand average waveform (blue), the spindle peak was centered at 0 lag. The middle histogram shows the temporal coupling of hippocampal sharp-wave ripples related to the peak of Spindles during the lag time 500 ms. To discard chance, coupling results were corrected by MonteCarlo (n = 1000) analysis. Below, raster plot showing all the sharp-wave ripples events coupled to the Spindle peak (at 0 lag) during the postnatal days 26 and 42. (b-c) Linear regression between the mean Spindle-SWR coupling count (events/min) and postnatal days P26-P42. These results showed a negative correlation between the coupling of Spindles and sharp-wave ripples throughout postnatal days P26-P42 for all the animals (n = 4). Linear regression, $r^2 = 0,552$ and p = 0,014. For the animals that discriminate the OPR task (n = 3) $r^2 = 0,5621$ and p = 0,02.

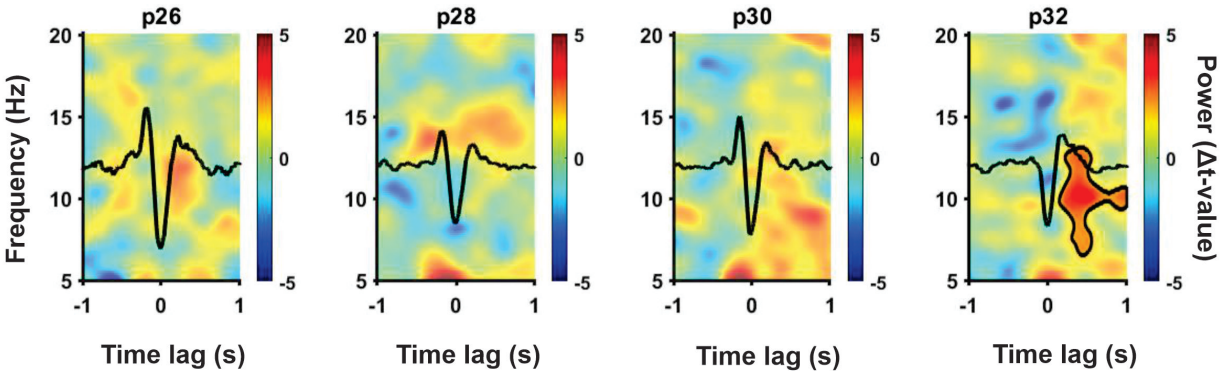

Figure 19: SO-triggered Spindle average spectrogram from cortical LFPs during the OPR retention phase. SO down-state centered at 0, +/- 1 s time lag. Note the power increase in the Spindle frequency range (9–16 Hz) at P32 around 500 ms from the SO down-state. Spindle power increasing is localized in the up-state of the SO band. Statistical comparisons were performed through a non-parametric permutation test (MonteCarlo, n = 1000) using a cluster alpha of 0.02 and with a significance mask of $p < 0.01$. Significant cluster at P32 ($p < 0{,}01$).

VII

Discussion

This study focused on the emergence of episodic memory during the transition from youth to adolescence in rats [8-11,13], and how this behavioral milestone is related to changes in slow oscillations, Spindles, and sharp-wave ripples [25-27] during sleep after memory encoding.

One of our main results was that hippocampal-dependent memory emerges late and gradually throughout postnatal development. The hippocampus is a structure that matures postnatally [23] then, the cognitive abilities that depend on this structure may appear together with this maturing process. Furthermore, the object-in-place memory task relies on the integrity of the hippocampus [12, 96, 97]; the present results are in agreement with the fact that hippocampal circuits continue maturing progressively after birth [98], being the circuits required for spatial navigation and memory the last to emerge near the fourth and fifth postnatal week (P28-P35) [98, 99]. Also, this onset of spatial memory coincides with the spatial tuning of the place-cells navigational system, which begins to take place around P23-P24 persisting till adulthood, an essential component for shaping the cognitive map [100].

We found that hippocampal-dependent memory appeared at not only P32,

but also that by that time reaches an adult-like profile (Fig. 7). Furthermore, this memory onset was independent of previous overtraining (P26, P28, and P30) (Fig. 9) since the rodents in the P32 without prior experience in the memory task (No Rep group) showed the same successful profile (Fig. 9a), supporting the idea that the emergence of memory capacities at P32 is related to neurodevelopment process and not other external factors.

Previously, has been described that rats could navigate using distal cues as a reference and to manifest a premature memory expression (i.e., object-zone preference) as early as P17 [29]. Later on, by P21, displaying short-retention time memory (5 min – 1 h) [28, 29, 101]. Our results are in line with those reported by Westbrook et al. (2014), who showed that since P26 rats were able to discriminate object-recognition tasks (i.e., object-location) when using distal and proximal cues [29], however, only at P31-P38 rats can display this types of memory for long retention times (4 h–24 h) [28-31]. Allocentric memory understood as spatial representations made by using external/distal environmental cues as a reference [114], has been the last manifestation of an episodic type of memories described to appear during adolescence (P38) [31]. However, in that study, the authors used different temporal windows, with the OPR test more spaced in time and without considering the sleep factor. Therefore, they may be overlooking critical days for memory onset in the hippocampus, authors mention that between day P31 (no object preference) and day P38 (preference for the displaced object), a noticeable switch in performance is observed [31]. In short, our data agree with previous research, confirming the postnatal appearance of this memory and suggesting that the most likely cause of this is the natural development of the brain and, mainly, the complete maturation of the hippocampus.

We observed that although some days there was no object preference, the differences between the juvenile and adult memory index progressively decreased

until day P32 (Fig. 7). Thus, we are in the presence of a gradual progression of this cognitive ability through development, with a substantial difference between day P26 and P32 (Fig. 8).

We compared the overtrained animals (from P26 to 32) with those tested for the first time on the day P32 (P32 NoRep, Fig. 9); however, they did not show any difference between them. Nevertheless, a subtle difference was observed when comparing against chance level, where only the overtrained group was able to distinguish the displaced object in the entire time course of the task, while the P32 NoRep, only discriminated in the first 4 min of the task. These minor details may partly explain the discrepancies found in literature about the onset of this spatial capability. Importantly, no differences in total exploration time or traveled distance were observed on the different days of the OPR task among groups (Fig. 9b-c), indicating that other factors such as motor skill could not account for these results.

To our knowledge, this is the first time where the entire temporal window when hippocampus-dependent memory appears (P26 to P32) has been explored. Using long retention times (3h), distal cues as spatial guidance, and 24 h spacing between successive exposures to one OPR task evaluation to another. We also ruled out the possible favorable effect of overtraining in this developmental time window. In addition, we combine behavioral analysis with sleep and its oscillations as a critical factor in episodic memory consolidation in the transition to adolescence in rats.

Based on these results, it was essential to take one more step forward by observing what was happening at the electrophysiological level. For this purpose, we successfully performed *in vivo* recordings of 4 rats that conducted the OPR task with sleep episodes between the sample and the test. Sleep stages were

distinguished through video recordings scoring [90, 102, 103] REM/NREM screening trough their oscillatory profile, as REM sleep is characterized for having a predominance of theta oscillation, and NREM sleep of slow oscillations [33]. We were able to successfully isolate NREM sleep windows from wake-REM states (Fig. 10 c-d), and thus, detecting SO, SWRs, and Spindle events in that stage(Fig. 11).

Our initial goal was to reach the three brain areas related to the origin of each oscillation (cortex, hippocampus, and thalamus); however, it was not possible to reach thalamic oscillations (Fig. 10 a-b). Nevertheless, we performed cortical Spindles detection, as has been widely reported before by the well-known corticothalamic circuitry which allow the detection of Spindles in both cortical and thalamic regions [52].

These results contributed to determine the role of sleep-oscillations during the postnatal window where hippocampus-dependent memory consolidates [74, 76, 79]. In this line, our second and third objectives pointed toward exploring if memory onset was sustained by the synchronization of the three cardinal NREM-oscillations as proposed in the "two-stage memory formation mechanism" and "the active system consolidation theory" described for adult models [75, 76]. Both theories argued that memory consolidation occurs due to a hippocampal-cortical dialogue that allows the phase-locking of the cortical slow-oscillations, the hippocampal sharp-wave ripples, and the thalamic Spindles [75-79].

First, we ruled out that the amount of NREM-sleep were proportional to performance (Fig. 12), which allowed us to focus on more specific oscillatory parameters. Our results were separated into two categories: (1) oscillatory characterization throughout development and (2) relationship between oscillatory parameters and behavior.

In the first category, we found that SO density increased with postnatal days (Fig. 13). In addition, SWRs density and frequency decreased with developmental days (Fig. 14). Also, we found an increased SO-Spindle temporal-coupling at the SO up-state (Fig. 17 b), in contrast to a Spindle-SWRs coupling decline along with development (Fig. 18 b-c). In both human and rodent studies, enough progress has been made to show that NREM-sleep decreases in the elderly, mainly the density of SO and Spindles [104, 105], encouraging the search for non-invasive techniques to restore sleep-oscillations to improve memory capacities [106]. The precise temporal coordination of slow oscillations and sleep Spindles is a fundamental mechanism of sleep-dependent memory consolidation [79, 107]. Recent studies in humans showed that the strength of coupling between SO-Spindles increases during brain maturation, suggesting that the transition from infancy to adolescence is critical for memory formation [93]. Our results in rodents, which showed a greater SO density and SO-spindles temporal coupling, could be reflecting parallelism with those pieces of evidence described for humans.

On the other hand, we know that SWRs are essential for memory consolidation [68], emerging among P14-P20 when they can be characterized as adults-like oscillations [66]. However, to date, only the work of Buhl (2015) has studied the relationship between SWRs parameters and postnatal days (up to P20). Their work showed that SWRs increased their power and established a constant frequency (around 140 Hz) throughout the P12-P20 postnatal window [66]. However, the SWRs-parameters have not been described furthermore than P20. And overtraining factor has not been considered during this temporal window.

More recent studies have shown that the density of SWRs increases during the first post-learning hour [59]. One possibility is that these results are in line

with those described by Wiegand et al. (2016), who showed that a decrease in both density and frequency of SWRs was associated with age [108]. However, it should be taken into account that the developmental period they used is quite far from our model. Another possibility is that what we are seeing is an effect of overtraining; even if we did not impact behavior, there could be differences at the electrophysiological level. For example, repeated memories are more prone to becoming less dependent on the hippocampus and more on the cortex [109]. Thus, we could see less hippocampal activity when comparing tasks with repetition versus single exposure in time. Therefore, it would be interesting to explore the effect of overtraining at the electrophysiological level in the future.

The hippocampus-cortex dialogue is one of the bases of the active consolidation model [75-79]. Coordination between SO-Spindles-SWRs is necessary for memory consolidation to occur [79, 82]. But as mentioned before, not much is known about how this coupling manifests along with postnatal development. Therefore, it is quite possible that the decrease in the density of the SWRs, and their Spindle-coupling, is a characteristic of this particular stage, being SWRs the last oscillatory event to get coupled to the SO-spindle events. Suggesting that more important than the density of coupled events in the SO up-state, we should pay attention to finer parameters of SWRs, and Spindle coupled events, or even at the spike level. In summary, there has been a lack of sleep-memory-related postnatal studies. These results could be setting a precedent.

In the second category, the relationship between oscillatory parameters and behavior, we found that the animals that discriminated the task had better performance, higher density, and longer duration of Spindles (Fig. 15). In agreement with those results, we did not see an increase in either the density or duration of Spindles along with development, which would indicate that the results we observed at OPR days are due only to post-task sleep. In turn, we observed

that better performance was associated with a lower density of SWRs (Fig. 16). Higher densities of post-learning spindles [59, 60], but no previous SWRs decrease have been reported, suggesting that this result could be a novel contribution to this area of study a further detailed experiment could be needed.

We did not observe other correlations between parameters of SO, Spindles, SWRs, or temporal coupling with memory (Supplementary Fig. 8, Table 3). However, this could be due to the small experimental number used and would require further confirmation.

Finally, as we did not find correlations between any oscillatory coupling pair density (SO-SPs, SPs-SWRs, SO-SWRs) with performance, we decided to explore using time-frequency spectrograms to observe the frequency ranges for Spindles and SWRs timed-locked to the down-state of SO events. Interestingly, by day P32, we observed an increase in the power of the Spindle frequency band in the up-state portion of the SO. This synchronized power increase was not observed in the previous days of the memory testing. But in the following days (P35 and P39), after the memory capacities emerged, significant clusters were observed with higher Spindle frequency ranges (14-20 Hz) (Supplementary Fig. 10). These results may suggest that, at first instance, a particular subset of SO-coupled Spindles of lower frequency (9-12Hz) could command the memory consolidation process, and later on, Spindles of higher frequencies would proceed. According to this, there is evidence in humans of two different subtypes of Spindles (fast and slow) during slow-wave-sleep that differ in frequency, SO-coupling, topography, and sensitivity to learning [107, 110, 111], in particular, slow Spindles which are mainly controlled by the cortical pathway [112]. Thus, reinforcing the proposal that these typologies may have distinct roles in the consolidation of hippocampal memories.

We also replicated this for the SWRs frequency band. We observed some

significant cluster of power spectrum at P26, P27, P31 and P39. It is noteworthy that on those days the SWRs are located whether preceding SO events and/or in the SO valley. Taxidis et al (2013) showed that SO-SWRs coupling would trigger an excitatory hippocampal balance when coupled to the SO up-state, or inhibitory when coupling occur at the SO down-state [113]. Demonstrating that there is still a long way to go to unravel the articulated mechanisms of hippocampal-dependent memory consolidation.

In conclusion, we wanted to evaluate how "The active system mechanism" and "The active system consolidation theory" fit with the postnatal emergence of hippocampus-dependent memory. Our results demonstrate that hippocampal dependent memory emerges at P32 independently of early overtraining. At electrophysiological level, we observed an increase in the amount of coupled SO-spindle events, and a decrease in the spindle-SWRs coupling during this stage which was not correlated with performance improvement. However, density and duration of the Spindles and SWRs density were associated with improved performance. Finally, an increase in Spindle power coupled to the ascending state of SO coincided with the successful manifestation of hippocampus-dependent memory on day P32. Hence, further investigations are needed. Taking these findings together, these results are of significant relevance to understanding the adult models of memory consolidation by combining behavioral and electrophysiological approaches to explain the emergence of episodic memory, which could be an excellent guide to explore the underlying mechanism of memory consolidation during sleep at early stages.

VIII

Supplementary

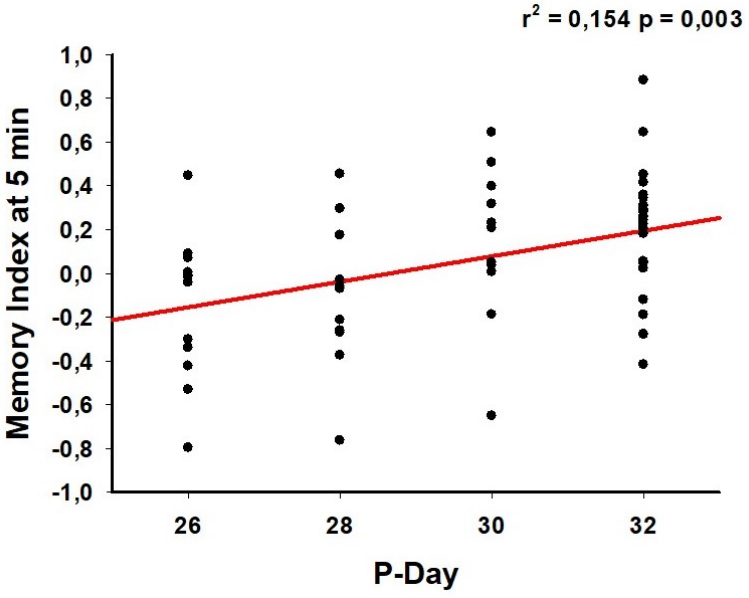

Supplementary Figure 1: Linear regression. Analysis was performed between the memory index at the OPR task using the final time (5 min) against P-days (P26, P28, P30, and P32). Observing that there is indeed a positive correlation between these variables (r^2 = 0,154; p = 0,003). P26 and P28 n=12, P30 =11 and P32 n=22.

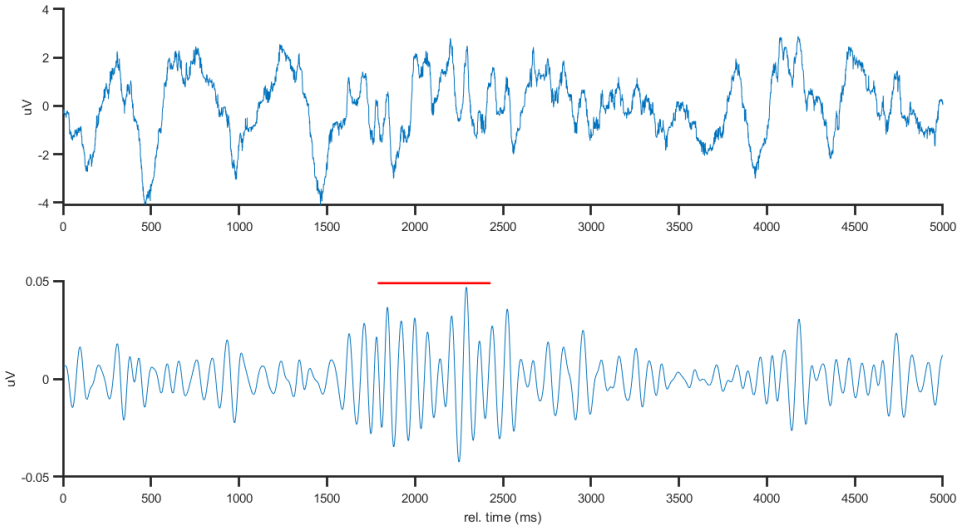

Supplementary Figure 2: Examples of detected sleep-oscillations events by the semi-automatic MATLAB routine used for detection. The broadband LFP (top) is decomposed into Spindle band (bottom) components. SO must have high amplitudes (black lines; middle) and sufficiently long durations to reach the thresholds. In addition, the Spindle band envelope must have exceeded an upper amplitude threshold for at least one bin, and the lower amplitude threshold for several bin until reach 500 ms. The red line represents the detected spindle duration.

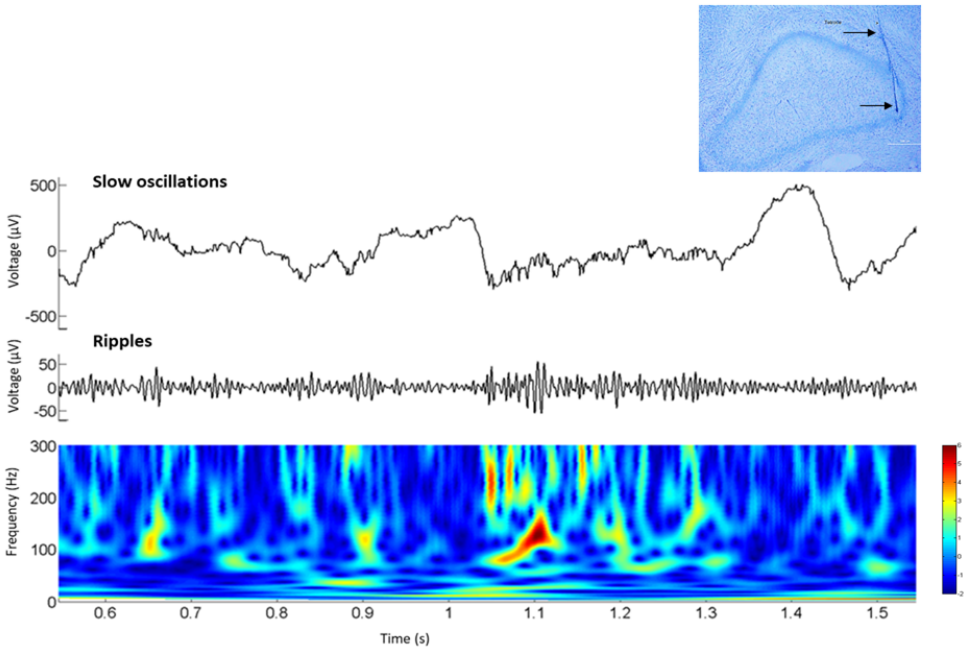

Supplementary Figure 3: Sharp-wave ripples at sleep. (Top) A representative cortical LFP raw signal and hippocampal filtered signal (SWRs, 100-300 Hz) from an implanted rat at a sleep state. (Down) Time-frequency power spectrum showing the respective power intensity for the SWRs frequency band (100-250 Hz) (-2, blue to 6, red). At the top and right portion of the figure, a Nissl staining showing the tetrode position targeting the CA3 hippocampal region for this recording example.

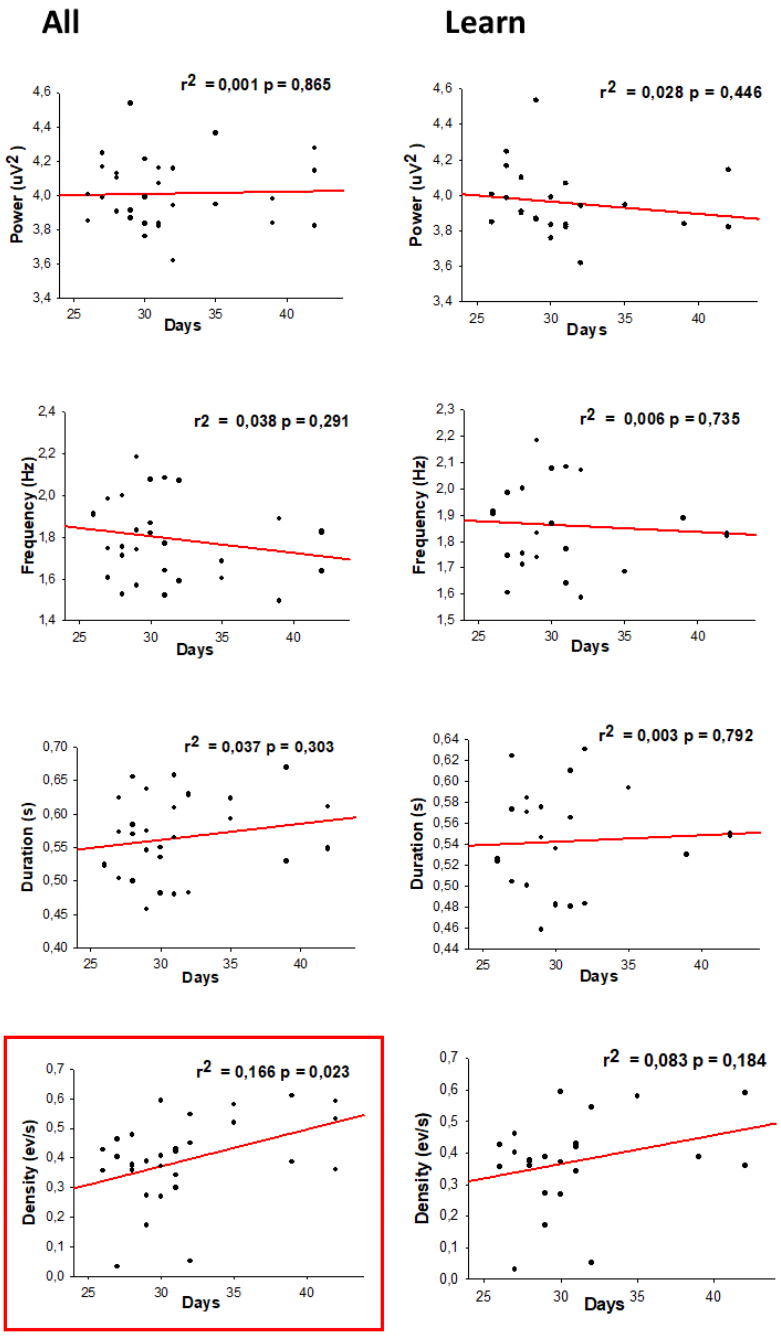

Supplementary Figure 4: Slow oscillation parameters. (On top)Liner regression for slow oscillation power, frequency, duration, and density against P-days for all the animals (n = 4). SO power $r^2 = 0,001$ and p = 0,865; SO frequency $r^2 = 0,038$ and p = 0,291; SO duration $r^2 = 0,037$ and p = 0,303 and SO density $r^2 = 0,166$ and p = 0,023. Then, (Below) linear regression for SO parameters for animals who discriminated the task (n = 3). SO power $r^2 = 0,028$ and p = 0,446; SO frequency $r^2 = 0,006$ and p = 0,735; SO duration $r^2 = 0,003$ and p = 0,792 and SO density $r^2 = 0,083$ and p = 0,184. Days of with missing dots occur because the animal did not sleep (P26) or a rat damaged his registration implant (AG14 at P32).

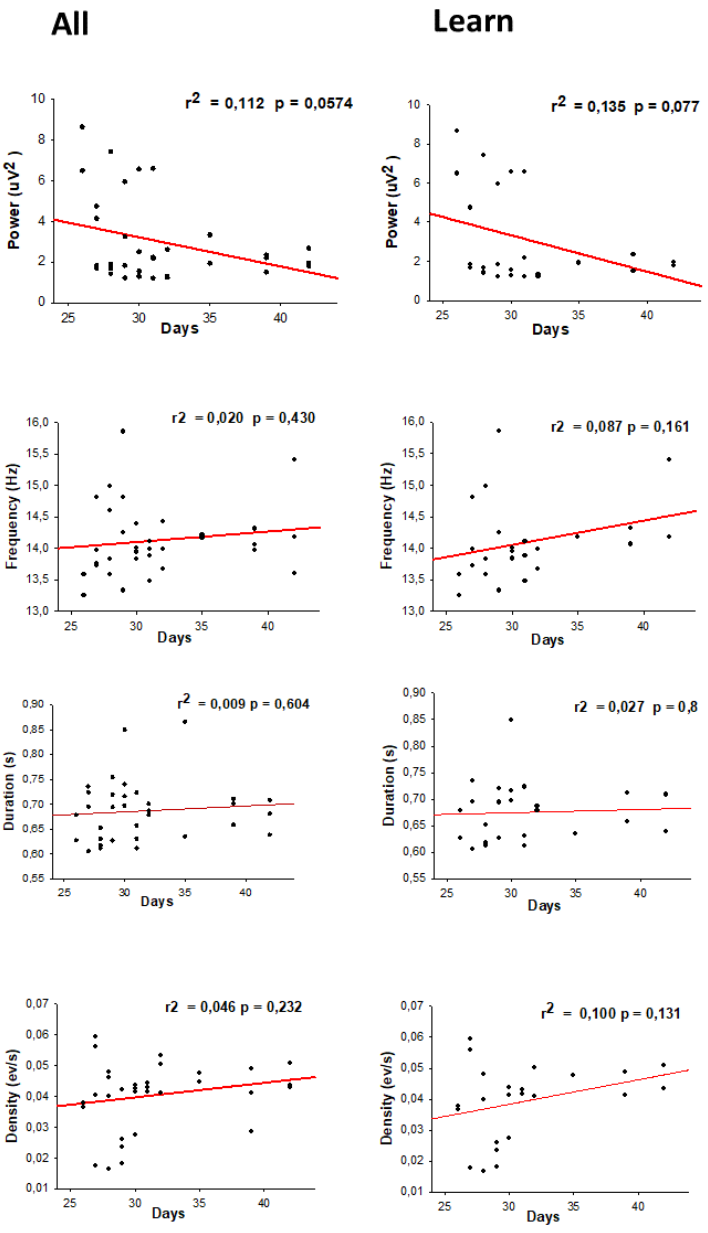

Supplementary Figure 5: Spindles parameters along development. (On top) Linear regression between spindles power, frequency, duration and density along P-days for all the animals (n = 4). Spindles power $r^2 = 0,112$ and p = 0,057; Spindles frequency $r^2 = 0,020$ and p = 0,430; Spindles duration $r^2 = 0,009$ and p = 0,604 and Spindles density $r^2 = 0,046$ and p = 0,232. Then, (Below) linear regression for Spindles parameters for animals who discriminated the task (n = 3). Spindles power $r^2 = 0,135$ and p = 0,077; Spindles frequency $r^2 = 0,087$ and p = 0,161; Spindles duration $r^2 = 0,027$ and p = 0,808 and Spindles density $r^2 = 0,100$ and p = 0,131. Days with missing black dots occur because the animal did not sleep (P26) or a rat damaged his registration implant (AG14 at P32).

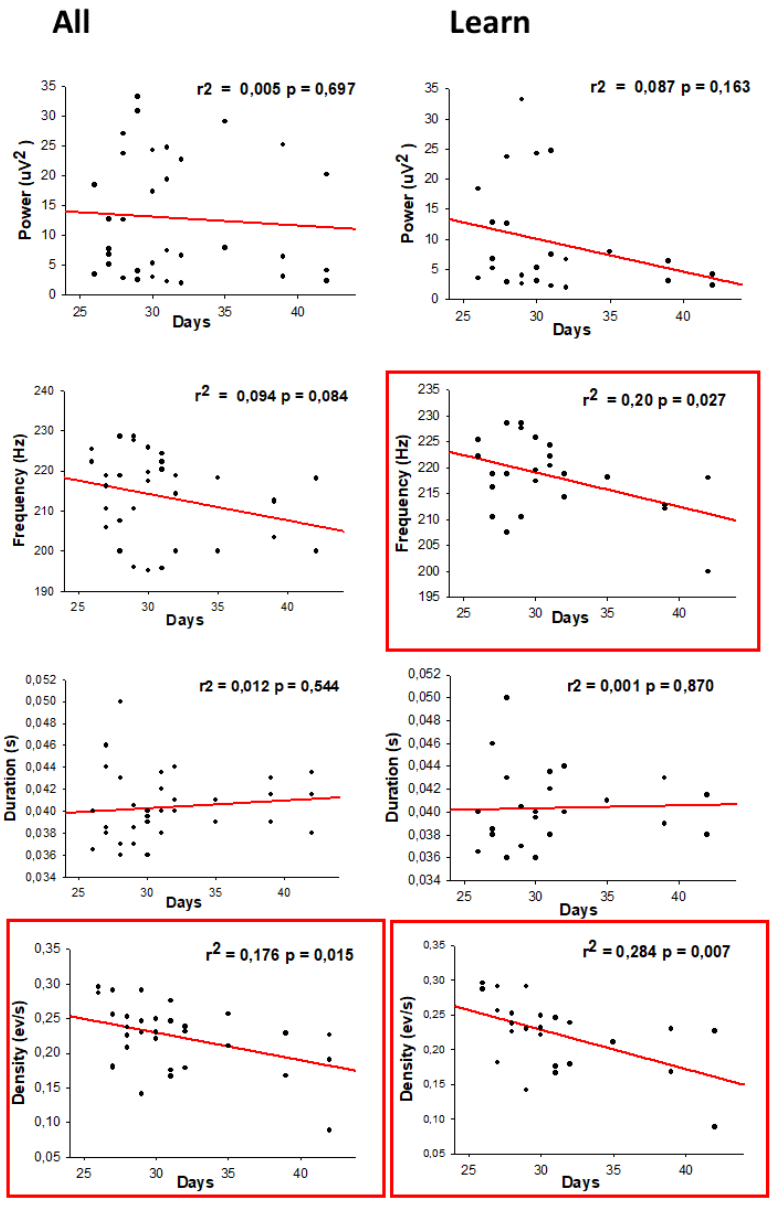

Supplementary Figure 6: SWRs parameters along development. On top, Linear regression for SWRs power, frequency, duration and density along P-days for all the animals (n = 4). SWRs power $r^2 = 0,005$ and p = 0,697; SWRs frequency $r^2 = 0,094$ and p = 0,084; SWRs duration $r^2 = 0,012$ and p = 0,544 and SWRs density $r^2 = 0,176$ and p = 0,015. Then, (Below) linear regression for SWRs parameters for animals who discriminated the task (n = 3). SWRs power $r^2 = 0,087$ and p = 0,163; SWRs frequency $r^2 = 0,200$ and p = 0,027; SWRs duration $r^2 = 0,001$ and p = 0,870 and SWRs density $r^2 = 0,284$ and p = 0,007. Missing dots on some days occur because the animal did not sleep (P26) or a rat damaged his registration implant (AG14 at P32).

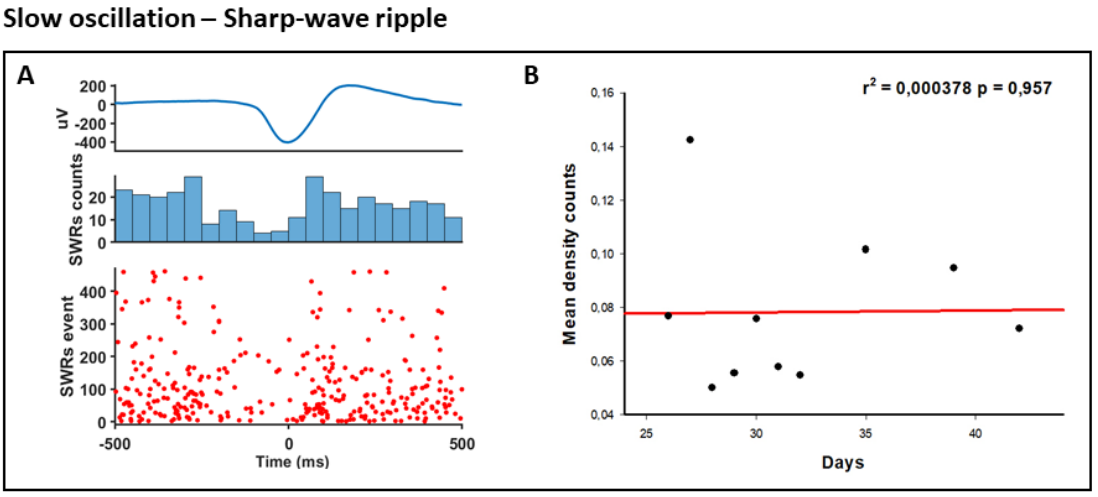

Supplementary Figure 7: SO-SWRs coupling along with the development. (a) From one animal as a representative example. On top, SO grand average waveform (line in blue), SO down-state centered at 0 lag. In the middle, a histogram showing the temporal coupling of hippocampal sharp-wave ripples related to the trough of the So. The time lag of -500 to 500 ms. All crosscorrelations were corrected by using the Monte Carlo analysis. Below, a raster plot showing all the sharp-wave ripples events related to the SO trough around 0 lag during P26- P42. (b) Linear regression for the mean number of counts (events/min) along with the postnatal days P26-P42. Density count between events was determined during NREM periods in the retention phase. These results show no correlation between the SO-SWRs temporal coupling and P-days for all the animals (n = 4) $r^2 = 0,000378$ and p = 0,957. And no correlation also for animals who discriminated $r^2 = 0,0154$ and p = 0,733 (not shown).

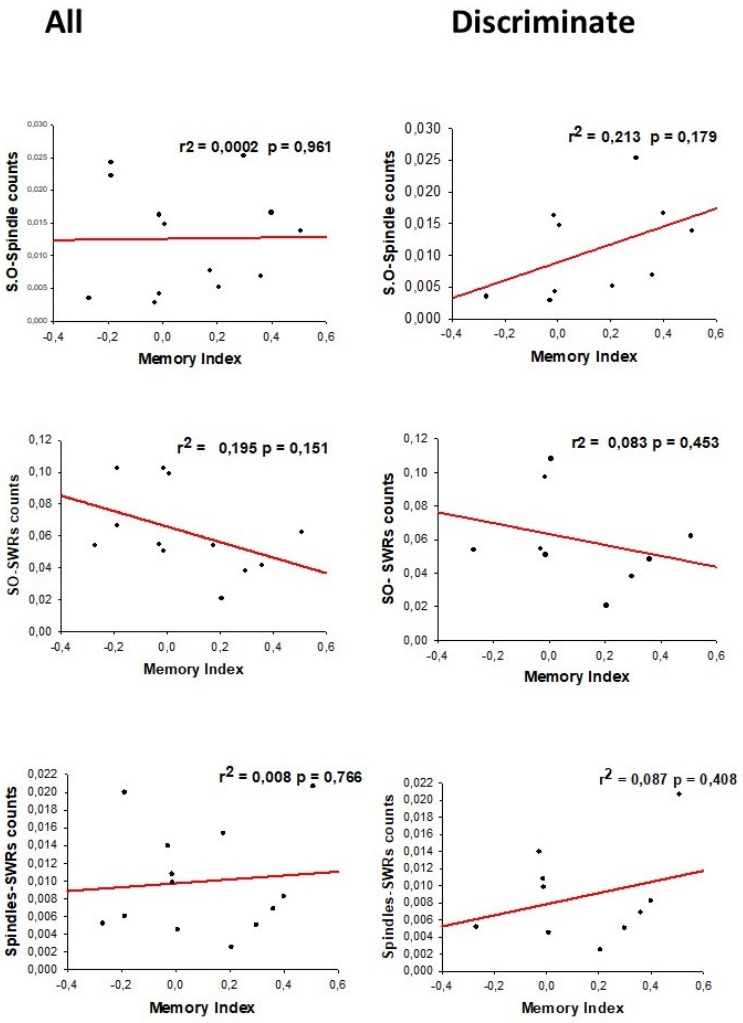

Supplementary Figure 8: Memory index versus oscillation coupling. On top, Linear regression of oscilations coupling counts against memory index, including all animales. SO-Spindles counts $r^2 = 0,0002$ and p = 0,961, SO-SWRs counts $r^2 = 0,195$ and p = 0,151 and Spindles-SWRs counts $r^2 = 0,008$ and p = 0,766 against memory index for all rats (n = 4). (Below) Linear regressions for SO-Spindles counts $r^2 = 0,213$ and p = 0,179, SO-SWRs counts $r^2 = 0,083$ and p = 0,453 and Spindles-SWRs counts $r^2 = 0,087$ and p = 0,408 against memory index for rats that discriminated the task (n = 3).

/P-Day	Slow oscillation	Spindles	Sharp-wave ripples
Slow oscillation	-	**All: r^2 = 0,586 p = 0,010** Discriminate: r^2 = 0,189 p = 0,209	All: r^2 = 0,0004 p = 0,957 Discriminate: r^2 = 0,015 p = 0,733
Spindles	-	-	**All: r^2 = 0,552 p = 0,014 Discriminate: r^2 = 0,562 p = 0,02**

/ Memory Index	All	Discriminate
S.O-Spindles	r^2 = 0,0002 p = 0,961	r^2 = 0,213 p = 0,179
S.O-SWRs	r^2 = 0,195 p = 0,151	r^2 = 0,083 p = 0,453
Spindles-SWRs	r^2 = 0,008 p = 0,766	r^2 = 0,087 p = 0,408

Table 3: Summary: Oscillations coupling versus P-days and memory index. On top, Oscillation coupling correlation with p-days. Below, oscillations coupling versus memory index in all rats (n = 4), discriminate (n = 3). The memory index was obtained from the test trials of the OPR task for each animal at 5 min. The r^2 and p value is detailed for each case. In red are shown the values that were significant ($p < 0{,}05$).

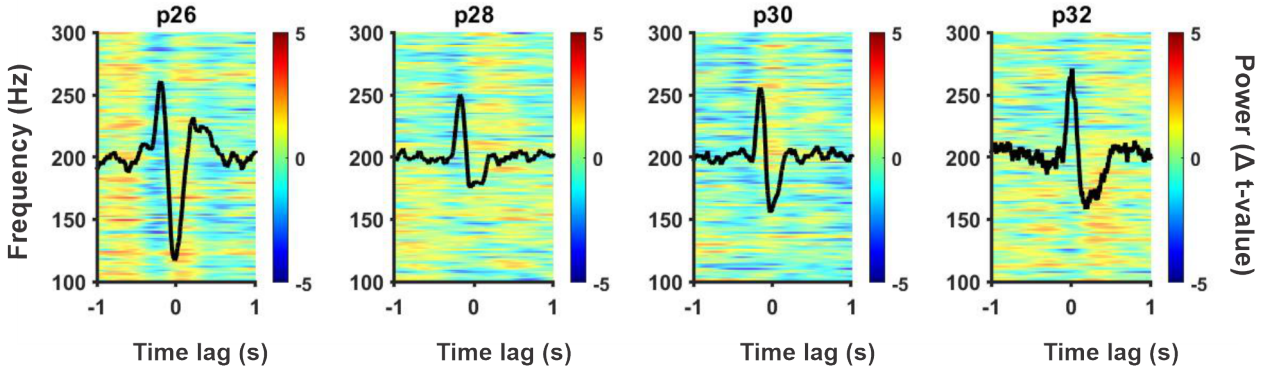

Supplementary Figure 9: SO-SWRs spectrogram. Average SWRs-triggered spectrogram, time-locked with cortical SO events during the OPR retention phase. SO down-state centered at 0, +/- 1 s time lag. Statistical comparisons were performed through a non-parametric permutation test (MonteCarlo, n = 1000) using a cluster alpha of 0.02 and with a significance mask of $p < 0.01$; however, no significative cluster were observed.

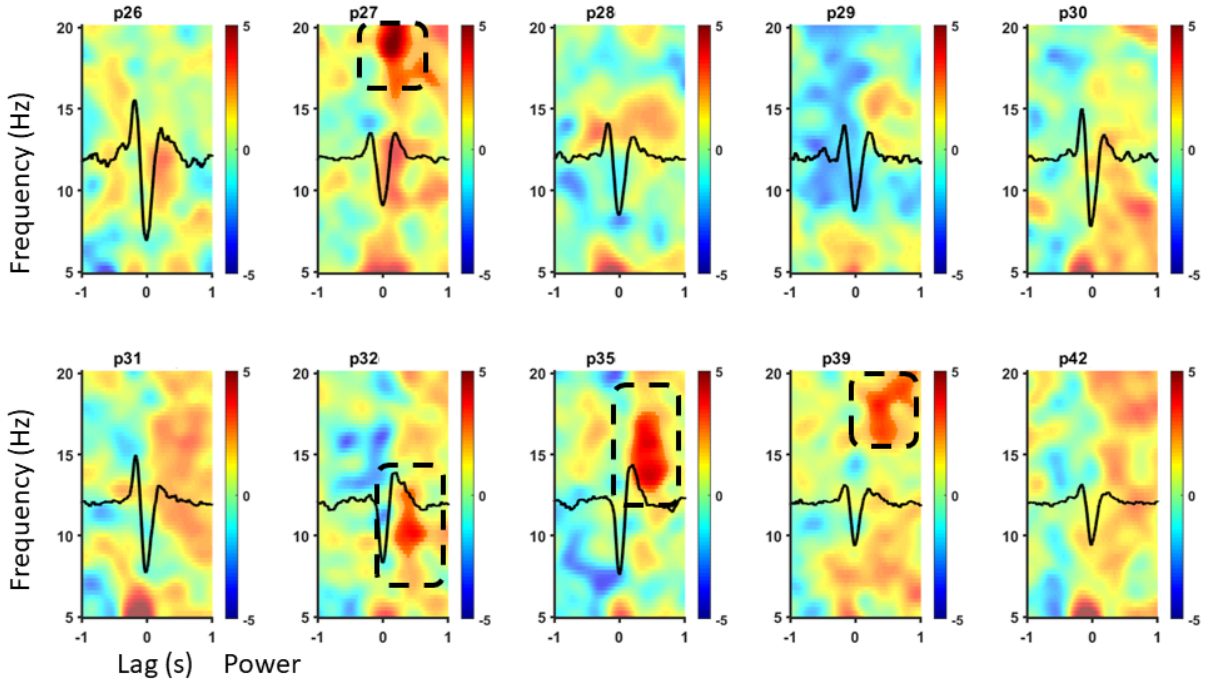

Supplementary Figure 10: SO-spindle spectrogram. Spindle-triggered average spectrogram from cortical LFPs during the OPR retention phase. Spectrogram during the developmental window P26-P42. SO down-state centered at 0, +/- 1 s time lag. Note the significant power increase at the spindle frequency range (9–17 Hz) since P32. The spindle's power increase is localized in the up-state of the SO. SO grand average in plotted in black. Statistical comparisons were performed through a non-parametric permutation test (MonteCarlo, n = 1000) using a cluster alpha of 0.02 and with a significance mask of p<0.01. Significant clusters at P27, P32, P35 and P39 (p < 0,01).

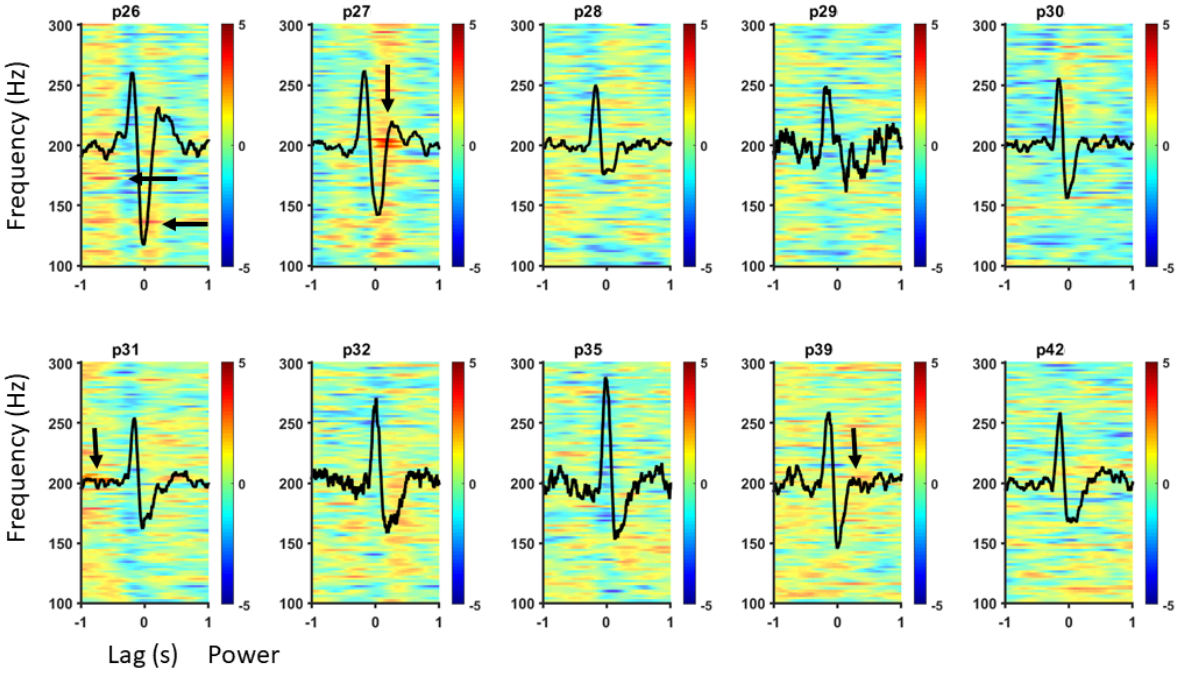

Supplementary Figure 11: SO-SWRs spectrogram. Average SWRs-triggered spectrogram during the developmental window P26-P42. The OPR task was performed only at P26, P28, P30 and P32. SO down-state centered at 0, +/- 1 s time lag. SO grand average in plotted in black. Statistical comparisons were performed through a non-parametric permutation test (MonteCarlo, n = 1000) using a cluster alpha of 0.02 and with a significance mask of p<0.01. Significant clusters at P26, p27, P31 and P39 (p < 0,01).

IX

References

1. Scoville WB, Milner B. (1957). Loss of recent memory after bilateral hippocampal lesions. J Neurol Neurosurg Psychiatry. 20(1):11-21. doi: 10.1136/jnnp.20.1.11. PMID: 13406589; PMCID: PMC497229.

2. Knierim JJ. (2015). The hippocampus. Curr Biol 25(23):R1116-21. doi: 10.1016/j.cub.2015.10.049. PMID: 26654366.

3. Neves G, Cooke SF, Bliss TV. (2008). Synaptic plasticity, memory and the hippocampus: a neural network approach to causality. Nat Rev Neurosci. 9(1):65-75. doi: 10.1038/nrn2303. Erratum in: Nat Rev Neurosci. 2012 Dec;13(12):878. PMID: 18094707.

4. Cellini N, Capuozzo A. (2018). Shaping memory consolidation via targeted memory reacti- vation during sleep. Ann N Y Acad Sci. doi: 10.1111/nyas.13855. Epub ahead of print. PMID: 29762867.

5. Tan HM, Wills TJ, Cacucci F. (2017). The development of spatial and memory circuits in the rat. Wiley Interdiscip Rev Cogn Sci. 8(3). doi: 10.1002/wcs.1424. Epub 2016 December 12. PMID: 27943643.

6. Barker GR, Banks PJ, Scott H, Ralph GS, Mitrophanous KA, Wong LF, Bashir ZI, Uney JB, Warburton EC. (2017). Separate elements of episodic memory subserved by distinct hippocampal-prefrontal connections. Nat Neurosci. 20(2):242-

250. doi: 10.1038/nn.4472. Epub 2017 January 9. PMID: 28067902.

7. Allen TA, Fortin NJ. (2013). The evolution of episodic memory. Proc Natl Acad Sci U S A. 18;110 Suppl 2(Suppl 2):10379-86. doi: 10.1073/pnas.1301199110. Epub 2013 Jun 10. PMID: 23754432; PMCID: PMC3690604.

8. Eichenbaum H, Yonelinas AP, Ranganath C. (2007). The medial temporal lobe and recognition memory. Annu Rev Neurosci. 30:123-52. doi: 10.1146/annurev.neuro 30.051606.094328. PMID: 17417939; PMCID: PMC2064941.

9. Ainge JA, Langston RF. (2012). Ontogeny of neural circuits underlying spatial memory in the rat. Front Neural Circuits. 1;6:8. doi: 10.3389/fncir.2012.00008. PMID: 22403529; PMCID: PMC3290765.

10. Burwell RD, Witter MP, Amaral DG. (1995). Perirhinal and postrhinal cortices of the rat: a review of the neuroanatomical literature and comparison with findings from the monkey brain. Hippocampus. 5(5):390-408. doi: 10.1002/hipo.450050503. Erratum in: Hippocampus 1996;6(3):340. PMID: 8773253.

11. Aggleton JP, Nelson AJD. (2020). Distributed interactive brain circuits for object-in-place memory: A place for time? Brain Neurosci Adv. 30;4:2398212820933471. doi: 10.1177/2398212820933471. PMID: 32954003; PMCID: PMC7479857.

12. Barker GR, Warburton EC. (2011). When is the hippocampus involved in recognition memory? J Neurosci. 20;31(29):10721-31. doi: 10.1523/JNEUROSCI.6413-10.2011. PMID: 21775615; PMCID: PMC6622630.

13. O'Keefe, J., Nadel, L. (1978). The hippocampus as a cognitive map. Oxford: Clarendon Press.

14. Nadel L. (1991). The hippocampus and space revisited. Hippocampus. 1(3):221-9. doi: 10.1002/hipo.450010302. Erratum in: Hippocampus 1992

Jan;2(1):92. PMID: 1669368.

15. O'Keefe J, Dostrovsky J. (1971). The hippocampus as a spatial map. Preliminary evidence from unit activity in the freely-moving rat. Brain Res. 34(1):171-5. doi: 10.1016/0006-8993(71)90358-1. PMID: 5124915.

16. Muller RU, Stead M. (1996). Hippocampal place cells connected by Hebbian synapses can solve spatial problems. Hippocampus. 6(6):709-19. doi: 10.1002/(SICI)1098-1063(1996)6:6¡709::AID-HIPO13¿3.0.CO;2-4. PMID: 9034857.

17. Jarrard LE. (1978). Selective hippocampal lesions: differential effects on performance by rats of a spatial task with preoperative versus postoperative training. J Comp Physiol Psychol. 92(6):1119-27. doi: 10.1037/h0077516. PMID: 755058.

18. Olton DS, Walker JA, Gage FH. (1978). Hippocampal connections and spatial discrimination. Brain Res 13;139(2):295-308. doi: 10.1016/0006-8993(78)90930-7. PMID: 624061.

19. Morris RG, Garrud P, Rawlins JN, O'Keefe J. (1982). Place navigation impaired in rats with hippocampal lesions. Nature. 24;297(5868):681-3. doi: 10.1038/297681a0. PMID: 7088155.

20. Morris RG, Schenk F, Tweedie F, Jarrard LE. (1990). Ibotenate Lesions of Hippocampus and/or Subiculum: Dissociating Components of Allocentric Spatial Learning. Eur J Neurosci. 2(12):1016-1028. doi: 10.1111/j.1460-9568.1990.tb00014.x. PMID: 12106063.

21. Maguire EA. (1997). Hippocampal involvement in human topographical memory: evidence from functional imaging. Philos Trans R Soc Lond B Biol Science. 29;352(1360):1475-80. doi: 10.1098/rstb.1997.0134. PMID: 9368936; PMCID: PMC1692049.

22. Maguire EA, Frith CD, Burgess N, Donnett JG, O'Keefe J. (1998). Knowing where things are parahippocampal involvement in encoding object

locations in virtual large-scale space. J Cogn Neurosci. 10(1):61-76. doi: 10.1162/089892998563789. PMID: 9526083.

23. Jabès, A., Lavenex, P. B., Amaral, D. G., Lavenex, P. (2011). Postnatal development of the hippocampal formation: a stereological study in macaque monkeys. The Journal of comparative neurology, 519(6), 1051–1070. https://doi.org/10.1002/cne.22549

24. Nadel L. (2021). Some implications of postnatal hippocampal development. Hippocampus. doi: 10.1002/hipo.23369. Epub ahead of print. PMID: 34133050.

25. Tulving, E. (2005). Episodic Memory and Autonoesis: Uniquely Human? In H. S. Terrace, J. Metcalfe (Eds.), The missing link in cognition: Origins of self-reflective consciousness (pp. 3–56). Oxford University Press. https://doi.org/10.1093/acprof:oso/9780195161564.003.0001.

26. Hayne H, Imuta K. (2011). Episodic memory in 3- and 4-year-old children. Dev Psychobiol. 53(3):317-22. doi: 10.1002/dev.20527. Epub 2011 Feb 8. PMID: 21400492.

27. Scarf D, Gross J, Colombo M, Hayne H. (2013). To have and to hold: episodic memory in 3- and 4-year-old children. Dev Psychobiol. 55(2):125-32. doi: 10.1002/dev.21004. Epub 2011 Dec 27. PMID: 22213009.

28. Ramsaran AI, Westbrook SR, Stanton ME. (2016). Ontogeny of object-in-context recognition in the rat. Behav Brain Res. 1;298(Pt A):37-47. doi: 10.1016/j.bbr.2015.04.011. Epub 2015 Apr 17. PMID: 25892362; PMCID: PMC4732722.

29. Westbrook SR, Brennan LE, Stanton ME. (2014). Ontogeny of object versus location recognition in the rat: acquisition and retention effects. Dev Psychobiol. 56(7):1492-506. doi: 10.1002/dev.21232. Epub 2014 July 3. PMID: 24992011; PMCID: PMC4786941.

30. Ramsaran AI, Sanders HR, Stanton ME. (2016). Determinants of object-in-context and object-place-context recognition in the developing rat. Dev Psychobiol. 58(7):883- 895. doi: 10.1002/dev.21432. PMID: 27753457.

31. Contreras MP, Born J, Inostroza M. (2019). The expression of allocentric object-place recognition memory during development. Behav Brain Res. 17;372:112013. doi: 10.1016/j.bbr.2019.112013. Epub 2019 June 5. PMID: 31173799.

32. Moser EI, Moser MB, McNaughton BL. (2017). Spatial representation in the hippocampal formation: a history. Nat Neurosci. 26;20(11):1448-1464. doi: 10.1038/nn.4653. PMID: 29073644.

33. McKenna J.T., Zielinski M.R., McCarley R.W. (2017). Neurobiology of REM Sleep, NREM Sleep Homeostasis, and Gamma Band Oscillations. In: Chokroverty S. (eds) Sleep Disorders Medicine. Springer, New York, NY. https://doi.org/10.1007/978-1-4939-6578-6-5.

34. Klinzing JG, Niethard N, Born J. (2019). Mechanisms of systems memory consolidation during sleep. Nat Neurosci. 22(10):1598-1610. doi: 10.1038/s41593-019-0467-3. Epub 2019 Aug 26. Erratum in: Nat Neurosci. 2019 Sep 11;: PMID: 31451802.

35. Buzsáki, G. (2006). Rhythms of the brain. Oxford University Press. https://doi.org/10.1093/acprof:oso/9780195301069.001.0001.

36. Lo CC, Chou T, Penzel T, Scammell TE, Strecker RE, Stanley HE, Ivanov PCh. (2004). Common scale-invariant patterns of sleep-wake transitions across mammalian species. Proc Natl Acad Sci U S A. 14;101(50):17545-8. doi: 10.1073/pnas.0408242101. Epub 2004 Dec 6. PMID: 15583127; PMCID: PMC536051.

37. Simasko SM, Mukherjee S. (2009). Novel analysis of sleep patterns in rats separates periods of vigilance cycling from long-duration wake events. Behav Brain Res. 23;196(2):228-36. doi: 10.1016/j.bbr.2008.09.003. Epub 2008 Sep 16.

PMID: 18835301; PMCID: PMC2617706.

38. Steriade M, McCormick DA, Sejnowski TJ. (1993). Thalamocortical oscillations in the sleeping and aroused brain. Science. 29;262(5134):679-85. doi: 10.1126/science.8235588. PMID: 8235588.

39. Massimini M, Huber R, Ferrarelli F, Hill S, Tononi G. (2004). The sleep slow oscillation as a traveling wave. J Neurosci. 4;24(31):6862-70. doi: 10.1523/JNEUROSCI.1318-04.2004. PMID: 15295020; PMCID: PMC6729597.

40. Nir Y, Staba RJ, Andrillon T, Vyazovskiy VV, Cirelli C, Fried I, Tononi G. (2011). Regional slow waves and spindles in human sleep. Neuron. 14;70(1):153-69. doi: 10.1016/j.neuron.2011.02.043. PMID: 21482364; PMCID: PMC3108825.

41. Battaglia FP, Sutherland GR, McNaughton BL. (2004). Hippocampal sharp wave bursts coincide with neocortical "up-state" transitions. Learn Mem. 11(6):697-704. doi: 10.1101/lm.73504. PMID: 15576887; PMCID: PMC534698.

42. Isomura Y, Sirota A, Ozen S, Montgomery S, Mizuseki K, Henze DA, Buzsáki G. (2006). Integration and segregation of activity in entorhinal-hippocampal subregions by neocortical slow oscillations. Neuron. 7;52(5):871-82. doi: 10.1016/j.neuron.2006.10.023. PMID: 17145507.

43. Cirelli C, Tononi G. (2015). Cortical development, electroencephalogram rhythms, and the sleep/wake cycle. Biol Psychiatry. 15;77(12):1071-8. doi: 10.1016/j.biopsych.2014.12.017. Epub 2014 Dec 24. PMID: 25680672; PMCID: PMC4444390.

44. Finelli LA, Borbély AA, Achermann P. (2001). Functional topography of the human nonREM sleep electroencephalogram. Eur J Neurosci. 13(12):2282-90. doi: 10.1046/j.0953-816x.2001.01597.x. PMID: 11454032.

45. Vyazovskiy VV., Olcese U, Lazimy YM, Faraguna U, Esser SK, Williams JC, Cirelli C, Tononi G. (2009). Cortical firing and sleep homeostasis. Neuron. 24;63(6):865-78. doi: 10.1016/j.neuron.2009.08.024. PMID: 19778514;

PMCID: PMC2819325.

46. Huber R, Ghilardi MF, Massimini M, Tononi G. (2004). Local sleep and learning. Nature. 1;430(6995):78-81. doi: 10.1038/nature02663. Epub 2004 Jun 6. PMID: 15184907.

47. Heynen AJ, Yoon BJ, Liu CH, Chung HJ, Huganir RL, Bear MF. (2003). Molecular mechanism for loss of visual cortical responsiveness following brief monocular deprivation. Nat Neurosci. 6(8):854-62. doi: 10.1038/nn1100. PMID: 12886226.

48. Ringli M, Huber R. (2011). Developmental aspects of sleep slow waves: linking sleep, brain maturation and behavior. Prog Brain Res. 193:63-82. doi: 10.1016/B978-0-444-53839-0.00005-3. PMID: 21854956.

49. Olini N, Kurth S, Huber R. (2013). The effects of caffeine on sleep and maturational markers in the rat. PLoS One. 4;8(9):e72539. doi: 10.1371/journal.pone.0072539. PMID: 24023748; PMCID: PMC3762801.

50. Lee YF, Gerashchenko D, Timofeev I, Bacskai BJ, Kastanenka KV. (2020). Slow Wave Sleep Is a Promising Intervention Target for Alzheimer's Disease. Front Neurosci. 30;14:705. doi: 10.3389/fnins.2020.00705. PMID: 32714142; PMCID: PMC7340158.

51. Loomis AL, Harvey EN, Hobart G. (1935). Potential Rhythms of the cerebral cortex during sleep. Science. 14;81(2111):597-8. doi: 10.1126/science.81.2111.597. PMID: 17739875.

52. Kandel A, Buzsáki G. (1997). Cellular-synaptic generation of sleep spindles, spike-and-wave discharges, and evoked thalamocortical responses in the neocortex of the rat. J Neurosci. 1;17(17):6783-97. doi: 10.1523/JNEUROSCI.17-17-06783.1997. PMID: 9254689; PMCID: PMC6573130.

53. Gramsbergen A. (1976). The development of the EEG in the rat. Dev Psychobiol. 9(6):501-15. doi: 10.1002/dev.420090604. PMID: 1001836.

54. Andrillon T, Nir Y, Staba RJ, Ferrarelli F, Cirelli C, Tononi G, Fried I. (2011). Sleep spindles in humans: insights from intracranial EEG and unit recordings. J Neurosci. 7;31(49):17821-34. doi: 10.1523/JNEUROSCI.2604-11.2011. PMID: 22159098; PMCID: PMC3270580.

55. Steriade M, Deschênes M, Domich L, Mulle C. (1985). Abolition of spindle oscillations in thalamic neurons disconnected from nucleus reticularis thalami. J Neurophysiol. 54(6):1473-97. doi: 10.1152/jn.1985.54.6.1473. PMID: 4087044.

56. Steriade M. (1997). Synchronized activities of coupled oscillators in the cerebral cortex and thalamus at different levels of vigilance. Cereb Cortex. 7(6):583-604. doi: 10.1093/cercor/7.6.583. Erratum in: Cereb Cortex 1997 Dec;7(8):779. PMID: 9276182.

57. Destexhe A, Contreras D, Steriade M. (1998). Mechanisms underlying the synchronizing action of corticothalamic feedback through inhibition of thalamic relay cells. J Neurophysiol. 79(2):999-1016. doi: 10.1152/jn.1998.79.2.999. PMID: 9463458.

58. Sejnowski TJ, Destexhe A. (2000). Why do we sleep? Brain Res. 15;886(1-2):208-223. doi: 10.1016/s0006-8993(00)03007-9. PMID: 11119697.

59. Eschenko O, Mölle M, Born J, Sara SJ. (2006). Elevated sleep spindle density after learning or after retrieval in rats. J Neurosci. 13;26(50):12914-20. doi: 10.1523/JNEUROSCI.3175-06.2006. PMID: 17167082; PMCID: PMC6674950.

60. Gais S, Mölle M, Helms K, Born J. (2002). Learning-dependent increases in sleep spindle density. J Neurosci. 1;22(15):6830-4. doi: 10.1523/JNEUROSCI.22-15-06830.2002. PMID: 12151563; PMCID: PMC6758170.

61. Clemens Z, Fabó D, Halász P. (2005). Overnight verbal memory retention correlates with the number of sleep spindles. Neuroscience. 132(2):529-35. doi: 10.1016/j.neuroscience.2005.01.011. PMID: 15802203.

62. O'Keefe J. (1976). Place units in the hippocampus of the freely moving rat. Exp Neurol. 51(1):78-109. doi: 10.1016/0014-4886(76)90055-8. PMID: 1261644.

63. Buzsáki G. (2015). Hippocampal sharp wave-ripple: A cognitive biomarker for episodic memory and planning. Hippocampus. 25(10):1073-188. doi: 10.1002/hipo.22488. PMID: 26135716; PMCID: PMC4648295.

64. Karlsson MP, Frank LM. (2009). Awake replay of remote experiences in the hippocampus. Nat Neurosci. 12(7):913-8. doi: 10.1038/nn.2344. Epub 2009 Jun 14. PMID: 19525943; PMCID: PMC2750914.

65. Roumis DK, Frank LM. (2015). Hippocampal sharp-wave ripples in waking and sleeping states. Curr Opin Neurobiol. 35:6-12. doi: 10.1016/j.conb.2015.05.001. Epub 2015 May 23. PMID: 26011627; PMCID: PMC4641767.

66. Buhl DL, Buzsáki G. (2005). Developmental emergence of hippocampal fast-field "ripple" oscillations in the behaving rat pups. Neuroscience. 134(4):1423-30. doi: 10.1016/j.neuroscience.2005.05.030. PMID: 16039793; PMCID: PMC1851000.

67. Jadhav SP, Kemere C, German PW, Frank LM. (2012). Awake hippocampal sharp-wave ripples support spatial memory. Science. 15;336(6087):1454-8. doi: 10.1126/science.1217230. Epub 2012 May 3. PMID: 22555434; PMCID: PMC4441285.

68. Girardeau G, Benchenane K, Wiener SI, Buzsáki G, Zugaro MB. (2009). Selective suppression of hippocampal ripples impairs spatial memory. Nat Neurosci. 12(10):1222-3. doi: 10.1038/nn.2384. Epub 2009 Sep 13. PMID: 19749750.

69. Ego-Stengel V, Wilson MA. (2010). Disruption of ripple-associated hippocampal activity during rest impairs spatial learning in the rat. Hippocampus. 20(1):1-10. doi: 10.1002/hipo.20707. PMID: 19816984; PMCID: PMC2801761.

70. Wang ME, Yuan RK, Keinath AT, Ramos Álvarez MM, Muzzio IA. (2015). Extinction of Learned Fear Induces Hippocampal Place Cell Remapping. J Neurosci. 17;35(24):9122-36. doi: 10.1523/JNEUROSCI.4477-14.2015. PMID: 26085635; PMCID: PMC4469738.

71. Rasch B, Born J. (2013). About sleep's role in memory. Physiol Rev. 93(2):681-766. doi: 10.1152/physrev.00032.2012. PMID: 23589831; PMCID: PMC3768102.

72. Walker MP, Stickgold R. (2004). Sleep-dependent learning and memory consolidation. Neuron. 30;44(1):121-33. doi: 10.1016/j.neuron.2004.08.031. PMID: 15450165.

73. Inostroza M, Binder S, Born J. (2013). Sleep-dependency of episodic-like memory consolidation in rats. Behav Brain Res. 15;237:15-22. doi: 10.1016/j.bbr.2012.09.011. Epub 2012 Sep 16. PMID: 22989412.

74. Binder S, Baier PC, Mölle M, Inostroza M, Born J, Marshall L. (2012). Sleep enhances memory consolidation in the hippocampus-dependent object-place recognition task in rats. Neurobiol Learn Mem. 97(2):213-9. doi: 10.1016/j.nlm.2011.12.004. Epub 2011 Dec 21. PMID: 22207008.

75. Marr D. (1971). Simple memory: a theory for archicortex. Philos Trans R Soc Lond B Biol Sci. 262(841):23-81. doi: 10.1098/rstb.1971.0078. PMID: 4399412.

76. Buzsáki G. (1989). Two-stage model of memory trace formation: a role for "noisy" brain states. Neuroscience. 31(3):551-70. doi: 10.1016/0306-4522(89)90423-5. PMID: 2687720.

77. Clemens Z, Mölle M, Eross L, Jakus R, Rásonyi G, Halász P, Born J. (2011). Fine-tuned coupling between human parahippocampal ripples and sleep spindles. Eur J Neurosci. 33(3):511-20. doi: 10.1111/j.1460-9568.2010.07505.x. Epub 2010 Dec 7. PMID: 21138489.

78. Staresina BP, Bergmann TO, Bonnefond M, van der Meij R, Jensen O,

Deuker L, Elger CE, Axmacher N, Fell J. (2015). Hierarchical nesting of slow oscillations, spindles and ripples in the human hippocampus during sleep. Nat Neurosci. 18(11):1679-1686. doi: 10.1038/nn.4119. Epub 2015 September 21. PMID: 26389842; PMCID: PMC4625581.

79. Latchoumane CV, Ngo HV, Born J, Shin HS. (2017). Thalamic Spindles Promote Memory Formation during Sleep through Triple Phase-Locking of Cortical, Thalamic, and Hippocampal Rhythms. Neuron. 19;95(2):424-435.e6. doi: 10.1016/j.neuron.2017.06.025. Epub 2017 Jul 6. PMID: 28689981.

80. Born J, Wilhelm I. (2012). System consolidation of memory during sleep. Psychol Res. 76(2):192-203. doi: 10.1007/s00426-011-0335-6. Epub 2011 May 4. PMID: 21541757; PMCID: PMC3278619.

81. Novitskaya Y, Sara SJ, Logothetis NK, Eschenko O. (2016). Ripple-triggered stimulation of the locus coeruleus during post-learning sleep disrupts ripple/spindle coupling and impairs memory consolidation. Learn Mem. 15;23(5):238-48. doi: 10.1101/lm.040923.115. PMID: 27084931; PMCID: PMC4836638.

82. Maingret N, Girardeau G, Todorova R, Goutierre M, Zugaro M. (2016). Hippocampo-cortical coupling mediates memory consolidation during sleep. Nat Neurosci. 19(7):959-64. doi: 10.1038/nn.4304. Epub 2016 May 16. PMID: 27182818.

83. Lindemann C, Ahlbeck J, Bitzenhofer SH, Hanganu-Opatz IL. (2016). Spindle Activity Orchestrates Plasticity during Development and Sleep. Neural Plast. 2016:5787423. doi: 10.1155/2016/5787423. Epub 2016 May 16. PMID: 27293903; PMCID: PMC4884844.

84. Altman J, Sudarshan K. (1975). Postnatal development of locomotion in the laboratory rat. Anim Behav. 23(4):896-920. doi: 10.1016/0003-3472(75)90114-1. PMID: 1200422.

85. Barker GR, Warburton EC. (2015). Object-in-place associative

recognition memory depends on glutamate receptor neurotransmission within two defined hippocampal-cortical circuits: a critical role for AMPA and NMDA receptors in the hippocampus, perirhinal, and prefrontal cortices. Cereb Cortex. 25(2):472-81. doi: 10.1093/cercor/bht245. Epub 2013 Sep 12. PMID: 24035904; PMCID: PMC4380082.

86. Ylinen A, Bragin A, Nádasdy Z, Jandó G, Szabó I, Sik A, Buzsáki G. (1995). Sharp wave-associated high-frequency oscillation (200 Hz) in the intact hippocampus: network and intracellular mechanisms. J Neurosci. 15(1 Pt 1):30-46. doi: 10.1523/JNEUROSCI.15-01-00030.1995. PMID: 7823136; PMCID: PMC6578299.

87. Pérez-Escudero A, Vicente-Page J, Hinz RC, Arganda S, de Polavieja GG. (2014). idTracker: tracking individuals in a group by automatic identification of unmarked animals. Nat Methods. 11(7):743-8. doi: 10.1038/nmeth.2994. Epub 2014 Jun 1. PMID: 24880877.

88. Negrón-Oyarzo I, Neira D, Espinosa N, Fuentealba P, Aboitiz F. (2015). Prenatal Stress Produces Persistence of Remote Memory and Disrupts Functional Connectivity in the Hippocampal-Prefrontal Cortex Axis. Cereb Cortex. 25(9):3132-43. doi: 10.1093/cercor/bhu108. Epub 2014 May 23. PMID: 24860018.

89. Paxinos, G. and Watson, C. (2006). The Rat Brain in Stereotaxic Coordinates. Sixth Edition, Academic Press, Cambridge.

90. Silversmith DB, Lemke SM, Egert D, Berke JD, Ganguly K. (2020). The Degree of Nesting between Spindles and Slow Oscillations Modulates Neural Synchrony. J Neurosci. 10;40(24):4673-4684. doi: 10.1523/JNEUROSCI.2682-19.2020. Epub 2020 May 5. PMID: 32371605; PMCID: PMC7294805.

91. Mölle M, Yeshenko O, Marshall L, Sara SJ, Born J. (2006). Hippocampal sharp wave-ripples linked to slow oscillations in rat slow-wave sleep. J Neurophysiol. 96(1):62-70. doi: 10.1152/jn.00014.2006. Epub 2006 Apr 12. PMID: 16611848.

92. Durán E, Oyanedel CN, Niethard N, Inostroza M, Born J. (2018). Sleep stage dynamics in neocortex and hippocampus. Sleep. 1;41(6). doi: 10.1093/sleep/zsy060. PMID: 29893972.

93. Hahn MA, Heib D, Schabus M, Hoedlmoser K, Helfrich RF. (2020). Slow oscillation-spindle coupling predicts enhanced memory formation from childhood to adolescence. Elife. 24;9:e53730. doi: 10.7554/eLife.53730. PMID: 32579108; PMCID: PMC7314542.

94. Eackermann. Ratpack. (2018). Github [https://github.com/eackermann/ratpack].

95. Maris E, Oostenveld R. (2007). Nonparametric statistical testing of EEG-and MEG-data. J Neurosci Methods. 15;164(1):177-90. doi: 10.1016/j.jneumeth.2007.03.024. Epub 2007 Apr 10. PMID: 17517438.

96. Mumby DG, Gaskin S, Glenn MJ, Schramek TE, Lehmann H. (2002). Hippocampal damage and exploratory preferences in rats: memory for objects, places, and contexts. Learn Mem. 9(2):49-57. doi: 10.1101/lm.41302. PMID: 11992015; PMCID: PMC155935.

97. Krüger HS, Brockmann MD, Salamon J, Ittrich H, Hanganu-Opatz IL. (2012). Neonatal hippocampal lesion alters the functional maturation of the prefrontal cortex and the early cognitive development in pre-juvenile rats. Neurobiol Learn Mem. 97(4):470-81. doi: 10.1016/j.nlm.2012.04.001. Epub 2012 Apr 10. PMID: 22521798.

98. Donato F, Jacobsen RI, Moser MB, Moser EI. (2017). Stellate cells drive maturation of the entorhinal-hippocampal circuit. Science. 17;355(6330):eaai8178. doi: 10.1126/sci- ence.aai8178. Epub 2017 February 2. PMID: 28154241.

99. Cacucci F, Salinas P, Wills TJ. (2017). Hippocampus: Activity-Driven Maturation of Neural Circuits for Navigation. Curr Biol. 5;27(11):R428-R430. doi: 10.1016/j.cub.2017.04.006. PMID: 28586670.

100. Farooq U, Dragoi G. (2019). Emergence of preconfigured and plastic time-compressed sequences in early postnatal development. Science. 11;363(6423):168-173. doi: 10.1126/science.aav0502. PMID: 30630930; PMCID: PMC6794005.

101. Cruz-Sanchez A, Dematagoda S, Ahmed R, Mohanathaas S, Odenwald N, Arruda-Carvalho M. (2020). Developmental onset distinguishes three types of spontaneous recognition memory in mice. Sci Rep. 30;10(1):10612. doi: 10.1038/s41598-020-67619-w. PMID: 32606443; PMCID: PMC7326931.

102. Van Betteray JN, Vossen JM, Coenen AM. (1991). Behavioural characteristics of sleep in rats under different light/dark conditions. Physiol Behav. 50(1):79-82. doi: 10.1016/0031-9384(91)90501-e. PMID: 1946735.

103. Tromp J, Lahaije M, Nijssen A. (1991). Sleep postures and power spectrum analysis of the EEG of the rat. Behav Processes. 22(3):151-5. doi:10.1016/0376-6357(91)90089-I. PMID: 24897175.

104. Ohayon MM, Carskadon MA, Guilleminault C, Vitiello MV. (2004). Meta-analysis of quantitative sleep parameters from childhood to old age in healthy individuals: developing normative sleep values across the human lifespan. Sleep. 1;27(7):1255-73. doi: 10.1093/sleep/27.7.1255. PMID: 15586779.

105. Campos-Beltrán D, Marshall L. (2021). Changes in sleep EEG with aging in humans and rodents. Pflugers Arch. 473(5):841-851. doi: 10.1007/s00424-021-02545-y. Epub 2021 Apr 1. PMID: 33791849; PMCID: PMC8076123.

106. Salfi F, D'Atri A, Tempesta D, De Gennaro L, Ferrara M. (2020). Boosting Slow Oscillations during Sleep to Improve Memory Function in Elderly People: A Review of the Literature. Brain Sci. 15;10(5):300. doi: 10.3390/brainsci10050300. PMID: 32429181; PMCID: PMC7287854.

107. Klinzing JG, Mölle M, Weber F, Supp G, Hipp JF, Engel AK, Born J. (2016). Spindle activity phase-locked to sleep slow oscillations. Neuroimage. 1;134:607-616. doi: 10.1016/j.neuroimage.2016.04.031. Epub 2016 Apr 18. PMID:

27103135.

108. Wiegand JP, Gray DT, Schimanski LA, Lipa P, Barnes CA, Cowen SL. (2016). Age Is Associated with Reduced Sharp-Wave Ripple Frequency and Altered Patterns of Neuronal Variability. J Neurosci. 18;36(20):5650-60. doi: 10.1523/JNEUROSCI.3069-15.2016. PMID: 27194342; PMCID: PMC5696526.

109. Takashima A, Nieuwenhuis IL, Jensen O, Talamini LM, Rijpkema M, Fernández G. (2009). Shift from hippocampal to neocortical centered retrieval network with consolidation. J Neurosci. 12;29(32):10087-93. doi: 10.1523/JNEUROSCI.0799-09.2009. PMID: 19675242; PMCID: PMC6664975.

110. Mölle M, Born J. (2011). Slow oscillations orchestrating fast oscillations and memory consolidation. Prog Brain Res. 193:93-110. doi: 10.1016/B978-0-444-53839-0.00007-7. PMID: 21854958.

111. Cox R, Schapiro AC, Manoach DS, Stickgold R. (2017). Individual Differences in Frequency and Topography of Slow and Fast Sleep Spindles. Front Hum Neurosci. 5;11:433. doi: 10.3389/fnhum.2017.00433. PMID: 28928647; PMCID: PMC5591792.

112. Hashemi NS, Dehnavi F, Moghimi S, Ghorbani M. (2019). Slow spindles are associated with cortical high frequency activity. Neuroimage. 1;189:71-84. doi: 10.1016/j.neuroimage.2019.01.012. Epub 2019 Jan 9. PMID: 30639838.

113. Taxidis J, Mizuseki K, Mason R, Owen MR. (2013). Influence of slow oscillation on hippocampal activity and ripples through cortico-hippocampal synaptic interactions, analyzed by a cortical-CA3-CA1 network model. Front Comput Neurosci. 5;7:3. doi: 10.3389/fncom.2013.00003. PMID: 23386827; PMCID: PMC3564232.

114. Ekstrom AD, Arnold AE, Iaria G. (2014). A critical review of the allocentric spatial representation and its neural underpinnings: toward a network-based perspective. Front Hum Neurosci. 10;8:803. doi: 10.3389/fnhum.2014.00803. PMID: 25346679; PMCID: PMC4193251.

X

10.1 Papers

- **García-Pérez M.A**, Irani M, Tiznado V, Bustamante T, Inostroza M, Maldonado PE and Valdés JL. Cortico-hippocampal oscillations are associated with the developmental onset of hippocampal-dependent memory. Front Neurosci. 2022 March. Manuscript ID: 891523. (Submitted, under review).

- Morales C, Morici JF, Espinosa N, Sacson A, Lara-Vasquez A, **García-Pérez MA**, Bekinschtein P, Weisstaub NV, Fuentealba P. Dentate Gyrus Somatostatin Cells are Required for Contextual Discrimination During Episodic Memory Encoding. Cereb Cortex. 2021 Jan 5;31(2):1046-1059. doi: 10.1093/cercor/bhaa273. PMID: 33026440. [https://pubmed.ncbi.nlm.nih.gov/33026440/]

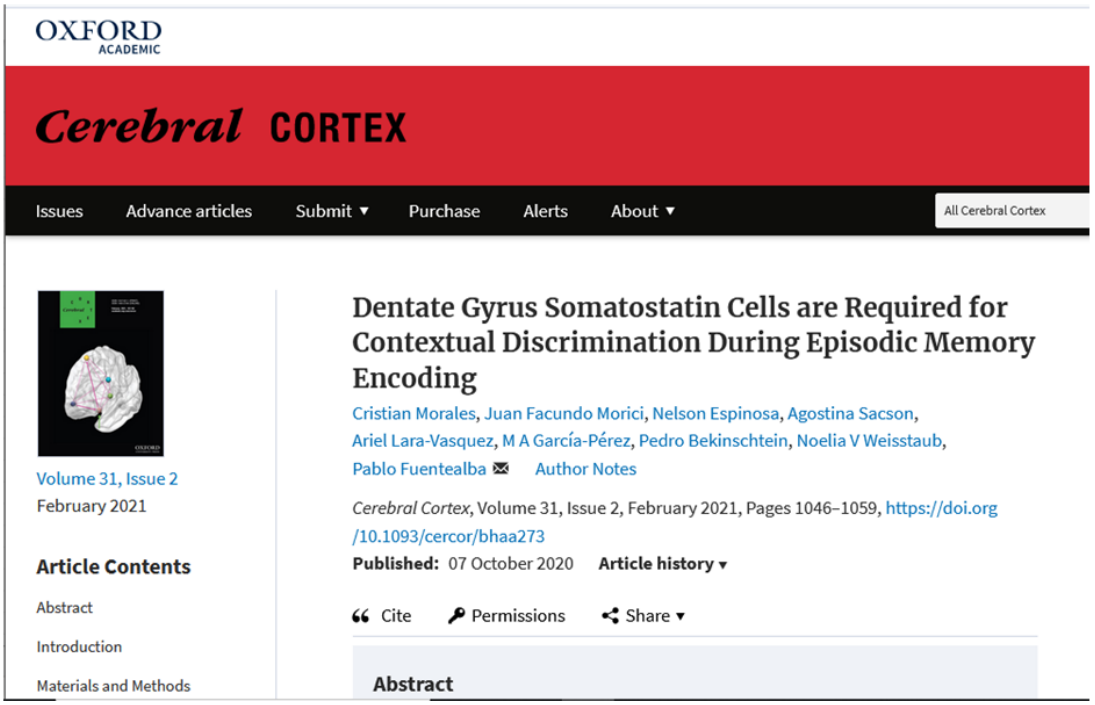

10.2 Poster presentations

10.2.1 International

- **García-Pérez M.A**, Irani M, Tiznado Vicente, Pedro Maldonado, José Luis Valdés. (2021). Allocentric episodic memory onset along postnatal development during sleep. SfN Global Connectome, Virtual meeting, January 11-13, 2021.

- **García-Pérez M.A**, Irani M, Tiznado Vicente, Pablo Fuentealba. (2019). Hippocampal Sharp-Wave Ripples and episodic memory onset along development. XXXIV Reunión Annual de la Sociedad Argentina de Investigación en Neurociencias (SAN), Villa Carlos Paz, Argentina 2019, October 3-5,2019.

- **García-Pérez M.A**, Valdivia Gonzalo, Espinosa Nelson, Tiznado Vicente,

Pablo Fuentealba. (2018). Spatial memory consolidation and sleep oscillations along development. XXXIII Reunión Annual de la Sociedad Argentina de Investigación en Neurociencias (SAN), Córdoba, Argentina 2018, October 23-26,2018.

- **García-Pérez M.A**, Valdivia Gonzalo, Espinosa Nelson, Tiznado Vicente, Pablo Fuentealba. (2018). Long-term spatial memory consolidation during sleep along developmental neuronal circuits maturation. Barcelona Computational, Cognitive and Systems Neuroscience (Barccsyn) 2018, May 24-25,2018.

10.2.2 National

- **García-Pérez M.A**, Irani M, Tiznado Vicente, Pedro Maldonado, José Luis Valdés. (2020). Allocentric episodic memory onset along postnatal development during sleep. XVI Reunión Annual de la Sociedad Chilena de Neurociencias, Virtual meeting, November 10-12,2020.

- **García-Pérez M.A**, Irani M, Tiznado Vicente, Pablo Fuentealba. (2019). Hippocampal Sharp-Wave Ripples and episodic memory onset along development. XV Reunión Annual de la Sociedad Chilena de Neurociencias, La Serena, Chile 2019, November 5-8,2019.

- **García-Pérez M.A**, Valdivia Gonzalo, Espinosa Nelson, Tiznado Vicente, Pablo Fuentealba. (2018). Spatial memory consolidation and sleep oscillations along development. XIV Reunión Annual de la Sociedad Chilena de Neurociencias, 90 Aniversario Reunión Conjunta. Puerto Varas, Chile 2018, November 20- 22,2018.

Allocentric episodic memory onset along postnatal development during sleep

García-Pérez M.A[1,2] , Irani M[3], Tiznado V[3], Maldonado P[2], Valdés JL[1].

1Laboratorio de Aprendizaje Memoria y Neuromodulación, Departamento de Neurociencia, Facultad de Medicina, Universidad de Chile.
2Laboratorio de Neurosistemas, Departamento de Neurociencia, Facultad de Medicina, Universidad de Chile.
3 Laboratorio de Neurodinámica de la Cognición, Departamento de Psiquiatría, Centro Interdisciplinario de Neurociencias UC, Pontificia Universidad Católica de Chile.

magarcia13@uc.cl

SUMMARY

Episodic memory relies on the ability of the hippocampus to process spatial information. This type of memory emerges late on postnatal lifetime, in correlation with hippocampal development. When this memory is build-up by using external/distal environmental cues is known as allocentric memory and, it is the latest form of episodic memory to emerge. Recently, it has been shown that allocentric memory is observed since postnatal day 18 (P18), but it is not fully developed until P28, when it reaches the adult-like form. However, it has been proposed that early reinforcement by allocentric task training could accelerate its adult-like expression.
Although the mechanisms of memory formation remain unclear, research has pointed out sleep as a memory promotor and oscillatory electrical rhythms during sleep, such as cortical slow waves (< 1Hz), and hippocampal sharp-wave ripples (SWRs,100-250 Hz) as correlates of memory consolidation. With the aim to determine whether allocentric reinforcement could anticipate the maturation of episodic memory in parallel with changes in oscillatory activity, we performed an object-in-place task with or without reinforcement and in vivo LFP recordings, throughout animal development, in the somatosensory and hippocampal cortices. Our results show that allocentric memory emerges around P32 (n=11, p< 0.042) independently of early reinforcement and, changes in the power and density of sleep SWRs accompany the emergence of memory consolidation.

Keywords: Behaviour, Spatial Memory, Development, Electrophysiology, Sleep.

INTRODUCTION

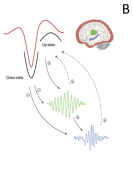

Figure 1. Sleep oscillations regulate memory consolidation during sleep. (A) The Active systems consolidation model suggest a loop-like dialog between neocortex (red), thalamus (green), and hippocampus (blue). The SO up-state mainly drives the generation of thalamic spindles which, in turn, act on hippocampal networks to synchronize ripples and ensemble reactivations to their excitable troughs. **(B)** The fine-tuned coupling of hippocampal SPW-Rs and cortical delta waves and spindles boosts next day performance in a spatial memory task. (a) Illustration of the object-in-place task at sleep condition. (b) Discrimination index (displaced object) during the first 2 min of exploration. Memory recall was observed only following coupled stimulation (coupled versus delayed, Wilcoxon matched pairs test; n = 9, Z = 2.67, **P = 0.008; coupled versus chance, Wilcoxon signed-rank test, n = 9, Z = 2.67, **P = 0.008; delayed versus chance, Wilcoxon signed-rank test, n = 9, Z = 1.48, P = 0.138). Error bars represent s.e.m. (Klinzing, 2019; Mainget, 2016)

RESULTS

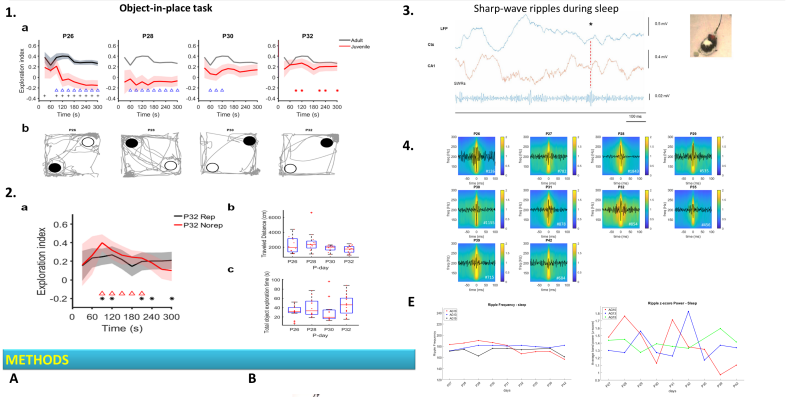

Figure 2. Sharp-wave ripples along development while performing an Object-in-place memory task. (1) Allocentric spatial-memory onset along development on the Object-place recognition (OPR) paradigm in juvenile Long Evans rats compared to adult's performance. Mean (+ SEM) exploration ratios during OPR at P26, P28, P30 and P32 compared to adult's index. Exploration index was calculated according to the formula: (Displaced object - Familiar object) / (Displaced object + Familiar object). These results show that juvenile rats were able to successfully perform an OPR task on P32, but not at P26, P28, and P30. When rats were compared to adults only at P32 the exploration index reaches adult level. Male adult rats, n=17 around P90 were used as a reference. Male pups, n=12 at P26, P28, and n=11 at P30 and P32 were used. Two-sided Wilcoxon signed-rank test compared to chance level was performed (*p<0.05, black for adults, and red for juvenile rats) in all cases. And two-sided Wilcoxon rank-sum test (*p<0.05, blue) was used for comparing adult vs juvenile performances. **(2)** Reinforcement of the task does not improve memory performance, mean (+ SEM) exploration ratios during OPR at P32 single exposure compared against P32 with early previous exposure. Male juvenile rats, n=8 for the single exposure P32 group were used. Male juvenile rats, n=11 for the early previous exposure P32 group were used. Two-sided Wilcoxon signed-rank test compared to chance level was performed (*p<0.05, black for adults, and red for juvenile rats) in all cases. And two-sided Wilcoxon rank-sum test (*p<0.05, blue) was used for comparing single exposure vs early previous exposure performances at P32 (p = 0.362). **(3)** Sharp-wave ripples identification at sleep. (Right) A representative implanted rat at sleep state, (left) cortical and hippocampal LFP raw signal, and hippocampal filtered signal (SWRs, 100-300 Hz) from an implanted rat at a sleep state. Showing examples of ripples (*). **(4)** Grand Average Ripple Spectrogram along days of development (n = 3). Ripples were detected form broadband signal (100–300 Hz) during sleep windows. Units are expressed in terms of s.d. from the mean. Number of events is indicated at the bottom of each image (E) Ripple Frequency and Average Power along days of development for each animal.

METHODS

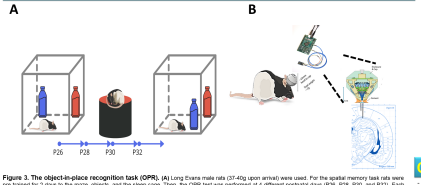

Figure 3. The object-in-place recognition task (OPR). (A) Long Evans male rats (37-40g upon arrival) were used. For the spatial memory task rats were pre-trained for 2 days to the maze, objects, and the sleep cage. Then, the OPR test was performed at 4 different postnatal days (P26, P28, P30, and P32). Each session consisted of 5 min in the maze with 2 identical objects for free exploration. Immediately after, 3h in the retention cage for LFP-recording while sleeping until P42, followed by 5 min in the maze with the same 2 identical objects but one of them were displaced from the familiar position. Visual cues were suspended on the wall of the room as a spatial reference. Electrophysiological recordings continued after P32 twice a week without the task (only sleep). **(B)** Left, an illustration of the microdrive implant and the INTAN recording system. Right, Microdrive illustration, and in detail the 4 Ni-Cr tetrodes final position at the posterior parietal cortex and dorsal hippocampus (CA1) (Modified from Eickenkamm 2016; Vogts J, 2013).

CONCLUSIONS

- Allocentric memory as discrimination in the OPR task emerges at P32, and reaches adult-like exploration index.
- Spatial memory emergence is independet of the early reinforcement of the task, suggesting that must be due to the development.
- SPW-Rs frequency remain stable along development during sleep, also preliminary data suggest that SPW-Rs power increases around P32 which could be an indicative of the memory consolidation mechanism. Further research is needed.

Acknowledgement: ANID 21171047, ICN09_015 and to the Congress Fellowship

Hippocampal Sharp-Wave Ripples and episodic memory onset along development

García-Pérez M.A [1,2], Irani M[1], Tiznado V[3], Valdés JL[2], Fuentealba P[1].

[1]Laboratorio de Circuitos Neuronales, Departamento de Psiquiatría, Centro Interdisciplinario de Neurociencias UC, Pontificia Universidad Católica de Chile.
[2]Laboratorio de Aprendizaje Memoria y Neuromodulación, Departamento de Neurociencia, Facultad de Medicina, Universidad de Chile.
[3]Laboratory for Brain-Machine Interfaces and Neuromodulation, Departamento de Psiquiatría, Centro Interdisciplinario de Neurociencias UC, Pontificia Universidad Católica de Chile.

magarcia13@uc.cl

SUMMARY

Episodic memory relies on the ability of the hippocampus to process spatial information. This type of memory emerges late on postnatal lifetime, in correlation with hippocampal development. When this memory is build-up by using external/distal environmental cues is known as allocentric memory and, it is the latest form of episodic memory to emerge. Recently, it has been shown that allocentric memory is observed since postnatal day 18 (P18), but it is not fully developed until P38, when it reaches the adult-like form. However, it has been proposed that early reinforcement by allocentric task training could accelerate its adult-like expression.

Although the mechanisms of memory formation remain unclear, research has pointed out sleep as a memory promoter and oscillatory electrical rhythms during sleep, such as cortical slow waves (< 1Hz), and hippocampal sharp-wave ripples (SWRs,100-250 Hz) as correlates of memory consolidation. With the aim to determine whether allocentric reinforcement could anticipate the maturation of episodic memory in parallel with changes in oscillatory activity, we performed an object-place task with or without reinforcement and *in vivo* LFP recordings, throughout animal development, in the somatosensory and hippocampal cortices. Our results show that allocentric memory emerges around P32 (n=11, p=0.042), independently of early reinforcement and, changes in the power and density of sleep SWRs accompany the emergence of memory consolidation.

Keywords: Neurosciences, Electrophysiology, Sleep, Behavior, Development.

INTRODUCTION

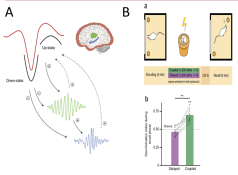

Figure 1. Sleep oscillations regulate memory consolidation during sleep. (A) The Active systems consolidation model suggest a loop-like dialog between neocortex (red), thalamus (green), and hippocampus (blue). The SO up-state mainly drives the generation of thalamic spindles which, in turn, act on hippocampal networks to synchronize ripples and ensemble reactivations to their excitable troughs. **(B)** The fine-tuned coupling of hippocampal SPW-Rs and cortical delta waves and spindles boosts next day performance in a spatial memory task. (a) Illustration of the object-in place task at sleep condition. (b) Discrimination index (displaced object) during the first 2 min of exploration. Memory recall was observed only following coupled stimulation (coupled versus delayed, Wilcoxon matched pairs test; n = 9, Z = 2.67, **P = 0.008; coupled versus chance, Wilcoxon signed-rank test, n = 9, Z = 2.67, **P = 0.008; delayed versus chance, Wilcoxon signed-rank test, n = 9, Z = 1.48, P = 0.138). Error bars represent s.e.m. (Klinzing, 2019; Maingret, 2016)

RESULTS

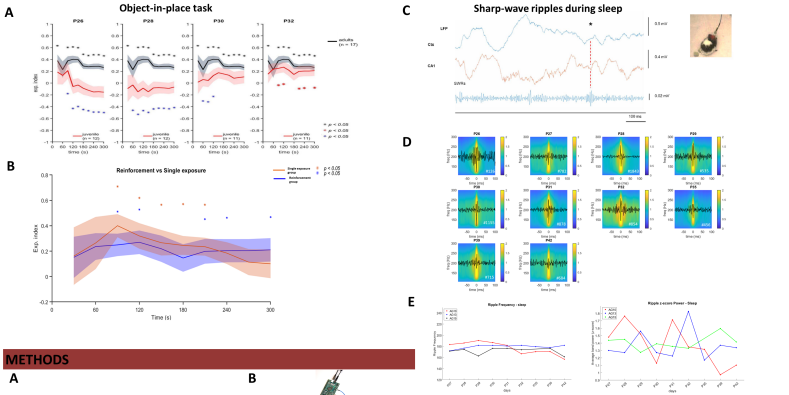

Figure 2. Sharp-wave ripples along development while performing an Object-in-place memory task. (A) Allocentric spatial-memory onset along development on the Object-place recognition (OPR) paradigm in juvenile Long Evans rats compared to adult's performance. Mean (+ SEM) exploration ratios during OPR at P26, P28, P30 and P32 compared to adult's index. Exploration index was calculated according to the formula: (Displaced object - Familiar object) / (Displaced object + Familiar object). These results show that juvenile rats were able to successfully perform an OPR task on P32, but not at P26, P28, and P30. When rats were compared to adults only at P32 the exploration index reaches adult level. Male adult rats, n=17 around P90 were used as a reference. Male pups, n=12 at P26, P28, and n=11 at P30 and P32 were used. Two-sided Wilcoxon signed-rank test compared to chance level was performed (*p<0.05, black for adults, and red for juvenile rats) in all cases. And two-sided Wilcoxon rank-sum test (*p<0.05, blue) was used for comparing adult vs juvenile performances. **(B)** Reinforcement of the task does not improve memory performance, mean (+ SEM) exploration ratios during OPR at P32 single exposure compared against P32 with early previous exposure. Male juvenile rats, n=8 for the single exposure P32 group were used. Male juvenile rats, n=11 for the early previous exposure P32 group were used. Two-sided Wilcoxon signed-rank test compared to chance level was performed (*p<0.05, black for adults, and red for juvenile rats) in all cases. And two-sided Wilcoxon rank-sum test (*p<0.05, blue) was used for comparing single exposure vs early previous exposure performances at P32 (p = 0.362). (C) Sharp-wave ripples identification at sleep. (Right) A representative implanted rat at sleep state, (left) cortical and hippocampal LFP raw signal, and hippocampal filtered signal (SWRs, 100-300 Hz) from an implanted rat at a sleep state. Showing examples of ripples (*). (D) Grand Average Ripple Spectrogram along days of development (n = 3). Ripples were detected form broadband signal (100–300 Hz) during sleep windows. Units are expressed in terms of s.d. from the mean. Number of events is indicated at the bottom of each image (E) Ripple Frequency and Average Power along days of development for each animal.

METHODS

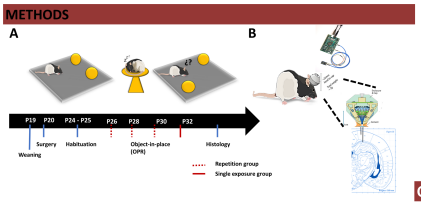

Figure 3. The object-in-place recognition task (OPR). (A) Long Evans male rats (37-40g upon arrival) were used. For the spatial memory task rats were pre-trained for 2 days to the maze, objects, and the sleep cage. Then, the OPR test was performed at 4 different postnatal days (P26, P28, P30, and P32). Each session consisted of 5 min in the maze with 2 identical objects for free exploration. Immediately after, 3h in the retention cage for LFP-recording while sleeping until P42, followed by 5 min in the maze with the same 2 identical objects but one of them were displaced from the familiar position. Visual cues were suspended on the wall of the room as a spatial reference. Electrophysiological recordings continued after P32 twice a week, without the task (only sleep). **(B)** Left, an illustration of the microdrive implant and the INTAN recording system. Right, Microdrive illustration, and in detail the 4 NI-Cr tetrodes final position at the posterior parietal cortex and dorsal hippocampus (CA1) (Modified from Eackermann 2016; Voigts J, 2013).

CONCLUSIONS

- Allocentric memory as discrimination in the OPR task emerges at P32, and reaches adult-like exploration index.
- Spatial memory emergence is independet of the early reinforcement of the task, suggesting that must be due to the development.
- SPW-Rs frequency remain stable along development during sleep, also preliminary data suggest that SPW-Rs power increases around P32 which could be an indicative of the memory consolidation mechanism. Further research is needed.

Acknowledgement: FONDECYT 1190375 and to the Congress Fellowship

Spatial memory consolidation and sleep oscillations development

García-Pérez M.A, Valdivia G, Espinosa N, Tiznado V, Fuentealba P.
Laboratorio de Circuitos Neuronales, Departamento de Psiquiatría, Centro Interdisciplinario de Neurociencias UC, Pontificia Universidad Católica de Chile.
magarcia13@uc.cl

SUMMARY

Sleep following encoding favors the formation of **episodic long-term memory** (Rasch and Born, 2013). In particular, slow wave sleep appears to support **hippocampus-dependent declarative memory consolidation**, i.e.; spatial tasks such as **object in place recognition (OPR)** (Inostroza and Born, 2013). It has been proposed that this process is supported by the phase-locking of three cortical rhythms: **neocortical slow oscillations, thalamic spindles, and hippocampal sharp wave-ripples** thus sustaining hippocampal-neocortical long-term storage (Sirota et al., 2003; Clemens et al., 2007; Mölle and Born, 2010; Latchoumane, et al. 2017; Staresina et al.,2015).

During **postnatal development** cortical oscillations related to cognitive functions and synaptic plasticity emerge in the network, such as sharp waves, theta, and gamma rhythms. Ripples begin to emerge at P14 (Lahtinen, et al, 2002; Buhl, Buzsaki et al 2005). Furthermore, allocentric spatial abilities emerge at an early stage, along with rat's sensorimotor repertoire (Altman J, et al., 1975; Tan H. 2017). We are particularly interested in the study of oscillation phase-locking related to memory consolidation during sleep, coupled with allocentric spatial emergence during development. To address this, Long Evans pup's rats were repeatedly trained in a spatial memory task (OPR) during several postnatal days. Our data shows that animals acquire the task at around P32, after several repetitions. Also, that this capability becomes comparable to adult along P26-P32. Moreover, we predict that interregional connectivity will be enhanced during that period, reflected in enhanced synchrony in thalamocortical networks during sleep. According to this, we will implant multichannel electrodes in the posterior parietal cortex, somatosensory thalamus, and dorsal hippocampus (CA1) for LFP and single units recording during sleep. We hypothesize that early spatial memory reinforcement following sleep may improve the oscillation phase-locking and in consequence long-term storage.

Keywords: Neurosciences, Electrophysiology, Sleep, Behavior, Development.

INTRODUCTION

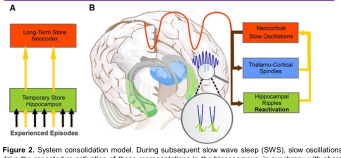

Figure 2. System consolidation model. During subsequent slow wave sleep (SWS), slow oscillations drive the repeated re-activation of these representations in the hippocampus, in synchrony with sharp wave-ripples and thalamo-cortical spindles (synchronizing feed-forward effect of the slow oscillation up-state). By synchronizing these events the slow oscillations support the formation of ripple-spindle events, which enable an effective hippocampus-to-neocortex transfer of the re-activated information for long-term cortical storage (Modified from Born J, 2012).

METHODS

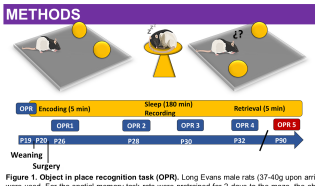

Figure 1. Object in place recognition task (OPR). Long Evans male rats (37-40g upon arrival) were used. For the spatial memory task rats were pretrained for 2 days to the maze, the object and the sleep cage. Then, the OPR test were performed for 4 consecutive days (P26, P28, P30 and P32) with one day of rest in between test. Each session consisted of 5 min in the maze with 2 identical objects for free exploration. Immediately after, 2h in the retention cage for sleep recording, followed by 5 min in the maze with the 2 identical objects but one of them is displaced from de familiar position. Visual cues were suspended on the wall of the room as spatial reference. Electrophysiological recordings continued after P32 twice a week without the task (only sleep). A last OPR task is performed at P90 to evaluate adult performance.

RESULTS

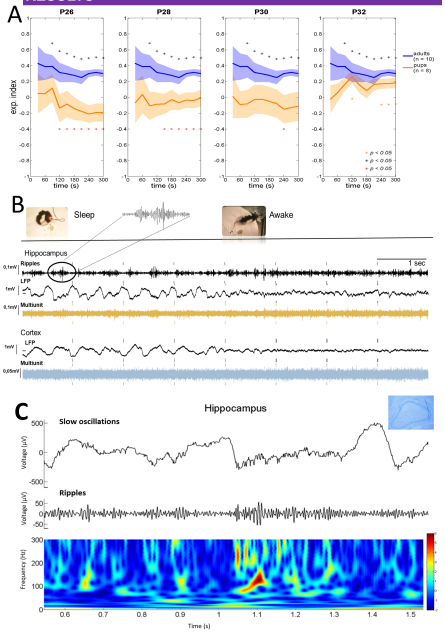

Figure 3. (A) Object in place recognition task performance. Exploration index for different postnatal days (male rats, n=8, P26-P32, *, orange). There is a significative discrimination of the novel object after the fourth reinforcemnt (P32) at minute 2,4 and 5 of exploration. Male and Female adult rats, n=10 at P90 were used (*, black). Two-sided Wilcoxon signed rank test compared to chance level was performed (*p<0.05) in both cases. Adult vs pup comparison is shown in red. **(B)** Multichannel recording. Scheme of LFP (raw signal) and multiunit recording (filtered at 500-5000 Hz) in Cortex, and LFP, multiunit and ripple (filtered at 100-250 Hz) signals during a sleep-awake transition at P32. **(C)** Hippocampal Sharp-waves ripples at rest state (NREM), on top slow oscillations detection filtered < 1Hz, below filtered-ripples, and finally Time–frequency spectra, power intensity (-2, blue to 6,red). In the corner a Nissl of the tetrode is shown as a reference.

CONCLUSIONS

According to this work, we were able to successfully evaluate at an early developmental stage, the *in vivo* oscillatory patterns during sleep after performing a OPR task. We observed that after the fourth consecutive day of OPR task (P32) there was a significant discrimination of the novel object during the initial phase of the exploration (2 min) and later at 4 and 5 min. Also, that this acquired discrimination becomes comparable to adult's. By the other hand, we could register LFP and multiunit signal at least two different regions of interest during sleep stage between P26-P32 (only P32 shown).

During this developmental stage (P26-P32), several functional and structural neuroplastic events occur in parallel to brain rhythms stabilization. Moreover, at this stage spatial memory has not been fully developed until P31. For all this, we intend to evaluate by electrophysiological recordings, the modulation of neocortical slow oscillations, thalamic spindles, and hippocampal sharp wave-ripples at sleep stage after a repetitive spatial memory task. These experiments, will allow us to determine the not previously described contribution of the oscillatory patterns synchronization during sleep in the behavioral correlate observed at P32. Finally, to address this, further analysis and greater experimental number will be required.

Acknowledgement: Conicyt Anillos PIA ACT 1414 and to the Congress Fellowship

Spatial memory consolidation and neuronal circuits synchronization during sleep along development

García-Pérez M.A, Valdivia G, Espinosa N, Tiznado V, Fuentealba P.
Laboratorio de Circuitos Neuronales, Departamento de Psiquiatría, Centro Interdisciplinario de Neurociencias UC, Pontificia Universidad Católica de Chile.
magarcia13@uc.cl

SUMMARY

Sleep following encoding favors the formation of **episodic long-term memory** (Rasch and Born, 2013). In particular, slow wave sleep appears to support **hippocampus-dependent declarative memory consolidation**, i.e.; spatial tasks such as **object in place recognition (OPR)** (Inostroza and Born, 2013). It has been proposed that this process is supported by the phase-locking of three cortical rhythms: **neocortical slow oscillations, thalamic spindles, and hippocampal sharp wave-ripples** thus sustaining hippocampal-neocortical long-term storage (Sirota et al., 2003; Clemens et al., 2007; Molle and Born, 2010; Latchoumane, et al. 2017; Staresina et al.,2015).

During **postnatal development** cortical oscillations related to cognitive functions and synaptic plasticity emerge in the network, such as sharp waves, theta, and gamma rhythms. Ripples begin to emerge at P14 (Lahtinen, et al, 2002; Buhl, Buzsaki et al 2005). Furthermore, allocentric spatial abilities emerge at an early stage, along with rat's sensorimotor repertoire (Altman J, et al., 1975; Tan H. 2017). We are particularly interested in the study of oscillation phase-locking related to memory consolidation during sleep, coupled with allocentric spatial emergence during development. To address this, Long Evans pup's rats were repeatedly trained in a spatial memory task (OPR) during several postnatal days. Our data suggest that animals acquire the task at around P32, after several repetitions. Moreover, we predict that interregional connectivity will be enhanced during that period, reflected in enhanced synchrony in thalamocortical networks during sleep. According to this, we will implant multichannel electrodes in the posterior parietal cortex, somatosensory thalamus, and dorsal hippocampus (CA1) for LFP and single units recording during sleep. We hypothesize that early spatial memory reinforcement following sleep may improve the oscillation phase-locking and in consequence long-term storage.

Keywords: Neurosciences, Electrophysiology, Sleep, Behavior, Development.

INTRODUCTION

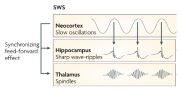

Figure 2. System consolidation model. During subsequent slow wave sleep (SWS), slow oscillations drive the repeated re-activation of these representations in the hippocampus, in synchrony with sharp wave-ripples and thalamo-cortical spindles (synchronizing feed-forward effect of the slow oscillation up-state). By synchronizing these events the slow oscillations support the formation of ripple-spindle events, which enable an effective hippocampus-to-neocortex transfer of the re-activated information. **(Modificated from Diekelmann S., 2010)**

METHODS

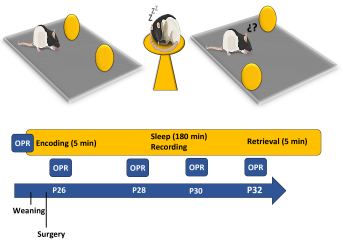

Figure 1. Object in place recognition task (OPR). Long Evans male rats (37-40g upon arrival) were used. For the spatial memory task rats were pretrained for 2 days to the maze, the object and the sleep cage. Then, the OPR test were performed for 4 consecutive days (P26, P28, P30 and P32). Each session consisted of 5 min in the maze with 2 identical objects for free exploration. Immediately after, 2h in the retention cage for sleep recording, followed by 5 min in the maze with the 2 identical objects but of them is displaced from de familiar position. This was repeated for 4 days with one day of rest in between test. Visual cues were suspended on the wall of the room as spatial reference cues.

RESULTS

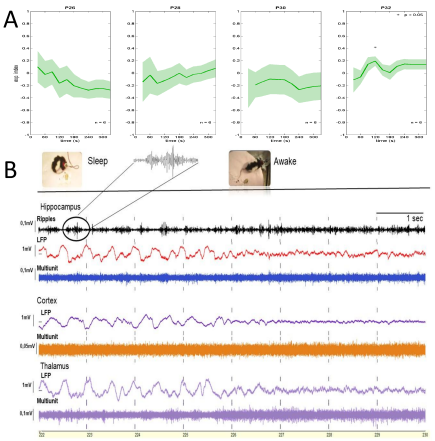

Figure 3. (A) Object in place recognition task performance. Exploration index for different postnatal days (P26-P32, n=6). There is a significative discrimination of the novel object after the fourth reinforcemnt (P32) at minute 2 of exploration **(P= 0,031). (B) Multichannel recording.** Scheme of LFP (raw signal) and multiunit recording (filtered at 500-5000 Hz) in Cortex and Thalamus, and LFP, multiunit and ripple (filtered at 100-250 Hz) signals during a sleep-awake transition at P32.

CONCLUSIONS

According to this work, we were able to successfully evaluate at an early stage the *in vivo* oscillatory patterns during sleep after performing a OPR task. We observed that after the fourth consecutive day of OPR task (P32) there was a significant discrimination of the novel object during the initial phase of the exploration (2 min). In addition, we could register LFP and multiunit signal at three different regions of interest during sleep stage between P26-P32 (only P32 shown).

During this developmental stage (P26-P32), several functional and structural neuroplastic events occur in parallel to brain rhythms stabilization. Moreover, at this stage spatial memory has not been fully developed until P31. For all this, we intend to evaluate by electrophysiological recordings, the modulation of neocortical slow oscillations, thalamic spindles, and hippocampal sharp wave-ripples at sleep stage after a repetitive spatial memory task. These experiments, will allow us to determine the not previously described contribution of the oscillatory patterns synchronization during sleep in the behavioral correlate observed at P32. Finally, to address this, further analysis and greater experimental number will be required.

Acknowledgement: Conicyt Anillos PIA ACT 1414 and to the Congress Fellowship

XI

Acknowledgments

This work represents the fruit of a dream and a passion for scientific knowledge. A challenge to continuously learn, and to be part of all those bold scientific women who have conducted research many times at the expense of omission and patriarchy. I am convinced that in the future, doing science or any other discipline will not be limited by gender. And that both, society, and educational institutions will really take care. I would like to dedicate my thesis to all those women and dissidents who struggle every day for a fair place in this society. To all those who have made them believe that their courage to express vulnerability and sensitivity were a weakness, because they are not.

This work also represents the support of many people, some transients, others who became friends, collaborators and/or inspiration.

First, I would like to thank wholeheartedly my tutors Dr. José Luis Valdés and Dr. Pedro Maldonado for showing me true scientific guidance and mentoring in a kind and respectful way. Also, for allowing me to finish my thesis in their laboratories with all the support and understanding that was possible. I would also like to thank Dr. Francisco Aboitiz and Dra. Claudia Saez for allowing this to happen.

I would also like to thank my thesis committee: Dr. Alexia Nuñez, Dr. Claudio Pérez-Leighton and Dr. Jorge Campusano who have guided and oriented

the development of my thesis in a very helpful and enlightening manner.

Special thanks to my collaborator, who also became a friend, Martin Irani, who offered me his hand in a very difficult period, showing me and teaching me in a friendly way that computational science could be an ally. He accompanied me until the end of my thesis, and he is currently enjoying a new challenge at the University of Illinois.

I would also like to thank my colleagues at the Pontificia Universidad Católica who either with their friendship, support or scientific expertise were fundamental for this stage: Cristián Morales, Rilda León and Vicente Tiznado. And to my colleagues at the Universidad de Chile, mainly Andrea Birkner, Tamara Bustamante, Miguel Concha, Camila Ramirez, Nicole, Benjamin and everyone at the Learning, Memory and Neuromodulation Laboratory and Neurosistemas Lab. Special thanks also to Carolina Lindsay who trough the Pandemic helped me to manage my work remotely with the best will.

I would also like to thank my fellow PhD students with whom I had the honor of sharing very good moments and friendship: Rilda León, Cristian Morales, Macarena Tejos, Marcos Domic, Vicente Medel, Sol Torruela, Josefina Vial, Juan Amaro and Andrea Sanchez.

On the other hand, I would like to thank the people who beyond science have always been there in a very special place of my heart, encouraging me and giving me strength when I did not seem to have it. My lovely friends Daniela Estay, Francisca Correa, Katherine Llull and Fernanda Rojas. Also, my great biochemist friends Valentina Camus and Paulina Rosa who have believed in me even when I could not.

None of this would have been possible without the support, unconditional love, and excellent example of my parents Hector Gacía and María Evangelista. I also want to extend my gratitude to my family and cousins, and specially to my grandmother whose steps in poetry and neuroscience I unknowingly followed.

Last but not least, I would like to thank my partner Rafael Pastene who with

his tenderness, loyalty and companionship has helped me to see the bright side of things during this last stage of my thesis.

Special thanks to: ANID 21171047, ICN09−015 and Proyecto Anillo ACT 172121